Towards Cleaner Fertilisers; Solution Ion-Exchange Methods for Reducing Cadmium Levels in Reactive Phosphate Rock

Timothy Dyche

Masters of Science Thesis

University of Waikato, 2022

Abstract

The aim of this study was to characterise reactive phosphate rock (RPR); a form of rock phosphate which can be used directly as fertiliser, and investigate the potential to reduce cadmium levels in RPR by application of calcium ion solutions derived from waste mussel shells.

Analytical techniques including ICP-MS, XRD, XRF, SEM-EDX, and FTIR were used in the characterisation of reactive phosphate rock, as provided by Terracare. These techniques allowed for changes to both the macro and trace element composition of reactive phosphate rock to be measured and monitored as it was subjected to a calcium ion solutions and variety of chemical and physical reaction conditions, with the aim of selectively extracting cadmium ions, by ion exchange with calcium, while leaving the general structure of RPR unchanged.

The solubility of phosphate ions in RPR was tested at varying pH, the intention being to determine the pH range of solutions that could be used for cadmium extraction while minimising phosphate losses.

Calcium ion solutions were applied to reactive phosphate rock under a range of different reaction conditions. Changes to calcium ion concentration, contact time, pH, temperature, microwave irradiation, use of different counter ions and addition of potential cadmium stabilising ligands were tested for their effects on reactive phosphate rock. Promising results were observed, with elevated levels of cadmium found in many extraction solutions. Calcium chloride solution of 1 mol L^{-1} concentration was found to be the most effective at extracting cadmium from RPR.

Mussel shells were characterised by analytical methods including ICP-MS, XRD, XRF, UV-Vis, and FTIR. The effects of heating to temperatures between 300°C and 900°C to the physical and chemical properties of mussel shells were studied. Mussel shells were used as a basis for calcium ion solutions by dissolving crushed mussel shell in mineral acids. These shell solutions were compared with solutions of pure calcium salts for their effectiveness in extracting cadmium ions.

Overall the results of this study indicate that it is possible for significant amounts of cadmium to exchange from RPR into calcium ion solutions with comparatively small phosphate losses. It appears that mussel shells could provide a suitable source of calcium ions for this purpose. Overall indications are that cadmium extraction from RPR by ion exchange with calcium ion solutions is a concept worthy of further research. If the preliminary results prove to be accurate then further developments have the potential to contribute to improved environmental outcomes for both the fertiliser and shellfish industries in New Zealand.

Acknowledgements

Firstly I would like to thank my supervisor Associate Professor Michael Mucalo for his support and guidance throughout this project.

Thank you to the University of Waikato for the opportunity for this MSc project and for providing the facilities and support required. I would like to thank all of the University of Waikato staff who have assisted with this project:
- Danielle Blackwell for running all of the ICP-MS samples from this project.
- Dr Megan Grainger for advice in interpreting ICP-MS results.
- Helen Turner for SEM-XRF analysis.
- Karla Watson and Annie Barker for their technical support and training.
- Annette Rodgers for particle sizer analysis. - Kirsty Vincent for XRD and XRF analysis and training on the ring mill.

Thank you to University of Waikato students Ali Almosabeh and Jing Xu for sharing the finding from their own research on mussel shells.

Terracare for supplying reactive phosphate rock and fertiliser samples. (Terracare has since merged with, and is now trading as Fertco).

North Island Mussels Ltd (NIML) for supplying greenshell mussel shell samples.

I would also like to thank my employer, New Seed Solutions, who have accommodated and supported my academic interests alongside my work commitments.

Finally I would like to thank my family, whose support and encouragement have made this all possible.

Contents

List of Figures

List of Tables

List of Abbreviations

°C	degrees Celsius
AAS	Atomic Absorption Spectroscopy
EDTA	Ethylenediaminetetraacetic acid
FTIR	Fourier Transform Infra-Red (Spectroscopy)
ICP-MS	Inductively Coupled Plasma - Mass Spectroscopy
NPK	Nitrogen Phosphorous Potassium (weight percentage ratio on fertiliser labels)
NZTDS	New Zealand Total Diet Survey
ppb	parts per billion
ppm	parts per million
RPR	Reactive Phosphate Rock
SEM-EDX	Scanning Electron Microscopy - Energy Dispersive X-Ray Analysis
SSA	Specific Surface Area
SSP	Single Super Phosphate
UV-Vis	Ultra-Violet Visible (light)
XRD	X-Ray Diffraction
XRF	X-Ray Fluorescence

1. Introduction

1.1 Phosphate fertiliser and the effects of cadmium contamination

1.1.1 Phosphorus in Nature

Phosphorus is essential for plant and animal life. It is found in numerous biological systems: nucleic acids (DNA/RNA), nucleotides (ATP/ADP), cell membranes (phospholipids), phosphate buffers regulate inter-cellular pH, calcium phosphate is the main component of bones.

On land phosphorus, in the form of phosphate, is absorbed by plants through their roots and from there enters the food chain. The natural phosphorus cycle is extremely slow, unlike nitrogen there is no atmospheric reservoir from which terrestrial reserves can be replenished.[2] Phosphorus on land is gradually washed into the sea where it ultimately precipitates and forms sediment.[3] The return of ocean sediment to the land via plate tectonics occurs over a geological time scale.[4] On a human scale farming removes phosphorus from the soil, it must be replenished by applying phosphate fertiliser. Though some phosphate fertilisers are produced from recycled products (such as sewerage sludge and blood & bone) the great majority are derived from mineral deposits known as Reactive Phosphate Rock (RPR).[5]

1.1.2 Reactive Phosphate Rock

A loosely defined rock type rock phosphate may originate from guano, sedimentary deposits from ancient sea beds, as well as igneous and metamorphic deposits. Phosphate minerals are generally deposited along with other rock types, giving rise to a large variation in appearance and composition of phosphate rocks.

Rock phosphates are classified by their reactivity to acid (usually citric or formic). Rock phosphate which dissolve to a significant degree in acid are classed as Reactive Phosphate Rock (RPR). The chemical basis for this reactivity is

carbonate substitution for phosphate within the calcium phosphate lattice.[6] Higher rates of carbonate substitution lead to higher reactivity.

RPR can be applied directly to the soil as a fertiliser.[7] Acids in the soil react with RPR to release phosphate ions. In this form phosphate availability is low, especially in pH neutral or alkaline soils. To increase phosphate availability rock phosphate is commonly treated with sulphuric acid to make single super phosphate. Further processing can occur to produce higher value fertilisers. Untreated RPR is used by organic farmers who are not permitted to use "artificial" fertilisers. It is also used in situations where are slow release of phosphate is preferred, such as where nutrient run off into waterways is of high concern.

Rock phosphate varies considerably in its appearance, chemical reactivity and elemental composition. It contains Calcium Phosphate in the form of Apatites; hydroxapatite and fluorapatite are the most common forms. Various other minerals may be present, typically significant quantities of Silicon, Iron and Aluminium along with a variety of trace elements. Some of these, including Uranium, Fluorine and Cadmium, are of concern for their toxicity. Of the contaminants found in rock phosphate Cadmium has been identified as the greatest threat to human and environmental health.[8]

1.1.3 Cadmium: Toxic Contaminant

Cadmium is a toxic, carcinogenic heavy metal.[9] It does not have any known biological function but is absorbed from the soil by plants and from there enters the food chain. In animals Cd is excreted slowly and accumulates in the internal organs, especially the kidneys. Due to the risk of accumulated Cd New Zealand law prohibits the sale of offal from animals over 30 months old. Cadmium can also enter the body via contaminated air or water, and from cigarette smoke. Acute cadmium poisoning damages the liver and kidneys, if cadmium is inhaled as a dust lung damage can occur. Chronic poisoning leads to impaired kidney function, softening of the bones and heightened incidence of cancer. Treatment of cadmium poisoning depends on the severity and the route by which the cadmium was ingested. Chelation with EDTA increases the rate at which Cd is excreted but also raises Cd levels in the kidneys, risking renal failure. In many cases there is no effective treatment.

Cadmium shows low mobility in soil. Continued application of contaminated fertiliser causes soil Cd to accumulate. In soil contaminated by repeated fertiliser application most of the cadmium remains in the surface soil, migration to lower soil strata or removal by run off are slow.[10] Waste water contaminated with cadmium is another area of concern. In some parts of the world sewage sludge spread on agricultural land is a significant source of cadmium contamination.[11] Research into removing Cd from contaminated water has considered a range of adsorbents

from phosphate rock[12] to recycled shellfish waste[13] to synthetic nano particles.[14] Improper disposal of industrial cadmium waste is another significant source of contamination. Cadmium pollution from mining waste in the Jinzu and Kakehashi rivers of Japan resulted in hundreds of cases of Itai-itai disease, the result of chronic cadmium poisoning.[15] The legal and legislative action that followed had far reaching implications for the responsibility of industry towards environmental and human health.

The dietary cadmium intake of New Zealanders is monitored through the New Zealand Total Diet Survey (NZTDS). The NZTDS was last conducted in 2016 and the results published in 2018.[16] The survey purchased, prepared and analysed around 130 foods representative of 90% of the total dietary intake of the New Zealand population. Foods were analysed for their nutritional content as well as a range of contaminants including agricultural chemicals, aluminium, arsenic, cadmium, lead, mercury and tin. Cadmium intake was broken down by age group, gender and food type. The food containing the highest Cd levels was oysters, though the survey notes that oyster intake varies considerably between individuals, with many people reporting that they never eat oysters. Mussels also had considerably elevated levels of Cd compared to other seafood and meats. Other foods contributing significantly to Cd intake include potatoes and bread. Overall the NZTDS concluded that New Zealand dietary cadmium intakes had remained stable over the preceding 20 years and were within World Health Organisation guidelines for cadmium exposure.

1.1.4 Fertilisers through History

Since ancient times farmers have fertilised their fields by spreading manure. By the middle ages it was recognised that crop rotation with beans improved yields of the subsequent crop, though the nitrogen fixing properties of legumes would not be fully understood until centuries later. In the late eighteenth to early nineteenth century the science of soil chemistry rose to prominence. Spurred by the desire of farmers and landowners to increase their yields the craze for "improving" combined advances in soil chemistry, agricultural machinery, drainage, irrigation, crop rotation, the introduction of novel crops (such as turnips for winter animal feed) and animal husbandry. The combination of many different approaches to increasing agricultural outputs gave rise to the modern science of agronomy. This took place alongside the social upheavals of the industrial revolution and the land reforms (enclosure of the commons) which resulted in a massive shift of population and labour to urban areas, while agricultural land came under the control of a far smaller number of people. More than ever before the focus of farming moved away from subsistence to a drive for profit and maximising productivity.

Nitrogen, in the form of nitrate, was identified as the most important element

for stimulating plant growth. Championed by Humphry Davy and other leading figures Peruvian guano emerged as the most sought after nitrate fertiliser of the time. Guano is the petrified build up of bird or bat droppings, most prominently found on rocky ocean island where large sea bird colonies nest.[17] Guano varies in potency by its location, in areas with high rainfall much of the nitrogen leaches out into the water.[18] Demand for guano soared and production was expanded to many other locations around the world. The nineteenth century guano trade altered the wealth of nations, it led to increased agricultural output and food security, and stimulated global trade. It also fuelled war, slavery and imperialism as previously valueless rocky islands were captured and exploited for their guano reserves.[19] Towards the end of the nineteenth century deposits of sodium nitrate or "Chilean saltpeter" became another important source of nitrate fertiliser.[20] In the twentieth century guano was supplanted by synthetic nitrate fertilisers. The Haber-Bosch process of converting nitrogen and hydrogen gasses to ammonia, first used on an industrial scale in Germany in 1913, allowed nitrate fertilisers to be produced artificially.[21] The scalability, low raw materials cost and high product quality of the Haber-Bosch process more than made up for the significant energy input required.

After nitrogen phosphorus was identified as the next most important element for plant growth.[22] The first phosphate fertiliser was bone meal. This waste product of the meat industry was crushed and returned to the soil, recycling its mineral content. The idea of increasing phosphate availability by reacting phosphate minerals with sulphuric acid was raised by German scientist Justus von Liebig in 1840. The first super phosphate fertiliser was patented by English agricultural scientist John Lawes in 1842. Lawes used pot plants and farm trials to test the effects of fertilisers on plant growth. He showed that bone meal treated with sulphuric acid was more effective in stimulating plant growth than untreated bone. As its use as a fertiliser increased demand for bones soon outstripped supply so increasingly novel and gruesome sources were found. The battlefields of Europe were picked clean, even Egyptian mummies were ground up for fertiliser. Eventually phosphate rock overtook bone as the major source of phosphate fertiliser.

Other important plant nutrients include Potassium, Sulphur, Magnesium and Calcium.[23] Potassium was originally obtained from the ash of burned wood or other plant matter. The element's name derives from potash or pot ash, from the method of producing potassium carbonate by leaching wood ash with water then evaporating the solution in iron pots. Potash has been an important product since the Bronze Age, used in the making of soap, textiles, glass and ceramics. Today potassium is mined from mineral deposits formed from ancient dried sea beds. Today KCl, KNO_3 and K_2CO_3 are used as fertilisers.[24] Sulphur can be used as a fertiliser in either its elemental form or as sulphate salts.[25] Today sulphur is produced as a by-product of the oil and gas industry, where it is removed as part of the refining process. Sulphuric acid can also be used agriculturally as a desiccant

which also has the secondary effect of a fertiliser. This use of sulphuric acid is in decline due to concerns over operator safety and to help meet pesticide reduction targets. As the amount of sulphuric acid required to desiccate a crop is relatively high switching to another product can dramatically reduce the gross amount of agrochemicals used. Of course, the actual environmental impact of agrochemical use cannot be calculated in such a simplistic way. Magnesium is found at the active site of chlorophyll and so is essential to all plant life.[26] Magnesium can be applied either as a highly soluble salt, such as $MgSO_4$ or as the low soluble MgO.[27] Magnesium deficiency can be a problem in farm animals, $MgCl_2$ is used as a supplement in their drinking water. Calcium is usually added to soil as lime ($CaCO_3$) to raise pH. Soluble Ca salts such as $Ca(NO_3)_2$ are also used in some situations, especially in hydroponic growing where there is no soil to provide a reservoir of Ca.

In the nineteenth century colonial New Zealand was settled, mainly by British immigrants, many of whom intended to farm. Cleared land was developed into pasture. Along with native grasses and tussock English grasses and clover were introduced by the mid eighteenth century. Clover remained the most important source of nitrogen to New Zealand pasture, reducing the need for costly guano or synthetic fertilisers. Even today clover is vital to New Zealand farming.[28] Although urea is used in large quantity it is notable that New Zealand has no ammonium nitrate fertiliser production and, due to its hazardous nature, only small quantities are imported.[29]

The scientific study of New Zealand soils and farming was and continues to be of great interest to the country. In 1878 the Canterbury College School of Agriculture (now Lincoln University) was founded. Their research showed that super phosphate was highly effective in increasing the fertility of New Zealand soils. To encourage local super phosphate manufacture, the government offered incentives for the production of sulphuric acid. New Zealand's first super phosphate manufacturing began in 1882, in Burnside near Dunedin.

During the twentieth century agriculture changed dramatically. Mechanisation massively decreased labour demands, grand irrigation schemes turned deserts into arable land, glasshouses allowed seasonal crops to be grown year round. Led by Norman Borlaug the "Green Revolution" of the mid twentieth century saw plant breeders develop high-yielding disease resistant varieties, massively increasing crop yields.[30] Intensive agriculture requires more fertiliser input to sustain soil nutrient levels. Demand for fertiliser continued to climb worldwide throughout the twentieth century and beyond.[31]

Since the latter part of the twentieth century and into the twenty first century the use of fertiliser has come under scrutiny for its broader environmental impact.[32] Excessive or improper fertiliser use results in nutrient run off. When fertilisers find their way into waterways the ecological balance is disturbed. In most freshwater

and coastal environments the limiting nutrient for algal growth is either nitrogen or phosphorus. The process of waterways becoming enriched with nutrients and the resulting increase in algal growth is known as eutrophication[33].[34] A sudden or sustained increase in nutrient levels in a waterway can result in an unsustainably high level of algal growth, resulting in an algal bloom.[35] This can cause murkiness, shading of lower water levels and decreased oxygen levels. Some algae excrete toxins which can poison other aquatic life. The effects of an algal bloom can make water unfit for human consumption, force authorities to close fisheries and lead to mass fish die-offs.[36]

Debate over the use of fertiliser is also influenced by the Organic Farming Movement. Proponents believe that food grown in a more "natural" way, without the use of artificial pesticides and fertilisers, are healthier for both the consumer and the environment.[37] Exact rules vary by certifying authority but fertilisers manufactured using an industrial chemical process such as single super phosphate are not permitted on organic farms. In some areas, especially Europe, Organic farming has become very popular and the organic lobby has become a powerful political force. It has been instrumental in banning or restricting the use of many agri-chemicals. Organic farming is not immune to nutrient run off. To achieve high yields organic growers may apply large quantities of manure or fertilisers manufactured from manure and other recycled products. Demand from organic growers has seen the supply of guano increase in the twenty first century. However concerns for the well-being of sea bird colonies, which sharply declined in population during earlier guano mining operations, will limit the supply of this natural resource.

Technology has allowed farmers to optimise their fertiliser usage and so help prevent nutrient run off. Soil analysis is now affordable and readily available, allowing farmers to identify exactly what nutrients need to be added to their fields. Analytical surveys allow farmers to map the nutrient levels across their fields. Using GPS guided tractors and automated fertiliser delivery systems optimal fertiliser dosing can be applied to all areas. Drone photography can be used to monitor crop health and to locate damaged fences and areas where animals are able to access waterways, another major cause of eutrophication.[38] Fertigation (applying soluble fertiliser with irrigation) allows farmers to deliver fertiliser at the optimal time for plant growth, minimising run off as the nutrients are rapidly absorbed by growing plants.[39] Advances in manufacturing produce fertilisers with controlled nutrient release, again reducing the risk of run off.

1.1.5 Fertiliser Labelling

Fertiliser labels show the composition of their contents as weight percentages of nitrogen (N), phosphorus (P) and potassium (K) - the three most important

"macronutrients" which plants require in relatively large quantities. This is known as the NPK ratio. The format in which these numbers are written can vary but the order is always consistent. For example single super phosphate typically contains 0% nitrogen, 9% phosphorus and 0% potassium giving an NPK ratio of 0:9:0. The nutrient ratio is sometimes extended to cover sulphur, magnesium and calcium. Further elemental analysis may be provided, listing individual elements and their weight percentage. A large number of elements are required by plants in small quantities and fertiliser manufacturers often promote the "micronutrient" content of their products.

NPK labelling is not an indication of molecular structure, it is possible for fertilisers to have the same NPK ratio but dramatically different chemical and physical properties. For example, nitrogen can be delivered in the form of urea; a crystalline organic solid, or as ammonia; an inorganic gas.

Most fertilisers meet at least one criterion for classification as a hazardous substance. Fertiliser labels contain hazard information concerning transport, storage and handling as required by law. In New Zealand fertilisers are classified and labelled according to the United Nations Transport of Dangerous Goods-Model Regulations (TDG) and the United Nations Globally Harmonized System (UN GHS), as applicable. Fertiliser suppliers are required to maintain Material Safety Data Sheets (MSDS) for all their products.

1.1.6 Cadmium Contamination on New Zealand Farmland

Prior to the 1990s most of the RPR imported to New Zealand came from the Pacific island of Nauru. The exhaustion of Nauru's phosphate reserves around 1990 coincided with an increased awareness of the impact of Cd contamination in phosphate fertiliser. The guano based Nauru RPR was particularly high in cadmium. As a result of decades of applying highly contaminated super phosphate many New Zealand farms showed high levels of Cd in their soil.[40] In response to concern over cadmium levels in farmland the New Zealand fertiliser industry adopted voluntary maximum Cd levels for phosphate fertiliser. Initially set at 420mg Cd/kg P in 1995, the limit was reduced to 340mg Cd/kg P in the same year and then to 280mg Cd/kg P in 1997 where it remains as of 2022 (the year of writing this thesis). Cd levels in New Zealand fertiliser are monitored by the Fertmark program, which analyses fertiliser samples from manufacturing plants. Cadmium levels are also monitored in New Zealand farm soils. Soil Cd levels fall within five "Tiers" (Tier 0 to Tier 4) which determine what if any restrictions on the application of phosphate fertilisers apply to that farm (Table1.1). Tier 0 represents natural background levels of Cd and Tier 4 heavy contamination. Type of farming also affects cadmium risk. Cropping and meat farming are of high risk while dairy is considered lower risk as relativity little cadmium is passed into the

milk. Nonfood crops such as forestry can be grown at high contamination levels.

Tier	Soil cadmium (ppm)	Management Required
Tier 0	<0.6	Within natural background levels. No restrictions on phosphate fertiliser application.
Tier 1	0.6 to <1.0	1^{st} stage restrictions
Tier 2	1.0 to <1.4	2^{nd} stage restrictions
Tier 3	1.4 to <1.8	3^{rd} stage restrictions
Tier 4	≤ 1.8	No more Cd without site specific investigation and risk assessment

Table 1.1: NZ voluntary Tiered Fertiliser Management System

Cadmium levels in RPR vary widely depending on the geographic origin of the mineral deposits. Even within the same deposit there can be significant differences in Cd concentration. Phosphate rocks are tested for their Cd levels, which along with total phosphate content and reactivity define the rocks' suitability for use as a fertiliser and therefore its commercial value. Fertiliser manufacturers must source RPR that meets the regulatory requirements for cadmium concentration in their area.

1.1.7 Manufacture of Phosphate Fertiliser

The most commonly used phosphate fertiliser in New Zealand is single super phosphate (SSP), also known as super phosphate or super. SSP is manufactured by applying sulphuric acid to rock phosphate. The process if simple, fast, and low cost. Rock phosphate is crushed to a fine sandy consistency and assayed for its phosphate content. A measured amount of sulphuric acid is applied and mixed. Apatite is converted to calcium sulphate (gypsum) and mono calcium phosphate $Ca(H_2PO_4)_2$. Mono calcium phosphate (MCM) is far more soluble in water that apatite. The resultant single super phosphate fertiliser has a sandy consistency and of variable colour, from dark grey to brown. During manufacturing care must be taken to apply the right amount of sulphuric acid and to avoid excess moisture. Too much water results in a sticky SSP that is difficult to spread mechanically onto the soil. As a result of this simple and efficient manufacturing process SSP is one of the cheapest fertilisers available. SSP is also a source of sulphur, which is deficient in many New Zealand soils, making it even more attractive as a fertiliser. Due to its low cost, wide availability and high agronomic effectiveness, single super phosphate is used extensively by New Zealand farmers.

To achieve even higher phosphate levels rock phosphate can be treated with phosphoric acid to form triple super phosphate (TSP). Double super phosphate (DSP) is the result of treating rock phosphate with a mixture of sulphuric and phosphoric acids. Phosphoric acid can also be reacted with ammonium to form di-ammonium phosphate (DAP). These and other phosphate compounds are blended with other fertiliser stocks into a vast array of commercial fertiliser products tailored to a multitude of different agronomic requirements.

1.1.8 The Future of Phosphate Fertiliser

With an increasing global population and demand for food driving the trend towards more intensive farming practices it is clear that demand for phosphate fertiliser will continue to rise. This in turn will increase demand for reactive phosphate rock. Awareness of the environmental and health effects of cadmium by governments and peoples will lead to further tightening of restrictions on Cd levels in fertiliser. An effective method to remove cadmium from rock phosphate would benefit human and environmental health while also increasing the supply of rock phosphate suitable for fertiliser production. Such a method must be effective in significantly reducing cadmium levels, be compatible with existing fertiliser production, be scalable, have low environmental impact and finally have a low enough cost to justify its implementation.

1.2 Removing Cadmium from Reactive Phosphate Rock

There are two approaches to removing cadmium from phosphate fertiliser. The first is to produce phosphoric acid and remove Cd in the solution phase. This method is effective and is in use commercially. The waste product of phosphoric acid production, phosphogypsum, is considered hazardous due to low level radioactivity. In the USA phosphogypsum has no approved use and so is stored in giant "stacks" covering many hectares.[41] By contrast for single super phosphate the gypsum produced by reaction of rock phosphate with sulphuric acid remains with the fertiliser and helps provide sulphur to the soil.

The second approach is to remove Cd from rock phosphate prior to super phosphate production. Leaching with an aqueous solution has been researched, often employing chelating agents to assist in the extraction of Cd. A suitable extracting agent must be effective in removing cadmium without dissolving a significant amount of phosphate. A variety of extracting agents have been tested including EDTA, ascorbic acid and hydrochloric acid.[42] The effects of concentration, temperature, liquid to solid ratio and contact time were examined.

Methods of improving leaching efficiency have also been studied. These include a serial extraction and microwave radiation.[43] Using microwave heating could potentially speed up or increase extraction efficiency while serial extraction usually results in higher extraction efficiency for a given volume of solution used. Another enhancement method studied is electrodialysis;[44] using electrical potential to facilitate the transport of Cd^{2+} ions from a dilute solution to a more concentrated one. This could both drive the extraction of cadmium ions from rock phosphate and decontaminate the primary extraction solution.

1.2.1 Removal of heavy metals by Calcium ion exchange

Calcium ions have been studied for their potential to displace heavy metals, including cadmium, from contaminated soil.[45] The working principal is that heavy metals typically bind to receptor sites on or within soil particles. Calcium ions displace other metal ions by competitively binding to receptor sites. The degree to which calcium ions will replace other metal ions depends on the relative affinities of the ions towards receptor sites, calcium ion concentration and the chemical and physical properties of the soil.[46] Calcium is an attractive candidate for ion exchange solutions as it is tolerated at high concentrations by environmental and biological systems, is economical and readily available.

1.3 Mussel Shells; Waste to Recycled Resource

1.3.1 Shellfish Farming: A Sustainable Protein Source

Aquaculture is the farming of water based life forms. Practised since ancient times aquaculture was developed in ancient Greece, Rome, China and Egypt. Artificial lagoons for fish farming were constructed in Hawaii at least 1000 years ago and there is evidence that Aboriginal Australians were using aquaculture as far back as 8000 years ago.[47] As well as food fish are also farmed for ornamental purposes. Cultured pearls revolutionised the pearl trade.[48] Goldfish, once reserved for Chinese emperors, became a popular pet world wide.

Today as through history the attraction of aquaculture is that it provides a stable and reliable source of fish and shellfish, compared to the unpredictable and often dangerous practice of fishing. In the late twentieth century as overfishing became a global problem aquaculture has increasingly become a source of sustainable seafood. Wild fish stocks are no longer able to provide for worldwide demand for seafood. Aquaculture, when conducted responsibly, can produce large quantities of sustainable food. Over the past 30 years aquaculture has undergone tremendous growth worldwide. In 1986-1995 the average global aquaculture production was 14.9 million tons per annum, representing 14.6% of the total seafood industry. In 2018 aquaculture production had risen to 82.1 million tons, 46% of the total seafood industry.[49] Over the same period capture fishery production rose from 86.9 to 96.4 million tons per annum. In 2017 only 65.8% of world fisheries were considered to be harvested sustainably, down from 90% in 1970. As world demand continues to increase it is clear that the aquaculture industry will continue to grow, likely becoming the largest source of seafood worldwide within the decade.

In the New Zealand aquaculture industry three species account for the great majority of production. These are Greenshell mussel *Perna canaliculus* (also known as Green lipped mussel), King Salmon *Oncorhynchus tschawytscha* and

Pacific Oyster *Crassostrea gigas*. Greenshell mussel farming is New Zealand's largest aquaculture activity both in terms of revenue and tonnage. In 2020 a total of 101657 tons of greenshell mussel was harvested, for a total revenue of $377 million, of which $332 million was from exports.[50] Muscles are exported in a variety of forms, the most popular being a frozen half-shell product, accounting for 64% of revenue.

Mussel Product	% Export Revenue 2020
Frozen Half-Shell	64%
Mussel Oil	13%
Frozen Whole	6%
Frozen Meat	5%
Powder	4%
Live	4%
Other	5%

Table 1.2: NZ Greenshell Mussel exports by products

New Zealand Greenshell mussel farming is noted for its high productivity and low environmental impact. Greenshell mussels have many desirable characteristics for aquaculture. They grow rapidly, have few natural predators, are able to thrive at high population density and are immobile - the adult form stays anchored to the same spot. Difficulties associated with greenshell mussel farming are mainly due to the juvenile spat. Mussel spats float freely in the water until they find a suitable location to adhere to. Spats may attach and detach several times before settling on a permanent location.

Greenshell mussel spat is sourced by three methods. The oldest and still largest harvest is from seaweed covered in attached spat that washes up on Te Oneroa-a-Tōhē (Ninety Mile Beach). There is significant variation in the size of this harvest from year to year. Spat cannot live long away from their natural habitat so packaging and logistics must be carefully controlled. The unpredictable nature of beach harvested spat has led the industry to develop more controlled sources. Wild spat are captured using specially made ropes suspended in the sea in areas with high spat concentration. This method is also variable in terms of supply but since spat are collected from multiple locations the overall risk is reduced. In 2015 SPATNZ, the first commercial greenshell mussel hatchery, began operations. Located near Nelson, SPATNZ breed mussels and raise their spat in a controlled environment. Rearing spat in a hatchery has several advantages. Spat grow faster and more evenly under controlled conditions allowing for the supply of optimal sized spat to farmers. This increases the survival rate of hatchery spat compared to wild spat. Hatcheries are also less susceptible to disease, weather conditions

and environmental hazards than wild capture. Selective breeding of greenshell mussels is another growing research area and one that naturally aligns itself to hatchery production. Historically greenshell mussel spat proved difficult to raise in hatcheries, this and the relatively low cost of wild spat created a barrier to development. Today the NZ mussel industry has ambitious plans for growth and recognises that an increased investment in hatchery spat is necessary to ensure high quality and sustainable spat supply to farmers.

Farmed Greenshell mussels are grown on long culture ropes suspended in seawater. Spat are seeded by placing the spat and seaweed inside a biodegradable cotton mesh stocking "mussock" surrounding the culture rope. Spat then relocate themselves to the rope. Many spat do not adhere to the rope or later release themselves and are lost. Spat losses at greenshell mussel farms are high, it is estimated that only 5% of spats survive through to harvest.

New Zealand greenshell mussel farming is noted for its low environmental impact, both compared to other forms of aquaculture and to other animal protein foods in general. As filter feeders mussels extract food from naturally occurring plankton floating in the water. Unlike many other forms of aquaculture mussels do not require supplemental feeding with fish or plant based products. Mussel farms are a net absorber of nutrients, so they do not contribute to eutrophication. Strict resource consent requirements demand that New Zealand mussel farms minimise their environmental impact. This places controls on the building of structures in the water, use of materials and on farming activities so that disturbance to the seabed and to other aquatic life is minimised. Biosecurity requirements are strictly enforced as both the government and industry recognise that maintaining biosecurity is essential to preventing damage to the environment and the seafood industry. New Zealand greenshell mussels have received international recognition for their sustainability. The Monteray Bay Aquarium Seafood Watch recommends NZ greenshell mussels as a "Best Choice" for seafood consumers.[51]

1.3.2 Waste Shells: Disposal and Recycling

Processing of greenshell mussels generates thousands of tons of waste shells every year. Disposal of waste shells presents a significant cost to the shellfish industry. Historically shells were often dumped back into the sea. This practice is now prohibited in New Zealand due to the risk of environmental damage and the spread of disease to shellfish populations. Disposal in landfill is common, but requires that the shells are first cleaned to prevent the foul odour of rotting seafood. Traditional disposal of shells in a designated pit or midden has been practised by shellfish eating societies all over the world. Māori shell middens are commonly found around the New Zealand coastline,[52] these provide valuable archaeological insight as well as helping to locate rua tūpāpaku (graves) and other sacred sites.

A more attractive alternative to waste shell disposal is recycling. There are several current commercial uses for waste shells. Egg farmers use crushed oyster shells as a calcium supplement for laying hens.[53] Shells are sold as a landscaping material for garden paths, flower beds and other decorative uses. Crushed shells are also marketed as a mulch or soil conditioner for gardens. Some types of shell are processed for nacre (mother of pearl), which has many ornamental uses.

1.3.3 Proposed Uses for Waste Shells

Though there are already a variety of recycled shell products on the market the supply of waste shells still far exceeds demand. A number of alternative uses for waste shells are currently being investigated or developed. Using crushed shells as a aggregate in cement has been trailed.[54] As shells are primarily composed from calcium carbonate in the form of aragonite they can also be used as a feedstock for producing lime (CaO and $Ca(OH)_2$). This practice has been used historically, for example in colonial North America oyster shells were used to produce lime mortar in the coastal Maryland/Virginia region.[55] As well as its use in construction lime is used as a filtration material, to correct pH in water treatment and in sugar refining. Crushed shells could potentially be used as a source of agricultural lime ($CaCO_3$) for use as a soil conditioner. $CaCO_3$ is also used as a "scrubber" at coal fired power stations, it is injected into the exhaust stream where it reacts with and removes pollutant SO_2 converting it to harmless $CaSO_4$.[56]

1.4 Extracting Heavy Metal from Rocks

Removal of heavy metals from rock has been practised and studied for thousands of years, the main application being metal mining. There are two main methods used: calcination and leaching.

1.4.1 Calcination

Calcination is the process of heating a solid substance, within a controlled atmosphere, in order to drive off a substrate. Calcination takes its name from the oldest and most common application: the manufacture of lime.[57] Here calcium carbonate is heated strongly to drive off carbon dioxide gas, leaving calcium oxide. Mercury is produced by calcination; when mercury ore is heated elemental mercury vapour is released, the vapour is then condensed and liquid mercury is collected. Prior to the availability of mineral acids the calcination method of salt cementation was used to separate gold from silver. Gold - Silver alloy was mixed with salt (NaCl) and other minerals then heated, causing the silver to be converted to volatile silver chloride.

Researching the potential of using calcination as a method for removing cadmium is unattractive due to high energy input required, the possibility that high temperatures may degrade or alter the RPR, and the difficulty and hazards of recovering a heavy metal from the vapour phase.

1.4.2 Leaching

Leaching is the process of soaking or washing a solid substance causing the target substrate to move into the liquid phase. There are several methods of extracting gold by leaching. Historically mercury was used, extracting gold as an amalgam. From the nineteenth century cyanide solutions have been used to extract gold as a water soluble complex. These methods both rely on highly toxic chemicals with the potential to cause significant damage to the environment and human health if mishandled.

Leaching has been investigated as a method of remediating cadmium contaminated agricultural land.[58] Cadmium shows low mobility in contaminated soil, remaining in the surface soil strata. This indicates that cadmium ions bind strongly to surface soil particles, possibly due to a high affinity for organic acids in the soil. Leaching techniques investigated for removal of cadmium from surface soil include use of chelating ligands such as EDTA to extract Cd ions as a soluble complex, and the use of calcium ion solutions to displace Cd by competing for binding sites.

Research into leaching of cadmium from contaminated soil parallels that of removing cadmium from reactive phosphate rock. However, the different nature of

the chemical binding of Cd ions within soil and RPR means it may be difficult to apply results from one to the other.

1.4.3 Heap Leaching

Heap leaching is a process used to extract soluble species from large quantities of porous solid material.[59] Heap leaching is used for the extraction of gold, copper, nickel and uranium. A typical set up consists of a large pile of crushed ore sitting on top of a watertight plastic liner. The leaching solution is introduced to the top of the ore heap, usually via drippers, it then percolates down through the ore and the "pregnant" solution is collected from the lining at the bottom. Often tailing or other low yielding ores are used for heap leaching due to its low cost and scalability. Heap leaching is a slow process, cycle times typically vary from one month to two years depending on the type of ore.

A bench test of heap leaching principles was set up using chromatography columns filled with RPR. Solutions were then added to the top of the column and allowed to percolate through the RPR. Contact time could be controlled by adjusting the column tap, covering the top of the column to prevent air pressure in the top of the column from equalising and using different plug materials to reduce flow rate. In this case the solution itself was analysed, if Cd levels increased after passing through the RPR column that would be considered as evidence of leaching.

1.4.4 Leaching Phosphate Losses

Leaching of reactive phosphate rock will result in some phosphate dissolving into solution. An ideal leaching solution would remove cadmium along with only a negligible amount of phosphate. Excess phosphate removal both devalues the treated RPR and further complicates the process of disposal or recycling of the used leaching solution. Measuring the phosphate concentration of the leachate assesses this aspect of its suitability.

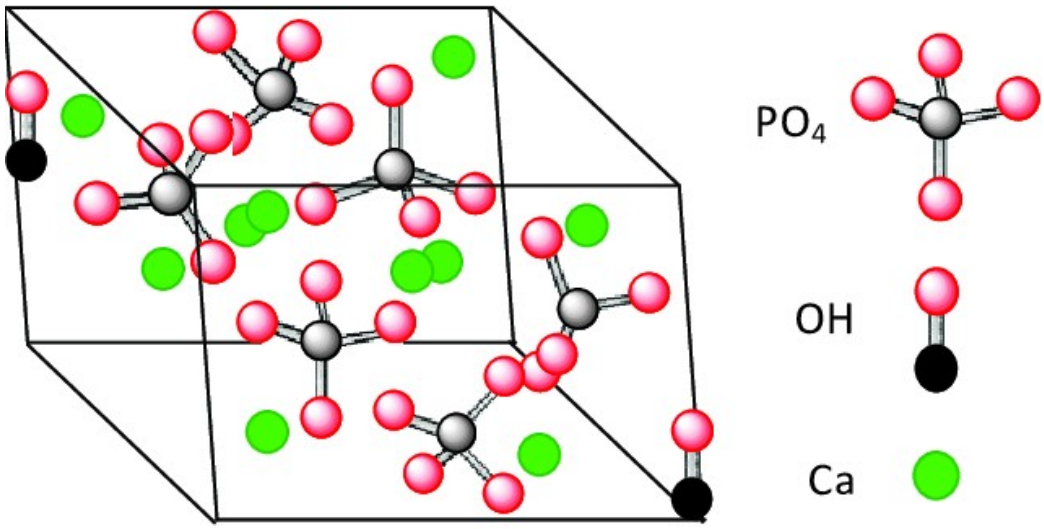

Figure 1.1: Unit cell of hydroxyapatite crystal.[1]

1.5 Ion Exchange in Apatites

Apatites are crystalline calcium phosphates with a general formula $Ca_5(PO_4)_3.X$, where X is the endmember,[60] as shown in Fig.1.1. Common endmembers are OH^- (hydroxyapatite), F^- (fluorapatite), Cl^- (chlorapatite) and CO_3^{2-} carbonate . Endmembers influence the chemical reactivity and physical properties of apatites. Apatites are found in a variety of minerals as well as the bones and teeth of animals. Apatites are noted for their ability to exchange both anions and cations from solution. Research into apatite ion exchange is of interest to a wide range of applications; including medical implants,[61] protein purification,[62] industrial catalysts and absorbents for removing heavy metal contamination.[63]

A public health application of apatite ion exchange is fluoridation of drinking water.[64] Tooth enamel is primarily comprised of hydroxyapatite. Exposure to fluoride ions in the mouth causes partial endmember substitution, converting some hydroxyapatite to fluorapatite. This hardens the enamel and helps prevent tooth decay. Fluoride is generally introduced through toothpaste and by fluoridation of municipal water supplies. In some areas excess fluoride is present in drinking water, generally from geogenic sources. This can lead to skeletal fluorosis, a potentially crippling disease.

As well as endmember subsitution the porous structure of apatite allows for exchange of Ca^{2+} and PO_4^{3-} ions with a variety of different anions and cations from solution. Notably carbonates are able to exchange with both the

endmember and phosphate positions, classified as A-type and B-type carbonates respectively. Carbonate exchanges more readily with the phosphate position under mild conditions whereas high temperature is required for significant endmember position exchange to occur.

The ability for apatites to exchange metal ions has lead to research into their use as absorbents for heavy metals. Apatites have shown potential for removal of a range of heavy metal contamination; including cadmium, caesium, strontium, uranium and plutonium. Apatites are able to reduce the levels of heavy metal ions contaminates in waste water by ion exchange with calcium.[65] This has potential uses in cleaning industrial and mining water prior to discharge and for removing heavy metals from sewage.

1.6 Experimental Techniques

1.6.1 ICP-MS

Inductively Coupled Plasma Mass Spectrometry (ICP-MS) provides an accurate and reliable analysis of a large number of elements with quantitation limits as low as 0.1 ppb.[66] ICP-MS is a mass spectrometry technique in which species are ionised using plasma generated by inductive heating of a gas (argon). ICP-MS contains two apparatus, an Inductively Coupled Plasma torch and a Mass Spectrometer.

The Inductively Coupled Plasma torch consists of three concentric quartz tubes surrounded by wire induction coils. The tip of the torch sits inside a vacuum chamber containing the mass spectrometer. High frequency electric current running through the coils induces a fluctuating magnetic field inside the torch. Charged particles within the fluctuating magnetic field oscillate rapidly, producing heat. The discharge gas (argon) flows through the outermost tube. A spark is used to initiate ionisation inside the torch then inductive heating increases the temperature to the point where some of the Ar atoms ionise, forming a plasma. Plasma is conductive so after the initial spark heat is sustained by inductive heating of the plasma itself. The inner most tube delivers the sample, along with argon carrier gas, to the centre of the plasma "flame". Sample species are ionised by the extreme temperature of the plasma. Between the inner and middle tubes another argon flow is used as a cooling gas to prevent the plasma from touching the top of the inner tube. The design of the plasma torch allows for temperatures far hotter than a chemical flame while maintaining precise control over sample ionisation inside the plasma. Samples are introduced to the carrier gas by nebuliser (for solutions) or vaporising (for solids, typically by laser ablation). Gaseous samples can be mixed into the carrier gas using appropriate valves and orifices.

Ions formed in the inductively coupled plasma are detected by mass spectrometer, a form of linear particle accelerator. An electric field accelerates ions towards the detector while a strong perpendicular magnetic field deflects their trajectory. Mass spectrometry detects ions by their mass to charge ratio. Lighter and more highly charged ions are deflected further.

In practice the vast majority of ions detected have +1 charge, formed by the loss of a single electron (first ionisation). Removing another electron (second ionisation) from an already positively charged ion requires significantly more energy. Having precise control over the plasma temperature allows ICP-MS to maximise the production of first ionisation ions with minimal secondary ionisation. For elements with high first ionisation energy, such as tungsten and osmium, helium may be used as the discharge gas instead of argon. Helium has higher ionisation energy than argon so produces a hotter plasma. The downside to using helium is higher cost, higher energy consumption and greater secondary ionisation of easily

ionised species. For these reasons argon is the preferred discharge gas for the majority of ICP-MS work.

Precise calibration of element detection is performed using standards of known concentration. Using Certified Reference Materials (CRMs) from accredited providers allows results to be compared with those from other ICP-MS facilities and for those results to be used for official purposes such as reporting to regulatory authorities or presenting in court.

Unlike other mass spectrometry techniques ICP-MS is able to receive a continuous sample injection. This allows for both very low detection limits (due to large samples) and for time resolved detection. For example the sample feed for ICP-MS can connect to Gas Chromatography (GG-ICP-MS) or Liquid Chromatography (LC-ICP-MS). Using laser ablation the composition of a solid object can be analysed by depth as the laser progressively digs into its surface. Continuous sampling also greatly speeds up throughput as multiple samples can be analysed in sequence without having to place samples individually inside a vacuum chamber and pump it down before each analysis.[67]

An advantage of ICP-MS over Atomic Absorption Spectrometry (AAS) is that ICP-MS is able to measure a large number of elements simultaneously. In contrast AAS can only measure one element at a time as the detector and flame must be adjusted for individual elements.[68]

A downside of inductively coupled plasma is that it produces many interfering species, especially Ar^+, ArO^+ as well as a multitude of other species arising from the sample.[69] For example selectivity of ^{56}Fe by ICP-MS is very low due to interference from ArO^+. Mixed samples can cause complex "matrix interference" as the sample species interfere with each other. One cause of matrix interference is the formation of polyatomic ions with masses that overlap with target atoms. Another is caused by changing the ionisation potential of an element compared to the standard. Matrix interference results in reading for elements being lower or higher than their true levels. A common example of matrix interference is the suppression of trace element signals in samples with high sodium concentration. Generally matrix interference increases with sample concentration in the plasma flame so can be controlled by reducing sample injection rates or using more dilute solutions.

1.6.2 UV-Vis Spectroscopy

Spectroscopy of Ultra Violet and Visible light (100 nm to 900 nm), is the most immediately accessible form of spectroscopy as most of the frequency range is visible to the eye. The energy of UV-Vis photons corresponds to many molecular electronic transitions. Electrons within a molecule are able to transition to a higher molecular energy level by absorbing a photon of corresponding energy. Electrons in

this excited state usually decay rapidly back to their original energy level, releasing one or more photos in the process. The overall result of this absorption and re-emission of photons is light scattering and an observed decrease in light transmitted through a material.

The relation between the concentration of a species in solution and its wavelength specific Absorbance is determined by the Beer-Lambert law[70] $A = \epsilon \ell c$ where A is absorbance: the logarithm of the ratio of incident light intensity to transmited light intensity, ϵ is extinction coefficient; a constant defining the attenuation strength of a species, ℓ is path length in cm, c is concentration in mol L^{-1}. Since the human eye can perceive brightness logarithmically the intensity of light passing through a coloured solution appears to be directly proportional to its concentration.

UV-Vis absorbance peaks of solutions are characteristically broad and smooth, small peaks often appear as "shoulders" on another nearby peaks. By comparison UV-Vis spectra of gasses peaks are typically narrower, and more fine structure may be visible.

A UV-Vis spectrometer consists of a light source, a monochromator, a sample path and a detector. Instruments vary considerably in design and operation, ranging from single wavelength to double beam scanning to CCD based instruments. The two principles of UV-Vis spectroscopy: colorimetry and diffraction were both developed separately before being combined into a single technology.

The oldest form of colorimetry is by visual comparison. Using a series of standards at known concentrations an unknown concentration is compared by eye. With a suitably coloured solution and the means to make accurate dilutions it is possible to determine concentrations by visual comparison to a surprising degree of accuracy. Extending this principle using an electronic light detector and a controlled light source is the basis of UV-Vis spectroscopy.

Separating "white" light into a monochromatic spectrum can be achieved using either a prism or a diffraction grating. Both are used in spectroscopy. Diffraction gratings allow for narrow wavelength bands while prisms can produce the entire frequency spectrum at once. The choice of monochromator depends on the type of detector used. Point detectors (photomultiplier tube) are generally paired with a diffraction grating, as found in most double beam instruments while area detectors (CCD) are generally paired with a prism. Double beam UV-Vis spectrometers can achieve excellent signal to noise ratio and frequency discrimination. Prism/CCD spectrometers allow very fast measurements of the entire spectrum and with no moving parts they can be used in many environments.

1.6.3 Particle sizing

Particle size is an important consideration for metal leaching. The size of RPR particles determines the surface area in contact with solution and is potentially an important factor in both the rate and efficacy of cadmium extraction.

Particle sizers use optical measurement techniques to determine the size of a population of small particles. Multiple different sizing techniques have been commercially developed to measure suspended particles, each suited to a particular range particle sizes and operator requirements.[71] For this project a Malvern Instruments Mastersizer 3000 was used. This instrument is able to measure the size of particles dispersed in a liquid over a broad range from 0.01μm to 3500μm. The Mastersizer works on the principle of laser light scattering. Inside the instrument laser light passes through the sample cell containing dispersed particles. Light is scattered by the particles and is detected by an array of sensors. By measuring the angle and intensity of light scatter through the sample cell particle size and concentration can be determined.

The optical properties of different materials vary greatly. Refractive index and absorption index of a material strongly effect the way light is scattered by a sample. The Mastersizer uses internal calibration files for a variety of different particle types. In order to obtain accurate results either the general composition of the particles must be known or its optical properties measured before using the Mastersizer.

1.6.4 FTIR Spectroscopy

FTIR (Fourier Transform Infra Red) Spectroscopy is an analytical method for measuring the absorption of infra-red light by a sample. FTIR spectroscopy is used to identify compounds by their molecular vibrational modes. Photons in the mid-IR spectral band (400-4000cm^{-1}) correspond to the energy of many molecular vibrational modes. There are two types of molecular vibrations: stretching and bending, corresponding to vibrations in length of a molecular bond (stretch) or vibrations in the angle between bonds (bend). FTIR spectra are highly specific to their compounds. It is often possible to identify an unknown substance by its IR spectrum. FTIR spectroscopy is also highly sensitive, only small quantities are required and detection of contaminants is possible at a relativity low level. Due to its high selectivity and sensitivity FTIR spectroscopy is widely used in both research and industry.

Only vibrational modes that result in a change in molecular dipole moment are observable by FTIR. This empirical rule can be formalised by quantum mechanics, the results give a set of selection rules which determine which transitions are "allowed" and which are forbidden. In many cased vibrational modes which are IR

forbidden can be observed using Raman spectroscopy, which has different selection rules).[72]

1.6.5 X-ray Fluorescence Spectrometry (XRF)

Fluorescence is the absorption an re-emission of electromagnetic radiation (light) by matter. Generally the re-emitted light is of longer wavelength (lower energy). The intensity and energy of florescent emissions are characteristic of the irradiated atoms/molecules.

Fluorescence usually results in emission of photos of lower energy than the absorbed photos. This occurs when an orbital electron absorbs photon energy, boosting them from their resting energy level (ground state) to a higher energy level (excited state). The electron then decays back to the ground state via a combination of non-radiative and radiative transitions. As some of the electron's energy is lost in a non-radiative way the emitted photon is of lower energy than the absorbed photon.

X-ray fluorescence uses high energy x-rays or gamma rays to energise a target. This high energy electromagnetic radiation causes ionisation by energising electrons enough to eject them from an atom/molecule. When an inner orbital electron is lost due to x-ray ionisation the "hole" is rapidly replaced by an electron from a higher energy outer orbital. This transition between orbitals releases a photon, with wavelength equivalent to the difference in energy between the two orbitals. The spectral lines are classified by the starting and finishing orbital of the transitioning electron. Manne Siegbahn, a Swedish physicist who was awarded the Nobel prize for his work in X-ray spectroscopy, developed the notation. Fluorescence peaks for each element are labelled in order of photon energy. K lines have the highest energy (corresponding to electrons ejected from the first electron shell), L lines (second electron shell) have the next highest energy, M lines and further lines follow in alphabetical order. Siegbahn notation pre-dates the SPDF orbital model, it becomes cumbersome to use when trying to match up complex spectral lines to their orbital transitions. To address this IUPAC notation, which combines Siegbahn line letters and orbital numbers in a systematic way, was introduced.[73]

As the number of orbital shells in an atom increases so does the number of possible XRF transitions. Since all detectable atoms show K lines these are generally the most useful when measuring the spectrum of a sample containing multiple elements. Software identifies the spectral lines by their wavelength and can compute the molar and weight percentage of each detected element by peak integration.

Light atoms are difficult to detect by XRF. The smallest species (H, He, Li^+) cannot be detected as they do not have available electrons in higher orbitals that

can replace a hole in the lowest orbital. Lighter elements produce lower energy fluorescence which is attenuated by air. Elements lighter than sodium are difficult to detect and are frequently excluded from analysis. By contrast, heavy elements are readily detected, making XRF an important tool for detecting heavy metal contamination.

XRF is considered to be a non-destructive analysis as the sample is not consumed however sample preparation requirements and exposure to x-ray radiation make it unsuitable for many sample types. XRF is widely used in earth sciences,[74] engineering and industrial applications to measure the composition of rocks, ceramics, glass, cement, paints and metals. Other users include forensic scientists, archaeologists, jewellers and art experts; XRF can be used to authenticate paintings by analysing paint composition.[75]

XRF instruments vary considerably in size, complexity and usage case. Ideally XRF measurements should be taken in a vacuum chamber to prevent signal loss from attenuation by air. The ideal sample shape is a flat disk, the thickness required depends on the composition; lighter elements require a thicker sample. This sample disk is rotated to minimise the effect of imperfect flatness. Measurement times of several hours may be required for maximum sensitivity. At the other end of the scale portable XRF instruments can be made small enough to be hand held. They can deliver results in seconds with irregular samples while providing enough precision for use in the field. X-ray radiation is most usually provided by a conventional X-ray generator (a high-powered cathode-ray tube). It is also possible to use X-rays from a synchrotron. Gamma rays from radioisotope decay are an alternative source of ionising radiation that do not require a power source, making them attractive for use in portable equipment.

1.6.6 Electron Microscopy

Electron microscopy is a technology that uses focused electron beams to create images.[76] Since accelerated electrons have much higher momentum and therefore much smaller Planck wavelengths than visible light electron microscopy is able to resolve much finer details than light microscopes. The diffraction limit of visible light means that ordinary optical microscopes cannot resolve features smaller than 200 nm. The most powerful scanning electron microscopes are able to resolve features smaller than 1 nm and transmission electron microscopes are able to resolve down to 50 pm.

There are two main types of electron microscope, Transmission Electron Microscope (TEM) and Scanning Electron Microscope (SEM).

TEM form an image by detecting electrons passing through a sample. Source electrons from an electron gun are focused on the specimen by a condenser lens. Electron lenses use magnetic or electric fields to steer the trajectories of

moving electrons. Electrons pass through the specimen and are then focused by a projector lens onto the detector. This technique can produce extremely high resolution but requires extremely thin specimens, generally less than 100nm thick. Specimens may also need staining with heavy metal ion solutions to provide image contrast. The high energy electron beam can damage specimens, especially from biological samples. Due to these limitations TEM is generally used at extremely high magnification, where SEM resolution is insufficient.

SEM energises the surface of a specimen using an electron beam scanning across a small area. The energised surface releases secondary electrons which are detected. The position of the scanning beam combined with the detected secondary electron counts builds up an image of the specimen surface. As secondary electrons have low energy they cannot penetrate far through matter. This means that although the primary electron beam may penetrate into a specimen only secondary electrons released very close to the surface will be detected. SEM instruments may feature additional detection modes as well as the standard secondary electron detector. Instruments are available to detect reflected (backscatter) electrons, measure current flow through a specimen and detect light emission from the energised surface.

SEM is able to create images of three-dimensional surfaces in extremely fine detail. The resolving power of SEM depends on the conductivity of the specimen surface. For many specimens a coating of gold or carbon is applied to increase resolution.

Energy Dispersive X-ray Analysis (EDX) is a spectroscopic technology used to analyse the elemental composition of specimens.[77] High energy electron colliding with atoms are able to cause ionisation, ejecting an electron from the atomic orbital shells. When the ejected electron comes from an inner orbital shell the hole left behind is quickly filled by an electron from an outer orbital. This electron transition releases energy in the form of a photon in the X-ray wavelength band. The elemental X-ray spectra of EDX are the same as those observed in X-ray Fluorescence (XRF) spectrometry. The difference being that ionisation is caused by collisions with high energy electron rather than absorption of X-ray radiation. See XRF section1.6.5 for further explanation of atomic X-ray spectra. SEM-EDX instruments use the SEM electron beam as the energy source for EDX analysis. The advantage of SEM-EDX is that the electron beam is extremely focused and it can be directed to precise locations on the SEM image. It is then possible to measure the elemental composition of very small areas of a specimen. With a RFR sample the composition of individual grains (approx. 0.1 to 0.4mm diameter) were measured. A limitation of SEM-EDX is that it is not possible to obtain meaningful EDX measurements with a metal/carbon coated specimen. For many specimens this means image resolution will be poor if EDX analysis is required.

1.7 Research aims

The aim of this Masters of Science project is to investigate the potential for the use of recycled mussel shells for reducing the cadmium content of reactive phosphate rock by ion exchange with aqueous calcium ions. The mussel shells will be used as a source of calcium ions. Flooding reactive phosphate rock with dissolved calcium ions may create conditions where cadmium ions in the RPR lattice are displaced into solution by calcium ions.

The main objectives of this study are:

- Characterise reactive phosphate rock using available analytic techniques.
- Study the effects of calcium salt solutions on RPR, test different concentrations, pH, temperature, contact time, anions, microwave heating and potential Cd^{2+} stabilising ligands. Use the results of these tests to optimise conditions for effective cadmium extractions. Initially calcium salts were used as to establish solution conditions that facilitate cadmium extraction.
- Study the stability of RPR when subject to these reaction conditions.
- Investigate the use of recycled mussel shells as a source of calcium ion solution. Prepare sample solutions by dissolving prepared mussel shell in acids. Compare the cadmium extraction potential of mussel shell solutions compared to standard calcium salt solutions.

From the results of these investigations we hope to establish whether calcium ion solutions have potential for use in extracting cadmium from reactive phosphate rock. We also hope to determine if recycled mussel shells have the potential to be a viable source of calcium ions for this purpose.

2. Experimental

2.1 General

Reactive Phosphate Rock and other fertiliser samples were provided by TerraCare, located in Te Awamutu, New Zealand. Samples were received in 2018. As of February 2022 TerraCare has merged with Fertco(Mt Maunganui); the TerraCare brand and many product names are no longer in use.

Greenshell mussel shells were supplied by North Island Mussels Ltd (NIML), located in Taurunga, New Zealand. Samples were received in July 2021. Shells were supplied coarsely crushed and were stored in a deep freezer.

All reagents were LR grade or higher.

UV-Vis spectra were recorded on a Cary 300 spectrometer.

FTIR spectra were recorded on a Perkin Elmar Spectrum 400.

ICP-MS analysis was performed by Waikato Mass Spectroscopy Facility.

SEM images and EDX analysis were recorded at University of Waikato School of Engineering - Electron Microscope Facility using a Hitachi S-4700 Field Emission Scanning Electron Microscope (SEM) with Quorum Technologies Cryo-system.

Powder XRD analysis was carried out using a Panalytical Empyrean XRD. Interpretation of results utilised HighScore software.

XRF analysis was carried out using a Bruker WDXRF S8 Tiger.

Particle sizing were recorded on a Malvern Mastersizer 3000.

Solution pH values measured on a Eutech Instruments pH 700.

2.2 Elemental Analysis of Reactive Phosphate Rock

Reactive Phosphate Rock samples were analysed for their elemental composition. Of particular interest was the ratio of Cadmium to phosphorus. Phosphate fertiliser is marketed and applied based on its phosphorus content, expressed as a percentage by weight. Since the amount of fertiliser required and therefore the amount of contaminate cadmium depends on the phosphorus content it is convenient to use the Cd:P ratio. By normalising cadmium to phosphorus content comparisons of the level of contamination can be made between different fertiliser types and samples. Since the amount of cadmium is fertilisers is very small compared to the amount of phosphorus the fertiliser industry uses the convention of multiplying the raw Cd:P ratio by one million. This means that unlike most ratios, which are completely dimensionless numbers, the Cd:P ratio is expressed in parts per million (ppm). This convention is used throughout this thesis. This unit of contamination is equivalent to mg Cd/kg P.

The fertiliser industry Cd:P ratio can be calculated using the following formula:

$$\text{Cd:P (ppm)} = ([\text{Cd}] \div [\text{P}]) \times 1000000$$

Where [Cd] and [P] are the mass concentrations of cadmium and phosphorus respectively. When comparing fertilisers care must be taken to ensure that the correct species are being measured. This thesis uses the New Zealand standard of reporting the mass of elemental phosphorus. Fertilisers manufactured in other countries often present the weight percentage equivalent of phosphate as PO_4 or P_2O_5. If this is case then it is necessary to use conversions.[78]

2.3 SEM-EDX

A sample of RPR was examined by Scanning Electron Microscope. The sample was not coated with carbon or platinum or otherwise treated before imaging. The RPR grain size was appropriate for the specimen stage so no other processing was required. RPR was applied to a conductive adhesive strip. The specimen holder was inverted to allow excess RPR to drop off. Specimen was then placed inside the SEM stage. An accelerating voltage of 20.0 kV was used and secondary electron mode. An SEM image of RPR was obtained and EDX was used to analyse the composition of 11 individual grains.

2.4 Particle size

As supplied RFR had a sandy consistency. Visually grain size appeared fairly uniform with the occasional larger pebble (generally under 5mm diameter). Larger particles could be broken up using a mortar and pestle but this appeared to be ineffective at reducing the size of the small grains. This was confirmed by measuring using a Malvern Mastersizer 3000 to measure the grain size of unprocessed and manually crushed RFR. Samples were suspended in water and measured. Dicalcium phosphate (refractive index 1.63) was chosen as a reference being the closest match chemically for RPR available from the standard values available in the software.

2.5 Phosphate UV-Vis Spectroscopy: Molybdenum Blue Complex

Phosphate concentrations were measured using UV-Vis spectroscopy via the molybdenum blue complex.[79] There are many different published methods for preparing molybdenum blue. The overall reaction consists of two steps. First molybdate ions coordinate around a phosphate ion under acidic conditions to form a Keggin ion. Second some of the molybdenum in the Keggin ion is reduced from Mo(VI) to Mo(V) producing an intense blue coloured complex. Several different reductants have been used, the exact nature of the complex and the absorbance peak vary depending on the reductant used. Despite these differences the linear relation between phosphate concentration and absorbtion peak intensity is still observed.

The method used here was based on a method for determining phosphate levels in soil samples,[80] with adaptation made for equipment used and sample preparation.

All glassware was washed with 1% nitric acid to remove adsorbed phosphate ion.

A standard ammonium molybdate solution was prepared. 0.25 g of ammonium molybdate was weighed into a 25 mL volumetric flask with about 10 mL distilled water. 8 mL of concentrated sulphuric acid was added. The flask was allowed to cool and filled to the mark with distilled water.

An ascorbic acid solution was prepared. 2.5 g of ascorbic acid was weighed into a 50 mL volumetric flask and diluted to the mark with distilled water.

Standard phosphate solutions were prepared. 0.220 g KH_2PO_4 was weighed into a 500 mL volumetric flask and diluted to the mark with distilled water, this gave a 300 ppm stock solution. Standard solutions of 3, 4.5, 6, 9, 12 and 15 ppm were prepared by pipetting 0.250, 0.375, 0.500, 0.750, 1.000 and 1.250 mL of 300 ppm stock solution into 25 mL volumetric flasks and diluting to the mark with distilled water.

To prepare the molybdenum blue spectroscopic solutions 0.2 mL of ammonium molybate standard, 0.5 mL of ascorbic acid solution, 1.5 mL distilled water and 1 mL of sample solution were pipetted into a test tube then heated for 20 min at 90°C in a block heater. For each standard solution two repeats were made. Two blank solutions were prepared using 1 mL distilled water in place of the sample solution. UV-Vis spectra were recorded on a Cary 300 spectrometer from 900-400 nm; plastic cuvettes; double beam mode, against blank solution. Recorded spectra showed a peak with maximum at 830 nm. There was also a weak shoulder peak around 600 nm. The location of these peaks was consistent between samples, only the intensity changed.

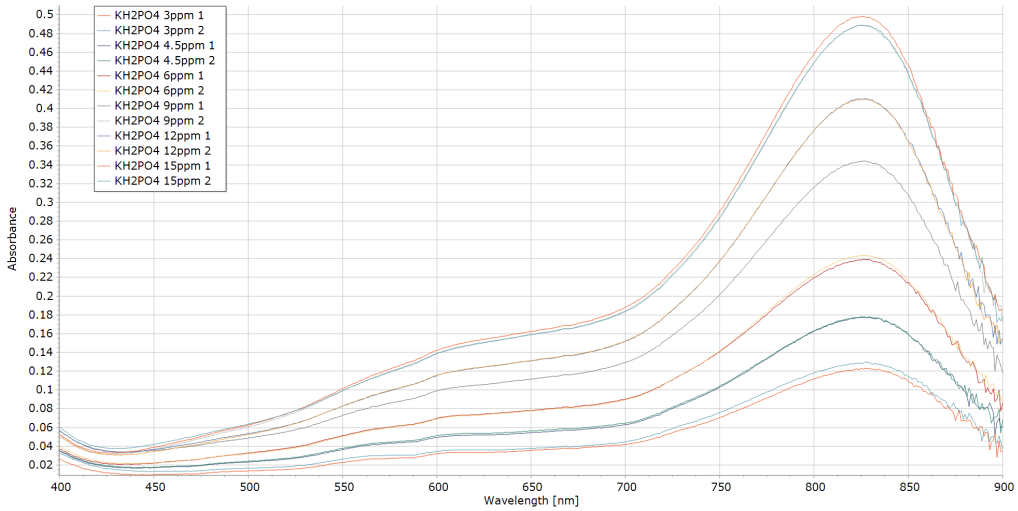

Figure 2.1: UV-Vis spectra of Molybdenum Blue Standards

Dilutions were made to sample solutions in order to obtain results that were within the boundaries of the calibration curve (3 ppm to 15 ppm). When sample solution absorbance was lower than the 3 ppm standard extrapolations were made. For this test precise determination of very low phosphate concentrations was not required as the aim was to determine at what pH value phosphate dissolution becomes unacceptably high.

Solutions of varying pH were prepared. 1 mL conc. HNO_3 and distilled water were added to a 100mL volumetric flask to form a 1% nitric acid solution. 0.1%, 0.01%, 0.001% and 0.0001% HNO_3 solutions were prepared by serial dilution. 4 mL glacial acetic acid and distilled water were added to a 100 mL volumetric flask to form a 4% acetic acid solution. 0.4%, 0.04%. 0.004% and 0.004% acetic acid solutions were prepared by serial dilution. 1g $NaHCO_3$ was dissolved in distilled water in a 100 mL volumetric flask to form a 1% $NaHCO_3$ solution. 0.1%, 0.01%, 0.001% and $NaHCO_3$ solutions were prepared by serial dilution.

10 mL of each solution were transferred to plastic 15 mL falcon tubes, in duplicate. Two tubes containing 10 mL distilled water were also used. The pH of the solution in each tube was recorded. 1 g of RPR was added to each falcon tube. Tubes were shaken and allowed to stand for 12 days (this extended time was due to the author being required to self isolate in accordance with Covid 19 orders in place at the time). The contents of the tubes were then filtered with paper filters to remove the RPR. The resulting liquid samples were tested for phosphate content using the molybdenum blue method. If the resulting absorbance values were outside the calibration curve samples were diluted with distilled water and the molybemnum blue process was repeated to produce results within the calibrated

concentration region.

2.6 ICP-MS Sample Digestion

ICP-MS instruments require samples to be injected in liquid or gas phase. In order to analyse RPR samples were first digested using "Sediment Digestion 2.0" method provided by Waikato Mass Spectrometry Facility. Later the protocol was modified due to difficulties encountered during analysis. Solid samples were dissolved in reverse Aqua Regia; a 3:1 mixture of concentrated nitric and hydrochloric acid. A higher concentration of nitric acid is preferred for compatibility with ICP-MS instrumentation. After digestion samples are diluted to give a 2% nitric acid solution, matching internal standards. A summary of the protocol is given here.

The digestion method is summarised here, all ICP-MS results from solid samples were prepared using this method unless otherwise stated.

RPR samples were dried at 50°C for 48 hours. Approximately 0.2 g of sample was accurately weighed into a 50 mL Falcon tube. 1 mL conc. HNO_3 and 0.33 mL conc. HCl were added. Samples were placed in digestion block with lids fitted loosely and left overnight overnight to pre-digest. The digestion block was heated to 50°C and samples were digested for 1 hour at this temperature. Type 1 water was added to the 50 mL mark. 10 mL of solution was filtered using 45 micron syringe filter into a 15 mL Falcon tube. This solution sample was submitted for analysis.

One blank solution was prepared for each batch submitted for ICP-MS analysis. Blank solutions were prepared using the same digestion method but no sample was added to the acid.

The original method used centrifuge to separate diluted solution from solid residue. We were instructed to use filtering instead as no suitable centrifuge was available.

A small amount of undissolved sediment remained after the digestion process.

The ICP-MS technician noted difficulties due to matrix effects, requiring additional dilution to obtain consistent results. All results provided were corrected for any additional dilutions performed.

Due to difficulties encountered with the ICP-MS instrumentation this method was modified to give a more dilute solution. In this case 1 mL of diluted solution and 9 mL of 2% HNO_3 in Type One water were filtered with a 45 μm syringe filter into a 15 mL falcon tube. This gave a final sample concentration of 10% of the original method. This reduced concentration gave results of sufficient precision while avoiding matrix interference and injector clogging reported using the original method.

For extraction solutions samples were diluted to 1% concentration for ICP-MS analysis. 100 μL of extration solution, 200 μL conc. HNO_3 and 9.7 mL of Type One water were filtered with a 45 μm syringe filter into a 15 mL falcon tube.

2.6.1 Untreated samples

In order to establish a baseline for contamination samples of untreated RPR (as received from supplier) were digested and submitted for analysis. Additionally samples of other commercial phosphate fertilisers were digested and analysed. The fertilisers submitted for analysis were “Superphosphate”, “Progresso”, “Replenish” and “Upgrade”. Finally a sample of cleaned, crushed greenshell mussel shell (*perna canaliculus*) was digested and analysed.

2.7 Calcium salt solution Cd extraction

Calcium ion solutions were tested for their potential to extract cadmium from RPR. The extraction principle is competitive displacement, Ca^{2+} and Cd^{2+} have the same charge and can occupy the same positions in an ionic lattice. It is hypothesised that in the presence of a relevantly high Ca^{2+} ion concentration Cd^{2+} will diffuse into solution as they are substituted by Ca^{2+} ion in the RPR crystal structure.

A number of cations with were considered for use as cadmium extraction agents. Primary criteria are that the ions must have be compatible with phosphate fertiliser (eg. non-toxic to plants and animals and not reactive with fertilisers and equipment) Secondary considerations are availability and cost. Calcium, magnesium, potassium and sodium ions were considered to be suitable candidates. A comparison of charge and ionic radius (Table2.1) shows that of these candidates Ca^{2+} is the closest match in size and charge to Cd^{2+}.

Ion	Charge	Effective Ionic radius (pm)[92]
Cd^{2+}	2+	95
Ca^{2+}	2+	100
Mg^{2+}	2+	72
K^{+}	1+	138
Na^{+}	1+	102

Table 2.1: Ionic Radii of Cd^{2+} and other cations

A simple test of this hypothesis was to place RPR and calcium salt solution in a conical flask and stir for a period of time, then measure the Cd content of the treated RPR. Potential influencing factors of Ca^{2+} concentration, counter ion, pH, contact time, RPR particle size and temperature were identified. Generally only one of these factors was varied while the others were held constant. Stirring RPR in distilled water was used as a control.

2.7.1 TDX001 Calcium Nitrate Leaching in Water, Acetic Acid and Sodium Carbonate Solutions

Calcium nitrate solutions of varying concentrations as well as distilled water, acetic acid and sodium carbonate solutions were tested for cadmium extraction potential. RPR was used as supplied, without any further processing. 0.8g of RPR and 20 mL distilled water were added to a conical flask along with a measured amount of $Ca(NO_3)_2$ or acetic acid or sodium carbonate was added. Flasks were then stirred for 31 hours. RPR residues were recovered by filtration with a Büchner funnel and paper filters before drying in an oven at 50°C for 48 hours. Dried RPR

were digested and submitted for ICP-MS analysis. A summary of each extraction solution is given in Table 2.2.

Flask	RPR (g)	H_2O	Solute
1	0.8058	20mL	-
2	0.8180	20mL	$Ca(NO_3)_2$ 1.6501g
3	0.7978	20mL	$Ca(NO_3)_2$ 0.8188g
4	0.8086	20mL	$Ca(NO_3)_2$ 0.3363g
5	0.8033	20mL	$Ca(NO_3)_2$ 0.1680g
6	0.7945	20mL	CH_3COOH 1mL
7	0.8012	20mL	$NaCH_3COOH$ 1.3996g

Table 2.2: TDX001 summary

2.7.2 TDX005 Calcium Nitrate Leaching at Varying pH

Calcium nitrate solutions of varying pH were tested for cadmium extraction potential. 1 mol L^{-1} calcium nitrate stock solutions were prepared by dissolving 16.4442 g and 16.4015 g $Ca(NO_3)_2$ in two 100 mL volumetric flasks. 20 mL of calcium nitrate solution was delivered to nine conical flasks and varying amounts of citric acid were added to each. A control flask containing 20 mL distilled water was also prepared. Solution pH levels were recorded. 0.8g of RPR was added to each flask. Flasks were stirred for 24 hours. RPR residues were recovered by filtration with a Büchner funnel and paper filters before drying in an oven at 50°C for 48 hours. Dried RPR were digested and submitted for ICP-MS analysis. Leaching solutions were recovered separately and the final pH of each was measured. A summary of each extraction solution is given in Table 2.3.

2.7.3 TDX006 Calcium Nitrate Leaching at Varying Temperature

The effect of increasing temperature to between 50°C and 90°C of cadmium extraction into calcium nitrate solution was tested. A 1 molL^{-1} calcium nitrate stock solution was prepared by dissolving 16.4178 g of $Ca(NO_3)_2$ in a 100 mL volumetric flask. Initial pH of this solution was 6.75. 20 mL of solution and 0.8 g RPR were placed in five conical flasks. An acidified 1 molL^{-1} calcium nitrate stock solution was prepared by dissolving 16.4214 g $Ca(NO_3)_2$ and 0.500 mL glacial acetic acid in a 100 mL volumetric flask. The initial pH of this solution was 3.22. 20 mL of solution and 0.8 g RPR were placed in five conical flasks.

Flask	RPR (g)	Solution	Citric acid (g)	pH (initial)	pH (final)
1	0.8058	H_2O (distilled)	0	5.07	7.06
2	0.8180	1M $Ca(NO_3)_2$	0	6.79	6.48
3	0.7978	1M $Ca(NO_3)_2$	0.1113g	1.88	2.80
4	0.8086	1M $Ca(NO_3)_2$	0.2508g	1.55	2.44
5	0.8033	1M $Ca(NO_3)_2$	0.5069g	1.34	2.17
6	0.7945	1M $Ca(NO_3)_2$	0.9975g	1.16	1.99
7	0.8012	1M $Ca(NO_3)_2$	0.0443g	2.59	3.63
8	0.8012	1M $Ca(NO_3)_2$	0.0136g	4.19	4.79
9	0.8012	1M $Ca(NO_3)_2$	0.0063g	5.72	5.74

Table 2.3: TDX005 summary

A SCILOGEX MS-H-Pro heater stirrer plate was used for heating/stirring. Stirring RPM was set at 400. Temperatures were set at 50, 60, 70, 80 and 90°C .

Each flask was heated and stirred for two hours. After this, RPR residues were recovered by filtration with a Büchner funnel and paper filters before drying in an oven at 50°C for 48 hours. Dried RPR were digested and submitted for ICP-MS analysis. Leaching solutions were recovered separately and the final pH of each was measured. A summary of each extraction solution is given in Table 2.4.

Flask	RPR (g)	Temp. (°C)	pH (final)
1	0.8065	50	6.58
2	0.8078	60	6.67
3	0.8032	70	6.87
4	0.8043	80	6.93
5	0.8001	90	6.90
6	0.7993	50	3.75
7	0.7996	60	3.71
8	0.7989	70	3.84
9	0.8017	80	3.79
10	0.8036	90	3.77

Table 2.4: TDX006 summary

2.7.4 TDX017 Leaching in Mussel Shell Derived Calcium Nitrate Solution at Varying Temperature

The effect of elevated temperature (20°C and 90°C) on cadmium extraction was tested with mussel shell derived calcium chloride solution. 25 mL of 0.1 molL^{-1} $CaCl_2$, from mussel shell dissolved in HCl, was added to each of four conical flasks. Initial solution pH was 5.21. 1 g of RPR was added to each flask. Two flasks were stirred at 20°C for 6 hours then allowed to stand overnight. The other two flasks were stirred at 90°C for 6 hours then allowed to stand overnight. RPR residues were recovered by filtration with a Büchner funnel and paper filters before drying in an oven at 50°C for 48 hours. Dried RPR were digested and submitted for ICP-MS analysis. Leaching solutions were recovered separately and the final pH of each was measured. Solutions were also prepared for analysis by ICP-MS. A summary of each extraction solution is given in Table 2.5.

Flask	RPR (g)	Temp. (°C)	pH (final)
1	1.0011	20	7.38
2	1.0034	20	7.41
3	1.0031	90	7.28
4	1.0041	90	7.23

Table 2.5: TDX017 summary

2.8 Column leaching Cd extraction

A column leaching set up was designed to increase contact time between RPR and solution while still having movement of solution. RPR was slurried with solution and loaded into a chromatography column. The column was then filled with solution and the tap opened slightly to allow solution to drip through at a controlled rate. To increase contact time it is possible to recycle the extraction solution by reloading the eluted solution into the column. It is also possible to carry out sequential extractions on the same RPR sample by using eluting multiple aliquots of solution through the column.

A range of calcium salt solutions were tested in this way, as well as distilled water and KCl and $MgCl_2$ solutions. All column leaching tests were carried out at room temperature (20-22°C).

2.8.1 TDX008 Small Scale Column Leaching with Water and Acidified Calcium Nitrate

To test the principle of column leaching a small scale set up using Pasteur pipettes was devised. Six pipettes were prepared. A small plug of cotton wool was pushed down to the neck then 2.5 g RPR was poured on top. The pipettes were placed in a test tube rack to hold them upright, with plastic sample tubes underneath to catch eluted solution.

An acidified calcium nitrate solution was prepared. 6.2239 g $Ca(NO_3)_2$ and 5 mL glacial acetic acid were dissolved in distilled water in a 100 mL volumetric flask. The initial pH was 2.20.

Pipettes 1, 2 and 3 were loaded with 1 mL distilled water. Pipettes 4,5 and 6 were loaded with 1 mL $Ca(NO_3)_2$ solution. All pipettes were covered with parafilm. After four days of being covered no liquid had eluted from any of the pipettes. With the tops covered it appeared that air could not enter the pipettes to replace liquid eluting from the bottom. This combined with surface tension inside the pipettes was enough to prevent any liquid from eluting.

The pipettes were uncovered and a further 1 mL of water/$Ca(NO_3)_2$ solution was added to each. Pipettes 4,5 and 6 the RPR column had been broken by gas pockets (see Fig. 2.3), elution from these pipettes was slower than pipettes 1,2 and 3. The pipettes were left overnight.

A further 2 mL of liquid was added to pipettes 1,2,3 and 5. Pipettes 4 and 6 1mL of liquid was added, as these pipettes had not eluted enough to receive any more.

Over the next three days the process of adding more solution to the pipettes was continued. The pipettes were then allowed to drain. For pipettes 1,2 and 3

(distilled water) a total of 11 mL was eluted through each pipette. For Pipettes 4,5 and 6 ($Ca(NO_3)_2$, acetic acid solution) 7 mL was eluted through pipette 4, 11 mL through pipette 5 and 10 mL through pipette 6.

Eluted liquid from pipettes 1,2 and 3 was combined into a single sample, pipettes 4,5 and 6 were combined into another liquid sample. These combined samples were submitted for ICP-MS analysis by the solution method. Solid RPR residues from pipettes 1,2 and 3 were combined into a single sample, as were residues from pipettes 4,5 and 6. The two combined RPR samples were dried 50°C for 48 hours then prepared for ICP-MS analysis by the digestion method.

2.8.2 TDX009 Column Leaching with Calcium Nitrate Solutions

Two glass chromatography columns of nominal 50 mL volume (approx. 1 cm internal diameter) with glass frits were used. Approximately 25 g of RPR was weighed then poured into each column.

For column 1 a 6.2% $Ca(NO_3)_2$, 5% acetic acid solution as prepared for TDX008 was used.

For column 2 a 20 mL of conc. HNO_3 was slowly added to 30 mL of distilled water. 15 g of $CaCO_3$ was added and stirred for two hours. After this time there was still some undissolved $CaCO_3$, this was removed by filtration.

20 mL of solution was added to each column and allowed to settle. After two hours standing, column 1 had multiple breaks in the column due to gas pockets. After this time only a few mL of solution had eluted from each column.

After three days of standing neither column had drained completely. Column 1 was broken by a large gas pocket, about 7 cm long. In order to released trapped gas the contents of each column were tipped out into beakers, mixed well and poured back into their columns. After this another 10 mL of solution was added to each column. After 10 minutes, column 1 formed three layers: liquid on top; a murky sediment layer, about 5 cm; and solid RPR. After 45 minutes the sediment layer had settled to a reduced size of about 2 cm. Column 2 formed a smaller sediment layer, about 1 cm, on top of the RPR. No more gas pockets were observed but drip rate was still very slow.

After sitting overnight very little solution had eluted through either column. Column 2 was broken by gas pockets again.

Columns again sat overnight, there was still no visible change in solution level for either column. Another 5 mL of solution was added to column 1 and 10 mL to column 2.

Columns sat for five days. At this time both columns had drained. Another 10 mL of solution was added to column 1 and 5 mL to column 2. In total 50 mL

of solution were added to each column. At this point column 1 had a hard gray sediment layer on top of the RPR; column 2 had a fluffy white sediment on top of the RPR.

Columns were left for two days, eluted solutions were collected into labelled containers. For column 1 approx. 30 mL of eluate was recovered; for column 2 approx. 35 mL of eluate was recovered. Column taps were left open overnight but no more solution eluted. RPR residues were removed from the columns and dried in an oven at 50°C .

2.8.3 TDX011 Column Leaching with Calcium Chloride Solutions

Two glass chromatography columns of nominal 50 mL volume (approx. 1 cm internal diameter) with glass frits were used. Approximately 20 g of RPR was weighed then poured into each column.

Solution 1: a 0.5 mol L^{-1} $CaCl_2$/1% acetic acid solution was prepared. 5.5579 g $CaCl_2$ and 0.5 mL acetic acid were added to a 50 mL volumetric flask. Distilled water was added to dissolve solids then filled up to the mark.

Solution 2: a 1 mol L^{-1} $CaCl_2$/1% acetic acid solution was prepared. 11.1144 g $CaCl_2$ and 0.5 mL acetic acid were added to a 50 mL volumetric flask. Distilled water was added to dissolve solids then filled up to the mark.

Columns 1 and 2 were filled with solutions 1 and 2 respectively. Columns were allowed to sit with taps open for six days. After this time, both columns were broken by gas bubbles. Column 1 still had about 25 mL of solution left in the column. In order to released trapped gas the contents of each column were tipped out into beakers, mixed well and poured back into their columns. Remaining solution was added to each column.

Columns were left for another six days. Column 1 was again broken by gas bubbles. Eluted solutions were collected into labelled containers. RPR residues were removed from the columns and dried in an oven at 50°C .

2.8.4 TDX012 Column Leaching with Calcium Chloride Solution and Calcium Nitrate Solution from Mussel Shells

Two glass chromatography columns of nominal 50 mL volume (approx. 1 cm internal diameter) with glass frits were used. Approximately 20 g of RPR was weighed then poured into each column.

Solution 1: a 0.5 mol L^{-1} $CaCl_2$/0.5% citric acid solution was prepared. 5.5521 g $CaCl_2$ and 0.2467 g citric acid were added to a 50 mL volumetric flask. Distilled

water was added to dissolve solids then filled up to the mark. The initial pH of this solution was measured as pH 1.85.

Solutions 2: Mussel shell solution prepared by Ali Almosabeh. Crushed shells were cleaned before being dissolved in HCl. The pH was then neutralised with $NaHCO_3$. The solution had a Ca^{2+} concentration of approximately 0.25 mol L^{-1}. The initial pH of this solution was measure as pH 5.54.

Columns 1 and 2 were filled with solutions 1 and 2 respectively. In both columns RPR reacted immediately to the liquid, forming gas pockets in the column. Each column was stoppered then tipped end over end until all RPR was wetted with solution.

After standing overnight all solution had eluted from both columns. The remaining solutions were added to each column.

After standing for two days all remaining solution had dripped out of the columns. Eluted liquids were added back to their respective columns and allowed to drain through again.

After four days all liquid had drained through both columns. Eluted liquids were collected into labelled containers. Approximately 40 mL of solution was recovered from each column. Another set of solutions was prepared. Solution 1: 5.5514 g $CaCl_2$ and 0.0122 g citric acid in a 50 mL volumetric flask, the initial pH was 4.56. Solution 2 mussel shell dissolved in HCl, as prepared by Ali Almosabeh, the initial pH was 5.45. The new solutions were added to their respective columns for a second extraction.

The next day column 1 had drained, added more solution. Column 2 had only half drained, there appeared to be a plug of precipitate on top of the RPR, after agitating the RPR surface and adding more solutions the column seemed to flow better. Column 1 RPR surface agitated as well.

After four days both columns had drained completely. About 47 mL of elute collected from each column. Solutions were prepared for a third extraction. Solution 1: 5.5516 g $CaCl_2$ and 0.0040 g citric acid in a 50 mL volumetric flask, the initial pH was 4.26. Solution 2 mussel shell dissolved in HCl, as prepared by Ali Almosabeh, the initial pH was 5.09. The new solutions were loaded into their respective columns for a third extraction.

After another four days eluates were poured back into their respective columns and allowed to drain for two days. Eluted solutions were collected into labelled containers. The RPR residues were removed from their columns and dried in an oven at 50°C .

2.8.5 TDX014 Column Leaching with Potassium Chloride Solution and Calcium Chloride Solution from Mussel Shells

Two glass chromatography columns of nominal 50 mL volume (approx. 1 cm internal diameter) with glass frits were used.

Solution 1: A 1 mol L^{-1} KCl solution was prepared. 7.4580 g KCl and 0.0081 citric acid were added to a 50 mL volumetric flask. Distilled water was added to dissolve solids then filled up to the mark. Initial pH = 4.71.

Solution 2: Mussel shell dissolved in HCl, as prepared by Ali Almosabeh. Crushed shells were cleaned then heated to 300°C in a muffle furnace before being dissolved in HCl. The pH was neutralised with $NaHCO_3$. The Ca^{2+} concentration was approximately 0.25 mol L^{-1} and the initial pH was 5.52.

Approximately 20 g of RPR was weighed for each column. RPR and solution was slurried together and poured into the column with taps closed. After 1 hour no gas pockets had appeared in the columns. Taps were left closed over the weekend.

After sitting for two days column 2 had drained out despite having tap closed. Eluate poured back into column but glass broke, spilling solution. Glass cracked around where column was clamped, upon inspection rubber on clamp had worn through and mettle was showing. RPR was removed and loaded into another column. About half of solution 2 was recovered, another 25 mL of shell solution was added. Taps were then opened and columns left overnight.

The next morning eluates were loaded back into the columns to run through again. After eluting for a second time the solutions were collected in labelled containers.

Another set of solutions was prepared. Solution 1: 7.4579 g KCl and 49 mg citric acid in a 50 mL volumetric flask, initial pH = 4.80. Solution 2: mussel shell dissolved in HCl, as prepared by Ali Almosabeh. Crushed shells were cleaned then heated to 300°C in a muffle furnace before being dissolved in HCl. The pH was neutralised with $NaHCO_3$. The Ca^{2+} concentration was approximately 0.25 mol L^{-1} and the initial pH was 5.77. The new solutions were added to their respective columns for a second extraction. After the solutions were loaded into the columns were allowed to sit overnight with their taps closed.

The next day the column taps were opened and the solutions allowed to flow through. The eluted solutions were loaded back into the columns and flowed through again. After eluting for a second time the solutions were collected in labelled containers.

Another set of solutions was prepared. Solution 1: 7.4507 g KCl and 61 mg citric acid were added to a 50mL volumetric flask, distilled water was added to dissolve the solids, then topped up to the mark. The initial solution pH was 4.59. Solution 2: mussel shell dissolved in HCl, as prepared by Ali Almosabeh. Crushed shells were cleaned then heated to 600°C in a muffle furnace before being

dissolved in HCl. The pH was neutralised with $NaHCO_3$. The Ca^{2+} concentration was approximately 0.25 mol L^{-1} and the initial pH was 12.5, citric acid added to reach pH = 5.77. New solutions were added to their respective columns for a second extraction. Solutions were loaded into column with taps closed and left overnight.

The next day the column taps were opened and the solutions allowed to flow through. Solution 2 was cloudy and yellow in colour, possibly from the "600°C " solution. After eluting for a second time the solutions were collected in labelled containers. The RPR residues were removed from the columns and dried in an oven at 50°C .

2.8.6 TDX015 Column Leaching with Water, Calcium Acetate, Calcium Nitrate and Magnesium Chloride Solutions

Four glass burettes of nominal 50mL volume (approx. 1cm internal diameter) with cotton wool plugs were used as columns.

Solution 1: A 1 mol L^{-1} $Ca(CH_3COO)_2$ solution was prepared. 15.16 mL of glacial acetic acid was added to 100 mL distilled water. 15.0142 g $CaCO_3$ was added slowly, with stirring, to the acetic acid solution. When all of the $CaCO_3$ had been added the solution was allowed to stir for 1 hour. The solution was diluted with distilled water to 150 mL. The initial pH was 5.04.

Solution 2: A 1 mol L^{-1} $Ca(NO_3)_2$ was prepared. 38.4205 g $Ca(NO_3)_2.4H_2O$ was dissolved in distilled water and diluted to 150 mL. A small amount of citric acid was added. The initial pH was 5.21.

Solution 3: A 1 mol L^{-1} $MgCl_2$ solution was prepared. 14.2867 g $MgCl_2$ (anhydrous) was dissolved in distilled water and diluted to 150 mL. A small amount of citric acid was added. The initial pH was 5.25.

Solution 4: distilled water; pH = 5.98.

Approximately 20 g of RPR was weighed for each column. Each solution was slurried with RPR then poured into a column with the tap closed. Columns were left to stand for two days.

After two days columns 2 and 4 had drained. These columns had Teflon taps, columns 1 and 3 had ground glass taps. All columns had minor gas pocket formation. Tapping on the glass columns released small bubbles and caused settling of the RPR. Taps were opened, column 3 was flowing slower than others. At the end of the day eluted solutions were added back to the columns. Taps were closed overnight.

The next day taps were opened again. None of the columns had leaked overnight. Column 3 flowed very slowly over this time. Columns were allowed to drain for 4 hours 45 min. Column 3 flowed very slowly over this time. The eluted

solutions were then placed in labelled containers. The column taps were closed and 50 mL of fresh solution was added to each column.

The next morning the column taps were opened. No leaks were observed. Column 1 nozzle was blocked with white precipitate, this was cleared. This precipitate is most likely $Ca(OH)_2$; compared to Cl^- and NO_3^- CH_3COO^- is a relatively strong conjugate base. It is able to accept a proton from H_2O, forming CH_3COOH and OH^-. Free OH^- ions will readily react with Ca^{2+} ions to form insoluble $Ca(OH)_2$.

The eluted solutions were poured back into their columns for four hours then they were allowed to drain for three hours. At this time columns 2, 3 and 4 had fully drained. Column 1 still had about 15 cm of liquid above the RPR, this was poured into the eluate. Solution samples were placed in labelled containers. The column taps were closed and 50 mL of fresh solution was added to each column.

The next morning the column taps were opened. Eluted solutions were poured back into their columns for seven hours, columns were then left to drain our overnight.

The next day Column 1 still had about 10 cm of liquid above the RPR, this was poured into the eluate. Solution samples were placed in labelled containers. The RPR residues were removed from their columns and dried in an oven at 50°C .

2.8.7 TDX018 Column Leaching with Calcium Chloride Solutions from Unheated Mussel Shell, Heated Mussel Shell, Lab $CaCl_2$ and Calcium Chloride Solution with EDTA

Four glass burettes of nominal 50 mL volume (approx. 1cm internal diameter) with cotton wool plugs were used as columns.

Solution 1: A 1 mol L^{-1} $CaCl_2$ solution was derived from mussel shell. About 20 g of unheated mussel shell was crushed in a mortar and pestle. Crushed shell was placed in a 500 mL conical flask, 150 mL of 2 mol L^{-1} HCl was added, slowly and with stirring. Considerable foaming occurred as the acid reacted with the shell, fast stirring and very slow addition of acid was required to prevent frothing over. Once all acid had been added the flask was stirred for one hour. The solution was then filtered to remove undissolved sediment. After filtration the solution was a very pale yellow colour. The initial pH was 5.98.

Solution 2: A 1 mol L^{-1} $CaCl_2$ solution was derived from heated mussel shell. About 20 g of 300°C heated mussel shell was crushed in a mortar and pestle. Heated shell was noticeably easier to crush than unheated shell. Crushed shell was placed in a 500 mL conical flask, 150 mL of 2 mol L^{-1} HCl was added, slowly and with stirring. A strong, pungent odour was produced. Considerable foaming occurred as the acid reacted with the shell, fast stirring and very slow addition of

acid was required to prevent frothing over. Once all acid had been added the flask was stirred for one hour. The solution was then filtered to remove undissolved sediment. After filtration the solution was bright yellow in colour. The sulphurous smell remained after filtering. The initial pH was 6.23.

Solution 3: A 1 mol L^{-1} $CaCl_2$ solution was prepared. 16.6574 g $CaCl_2.2H_2O$ was dissolved in 150 mL of distilled water. The initial pH was 6.12

Solution 4: A 1 mol L^{-1} $CaCl_2$ solution with 0.1% EDTA was prepared. 16.6594 g $CaCl_2.2H_2O$ and 0.1653 g EDTA were dissolved in 150 mL distilled water. The pH of this solution was 2.77. $NaHCO_3$ was added to raise the pH above 4. After neutralising the initial pH was 4.80.

UV-Vis spectra of solutions 1 and 2 were recorded.

Approximately 20 g of RPR was weighed for each column. Each solution was slurried with RPR then poured into a column with the tap closed. Columns were left to stand for two days.

Column taps were opened. Column 3 broke, spilling solution all over the bench. About 20 mL was recovered. RPR and remaining solution were transferred into a new column.

The next day eluted solutions were poured back into the columns. The columns were allowed to drain, after three and a half hours about 40 mL of eluted solution was recovered from each of columns 1, 2 and 4; about 10 mL was recovered from column 3. Solution samples were placed in labelled containers. The column taps were closed and 50 mL of fresh solution was added to each column.

The next day taps were opened, as solutions eluted they were poured back into their columns until for four hours, after this the columns were allowed to drain for 3 hours 45 min. The eluted solution samples were placed in labelled containers. The column taps were closed and 50 mL of fresh solution was added to each column.

The next day taps were opened, as solutions eluted they were poured back into their columns for seven hours, then columns were allowed to drain overnight. The next morning the eluted solution samples were placed in labelled containers and the RPR residues were removed from the columns and dried in an oven at 50°C .

Figure 2.2: RPR column leaching set up

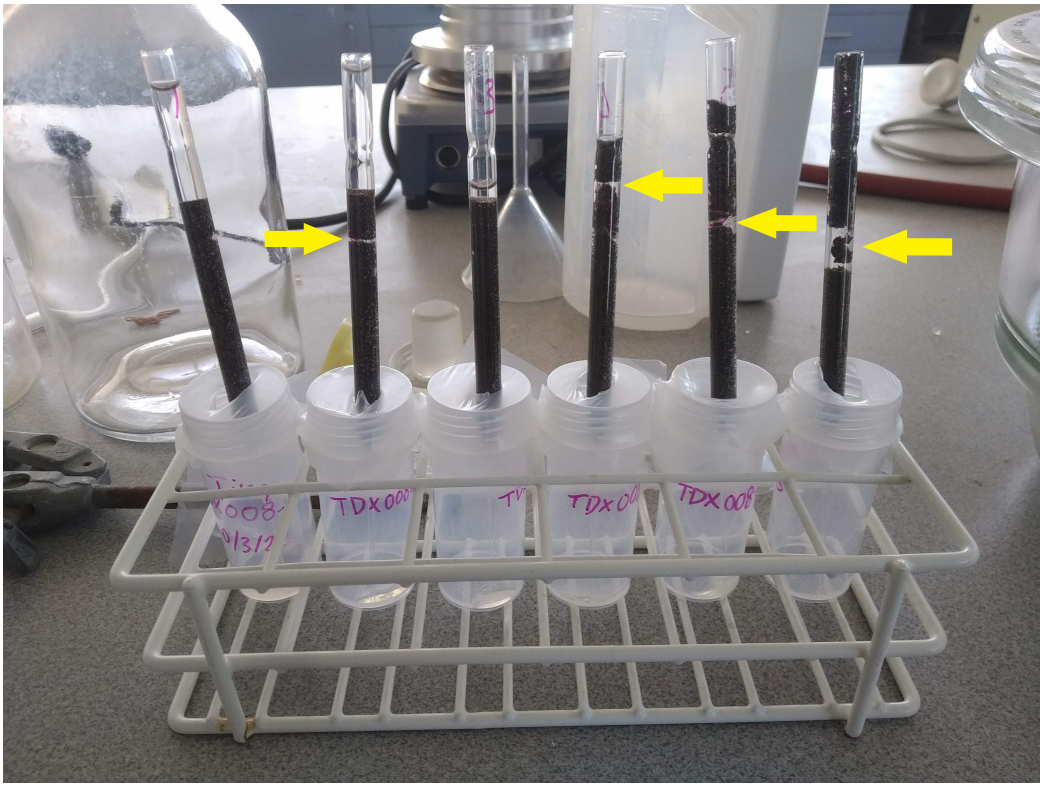

Figure 2.3: TDX008 pipettes; arrows indicate locations of gas pocket formation within the RPR column.

2.9 Microwave assisted Cd extraction

Microwave radiation produces rapid heating. Domestic microwave ovens use a cavity magnetron to generate radiation with a nominal 2.45 GHz frequency. This radiation causes dielectric heating in polar molecules such as water. The molecules rotate rapidly to align their dipoles to the fluctuating electromagnetic field. Non-polar molecules are not affected in this way. Due to the strong dependence on molecular structure it is possible to observe effects from microwave irradiation that differ from conventional heating. For example a short burst of microwave radiation may induce intense localised heating in a mixed substance. This can potentially be useful in chemical reactions if it allows the target substrate to be heated selectively.[81]

An NEC 800W domestic microwave oven was used. Microwave power was set to "LOW" in order to prevent boil over with the small volumes of solution used.

2.9.1 TDX010 $CaCl_2$ Solution Leaching

An 1 molL^{-1} $CaCl_2$ with 2% acetic acid solution was prepared. 11.1118 g $CaCl_2$ and 2 mL glacial acetic acid was dissolved in distilled water in a 100 mL volumetric flask then filled to the mark. The solution pH was 2.18. 20mL of solution was added to each of five 50 mL conical flasks. 20 mL distilled water was added to another 50 mL conical flask. 0.8 g of RPR was added to each flask. Flask 1 received no microwave irradiation. Flasks 2 to 5 were microwaved (MED power, 800 W microwave oven) for 1 minute. At medium power boiling was observed after 25 seconds and at 1 min was close to boiling over. For further heating LOW power was used. Flasks 3, 4 and 5 were microwaved on LOW for 2, 5 and 10 minutes respectively. RPR weight and microwave irradiation time for each flask are recorded in 2.6. To ensure that even cooled and well mixed solutions each flask was stirred for 2 hours at room temperature (21°C). RPR and solution were separated by Büchner funnel with paper filters. RPR residues were dried in an oven at 50°C for 24 hours then were prepared by digestion method for ICP-MS analysis.

2.9.2 TDX016 $CaCl_2$ Solution Leaching

A 1 mol L^{-1} $CaCl_2$ solution was prepared. 11.1192 g $CaCl_2$ was dissolved in distilled water in a 100 mL volumetric flask then filled to the mark. The solution pH was 4.93. 20 mL of solution was added to five 100 mL conical flasks. 20 mL distilled water was added to another 100 mL conical flask. 0.8 g of RPR was added to each flask. Flask 1 received no microwave irradiation. Flasks 2 to 5 were microwaved (LOW power, 800 W microwave oven) for between 2 and 12 minutes. Flask 6 was microwaved for 12 minutes. RPR weight and microwave irradiation

Flask	RPR (g)	Liquid	Microwave Time MED (min)	Microwave Time LOW (min)
1	0.7995	1M $CaCl_2$	0	0
2	0.8021	1M $CaCl_2$	1	0
3	0.8026	1M $CaCl_2$	1	2
4	0.8008	1M $CaCl_2$	1	5
5	0.8019	1M $CaCl_2$	1	10

Table 2.6: TDX010 summary

time for each flask are recorded in 2.7. To ensure that evenly cooled and well mixed solutions resulted each flask was stirred for 2 hours at room temperature (21°C). RPR and solution were separated by Büchner funnel with paper filters. Filtered solutions were stored in plastic sample tubes. RPR residues were dried in an oven at 50°C for 24 hours. ICP-MS samples of the six RPR residues and six solutions were prepared and submitted for analysis.

Flask	RPR (g)	Liquid	Microwave Time (min)
1	0.8014	1M $CaCl_2$	0
2	0.8035	1M $CaCl_2$	2
3	0.8018	1M $CaCl_2$	4
4	0.7993	1M $CaCl_2$	6
5	0.8031	1M $CaCl_2$	12
6	0.8041	H_2O	12

Table 2.7: TDX016 summary

2.9.3 TDX020 $CaCl_2$ and Ligand Solution Leaching

$CaCl_2$ solutions of concentrations 1, 2 and 3 mol L^{-1} were tested for their Cd extraction potential with microwave heating. 1 mol L^{-1} $CaCl_2$ solutions containing potential Cd stabilising ligands (Mercaptosuccinic acid, Potassium Bitartrate and EDTA) were tested for their Cd extraction potential with microwave heating.

A 1 mol L^{-1} $CaCl_2$ solution was prepared. 11.1158 g $CaCl_2$ was dissolved in distilled water in a 100 mL volumetric flask then filled to the mark. A 2 mol L^{-1} $CaCl_2$ solution was prepared. 4.4461 g $CaCl_2$ was dissolved in distilled water in a 20 mL volumetric flask then filled to the mark. A 3 mol L^{-1} $CaCl_2$ solution was

prepared. 6.6651 g $CaCl_2$ was dissolved in distilled water in a 20 mL volumetric flask then filled to the mark.

Six 100 mL conical flasks were used. To flask 1 20 mL of 1 mol L^{-1} $CaCl_2$ solution was added. To flask 2 20 mL of 2 mol L^{-1} $CaCl_2$ solution was added. To flask 3 20 mL of 3 mol L^{-1} $CaCl_2$ solution was added. To flask 4 20 mL of 1 mol L^{-1} $CaCl_2$ solution and about 20 mg Mercaptosuccinic acid was added. To flask 5 20 mL of 1 mol L^{-1} $CaCl_2$ solution and about 20mg Potassium Bitartrate was added. To flask 6 20 mL of 1 mol L^{-1} $CaCl_2$ solution and about 20 mg EDTA was added.

The pH of the solution in each flask was measured. For flasks 4, 5 and 6 the initial pH values were below 4 so Na_2CO_3 was added to neutralise.

0.8 g of ring mill crushed RPR was added to each flask. A summary of the RPR weight, $CaCl_2$ concentration, ligand and pH are summarised in 2.8.

Each flask was microwaved on LOW power for 12 minutes.

To ensure that even cooled and well mixed solutions resulted each flask was stirred for 2 hours at room temperature (21°C). RPR and solution were separated using a Büchner funnel with paper filters. Filtered solutions were stored in plastic sample tubes. RPR residues were dried in an oven at 50°C for 24 hours. ICP-MS samples of the six RPR residues and six solutions were prepared and submitted for analysis.

Flask	RPR (g)	Liquid	Ligand	pH
1	0.8079	1M $CaCl_2$	-	5.15
2	0.8021	2M $CaCl_2$	-	5.15
3	0.8031	3M $CaCl_2$	-	5.05
4	0.8039	1M $CaCl_2$	Mercaptosuccinic acid (21.2 mg)	6.19
5	0.8036	1M $CaCl_2$	Potassium Bitartrate (22.2 mg)	6.34
6	0.8076	1M $CaCl_2$	EDTA (23.1 mg)	6.08

Table 2.8: TDX020 summary

2.10 FTIR Spectroscopy

FTIR spectra were recorded using a Perkin Elmar 400 using Spectrum software. Measurement were recorded over the range from 4000 cm^{-1} to 450 cm^{-1}. A background level was recorded before each session using an empty sample disc holder. Spectragryph v1.2.15 software was use for analysis and presentation of spectra.

Samples were prepared as 10 mm diameter KBr discs. A small quantity of KBr and sample were finely ground together using an agate mortar and pestle. The quantity of sample was no more than 10% of the quantity of KBr. The KBr/sample mix was packed into a die set and pressed at 11 t pressure for about 5 minutes, no vacuum was used. Pressed discs were placed into a 10 mm disc holder and spectra were recorded immediately. The KBr used was stored at 100°C to prevent it from absorbing water. However a recorded spectrum of the supplied KBr2.4 shows significant absorbance peaks at 3453 cm^{-1} and 1638 cm^{-1}, characteristic of H_2O vibrational peaks. It is not clear if residual water is present in the oven stored KBr or if it is picked up in the disc making process. Since all recorded spectra show these peaks it is not possible to determine with confidence if any of the samples contain H_2O. There is also a small peak at 1385 cm^{-1}, indicative of nitrate. Again it is not clear where this contamination originated from. The KBr spectrum shows a slight baseline slope, this can be automatically corrected for in the Spectrum software, if this correction was used it is noted with the spectrum.

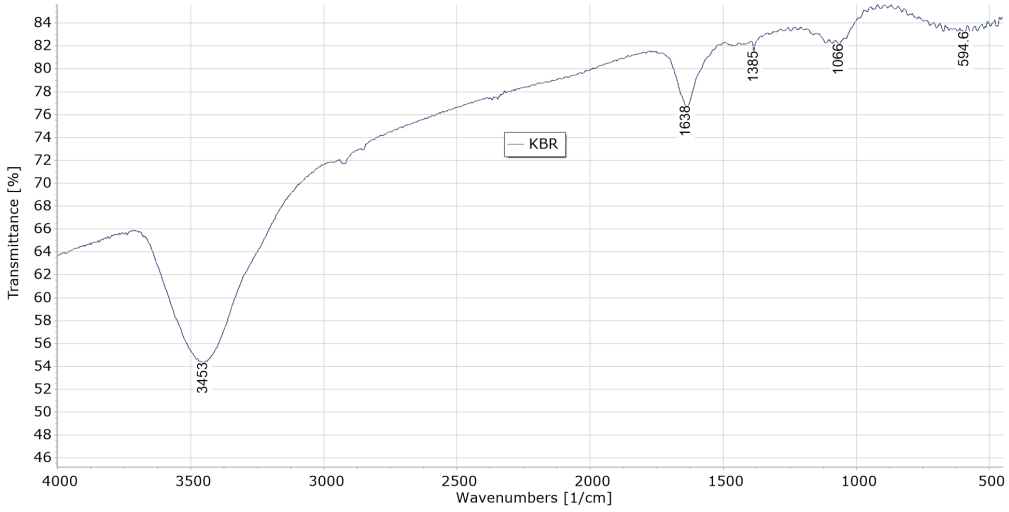

Figure 2.4: FTIR spectrum of supplied KBr

2.11 X-Ray Fluorescence and X-Ray Diffraction

2.11.1 Sample Crushing

Powder XRD analysis requires finely crushed samples. Samples of RPR, superphosphate fertiliser and mussel shell were dried at 105°C for 48 hours. Samples were then mechanically crushed using a ring mill with tungsten carbide head. The mill head consists of a round bowel with lid and a smaller round puck sitting inside. The puck is able to slide freely inside the bowl but not tumble end over end. To use the mill a sample is placed inside the mill head, the head is placed in the mill and secured by air bag clamp. The mill head is spun using a powerful eccentric motor. The jarring motion of the mill head causes the puck to bounce around inside the bowl, grinding and pulverising the sample between the puck and the wall of the bowl. Tungsten carbide is the preferred material for grinding, due to its hardness almost all minerals can be crushed with minimal wear to the head. The only contamination that tungsten carbide can leave is carbon (not detected) and tungsten (not of interest for our samples). A milling time of 45-60 seconds was used. Milled samples were sealed in plastic snap-lock bags.

2.11.2 Loss on Ignition

2-3 g of each sample were weighed into porcelain crucible. Crucibles were heated to 1100°C for 60 minutes in a muffle furnace. Crucibles were allowed to cool inside the furnace with the door open until it was safe to handle them with tongs, crucibles were then placed in a desiccator for further cooling. Cooled crucibles were then re-weighed. Percentage loss for each sample was calculated for use in XRF calculations.

2.11.3 XRF

For major element analysis XRF samples were prepared as fusion disks using Type 57:43 X-ray Flux (57% Lithium Tetraborate, 43% Lithium Metaborate). 8.00 g of flux was weighed into a platinum crucible. 0.80 g of sample was weighed on a weigh boat, the sample was then added to the crucible and the boat re-weighed to determine the exact weight of sample added. The crucible was loaded into a Claisse Le Ne Fluxer, using the pre-loaded program of 1100°C fusion. Fusion disks were labelled and crucibles were cleaned with citric acid solution in an ultrasonic bath.

For trace element analysis about 7 g of sample powder was weighed into a paper cup. About five drops of PVA glue were added and stirred together. The

mixture was pressed into a sample holder and dried in an oven at 60°C until the glue set.

2.11.4 XRD

Sample powders were loaded into sample holders and racked into an auto loader.

2.12 Mussel Shell Solutions

Mussel shells were used as a starting material for calcium salt solutions.

2.12.1 Mussel Shell Preparation

Mussel Shells were previously prepared by another student Ali Almosabeh. The as supplied mussel shells were coarsely crushed and contained mussel residues. Shell samples were first cleaned with and samples were heated in a muffle furnace to 300°C , 600°C and 900°C . Cleaned and heated shell samples were then used for preparation of solutions.

2.12.2 Dissolving Mussel Shells in Acid

Chloride solutions of mussel shells were prepared from unheated shells and shells which had been heated to 300°C . To obtain a solution of known concentration and neutral pH a known amount of HCl was added to excess mussel shell. The reaction mixture was then filtered to remove shell residues. Assuming all HCl reacts with $CaCO_3$ to form $CaCl_2$ 2 molL^{-1} HCl will be required to form a 1 mol L^{-1} $CaCl_2$ solution. Actual $CaCl_2$ concentration will be slightly lower, but as mussel shell is approximately 96% $CaCO_3$ the difference should be minor.

About 20 g of shell was crushed in a mortar and pestle then placed in a 500 mL conical flask. Unheated shell was much harder to crush than 300°C heated shell. 150 mL of 2 mol L^{-1} was added, slowly with stirring. Significant foaming occurred as the acid was added. Once all the acid had been added flasks were stirred for 1 hour then filtered. Unfiltered solutions were turbid and grey-black in colour 2.5. Filtered solutions were clear, unheated shell solution was very pale yellow, almost colourless while 300°C shell solution was a strong yellow colour 2.6. On reacting with HCl the 300°C shells produced and strong pungent, sulphurous smell. This smell persisted after filtering. Unheated shell solution did not smell strongly. The pH of filtered solutions were recorded: unheated shell solution pH = 5.98; 300°C shell solution pH = 6.23.

Figure 2.5: Unfiltered mussel shell solutions. Unheated (left), 300°C (right)

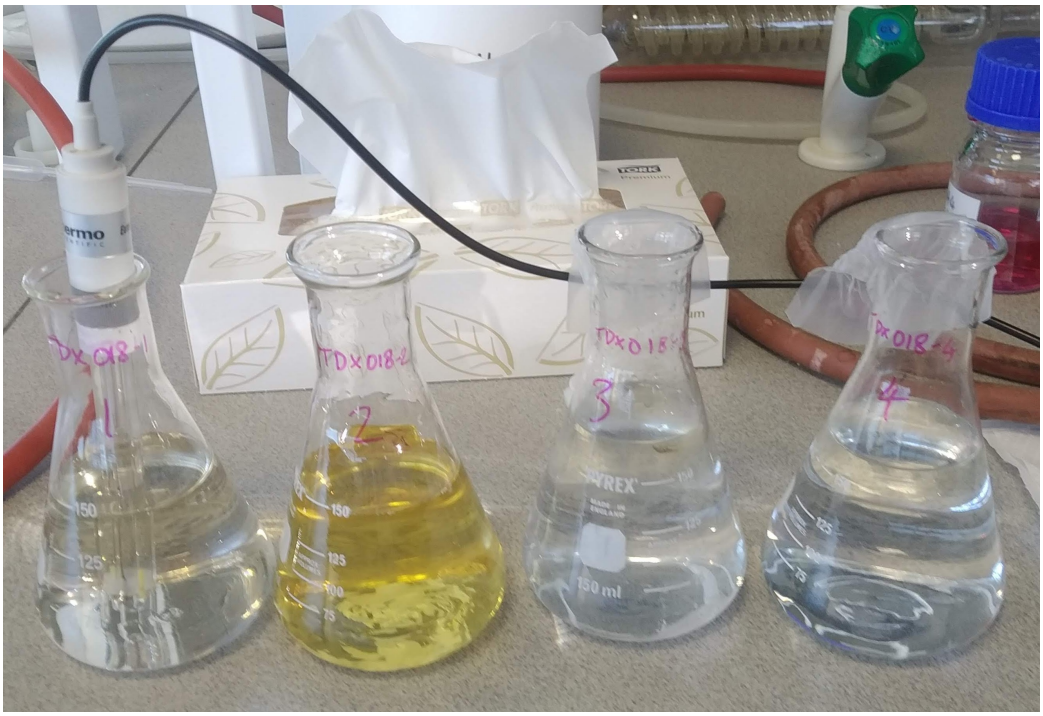

Figure 2.6: Filtered shell solutions unheated (1), 300°C (2). Also 1 mol L^{-1} $CaCl_2$ (3) and 1 mol L^{-1} $CaCl_2$ with EDTA (4)

3. Results and Discussion

3.1 Characterisation of RPR

3.1.1 Optical Microscopy

Using a stereo viewer microscope at 40x magnification a sample of RPR, as supplied by Terracare, were observed and photographed (Fig.3.1). Grains appeared smooth, with irregular shape and colour. A variety of colours were observed, ranging from white to brown and grey.

3.1.2 Scanning Electron Microscopy

An SEM image of RPR was obtained. Irregular shaped grains with approximate sizes of 0.1 to 0.4 mm were observed. As the specimen had not been coated with a conductive material resolution was limited. Grains appeared to vary in their surface texture, some smooth, others "fuzzy" but there is little detail visible. Visually it is possible to see dark and light coloured grains but this distinction is not visible on the SEM image.

Eleven individual RPR grains were analysed by SEM-EDX. Instrument calculated elemental compositions for each grain are shown in Table3.1. K line fluorescence was used for composition calculations, L and M lines (when detected) were not used.

Significant levels of calcium, phosphorus, oxygen and silicon were detected on all grains. Aluminium and iron were detected on some grains. EDX also indicated the presence of bromine on some grains, this is believed to be an instrument error. Bromine and aluminium have very similar EDX signals and the two are known to produce false readings when there is insufficient signal to noise ratio.

3.1.3 RPR X-ray Fluoresce

XRF results for RPR were outside the preferred range for accuracy with only 97.6% of the sample mass accounted for by calculated results. A likely cause of this

Grain	Ca	P	O	Si	S	Al	C
1.	37.79%	13.30%	40.20%	2.80%	5.39%	0.52%	-
2.	51.52%	15.90%	29.23%	1.20%	1.50%	-	-
3.	42.90%	16.36%	333.03%	1.68%	2.66%	-	2.52%
4.	44.04%	11.09%	31.39%	7.50%	2.64%	1.28%	2.05%
5.	43.76%	18.08%	28.92%	1.06%	-	-	2.81%
6.	39.07%	15.51%	39.57%	2.94%	1.94%	0.97%	-
7.	39.55%	15.00%	37.29%	1.51%	1.16%	0.36%	5.13%
8.	35.26%	13.6%	41.75%	3.47%	2.25%	0.65%	2.44%
9.	30.83%	11.43%	41.52%	11.09%	3.76%	1.37%	-
10.	44.75%	14.42%	36.87%	1.65%	2.01%	0.29%	-
11.	41.55%	15.39%	37.63%	3.07%	1.32%	0.36%	0.67%

Table 3.1: SEM-EDX instrument calculated elemental composition

inaccuracy is instrument parameters not being optimised for this type of mineral. Despite this the calculated results were in line with expectations from EDX and ICP-MS. The dominant elements were calcium and phosphorous, with significant levels of carbon, silicon, aluminium, iron, potassium and sulphur; with traces of many other elements.

Sample	SiO_2 (%)	Al_2O_3 (%)	TiO_2 (%)	MnO (%)	Fe_2O_3 (%)
RPR	5.53	1.11	0.091	0.018	0.78728
Sample	MgO (%)	CaO (%)	Na_2O (%)	K2O (%)	P2O5 (%)
RPR	0.631	45.528	1.61	0.22	28.798
Sample	SO3 (%)	SrO (Sr - ppm)	BaO (Ba - ppm)	CO2 (%)	Sum (%)
RPR	3.61	2067	125	9.40	97.648

Table 3.2: RPR XRF results - Majors

3.1.4 RPR X-ray Diffraction

The best Highscore match to the recorded scatter pattern was for a single compound Calcium Phosphate Fluoride (Fluorapatite) with a score of 75, Displacement [°2Th.] of 0.000 and Scale Factor of 0.981. The expected major component of RPR was hydroxyapatite. The structural difference between hydroxyapatite ($Ca_5(PO_4)_3OH$)and fluorapatite ($Ca_5(PO_4)_3F$)is minor, with a single OH^- ion replaced by an F^- ion. Both minerals have the same crystal structure and very similar physical properties. Hydroxyapatite absorbs fluoride ions to form fluorapatite.

Sample	Sc (ppm)	V (ppm)	Cr (ppm)	Co (ppm)	Ni (ppm)
RPR	50	82	142	3	17
Sample	Cu (ppm)	Zn (ppm)	Ga (ppm)	As (ppm)	Rb (ppm)
RPR	17	97	1	20	11
Sample	Sr (ppm)	Y (ppm)	Zr (ppm)	Nb (ppm)	Mo (ppm)
RPR	2040	77	44	2	11
Sample	Sn (ppm)	Sb (ppm)	Cs (ppm)	Ba (ppm)	La (ppm)
RPR	0	6	18	101	17
Sample	Ce (ppm)	Nd (ppm)	Pb (ppm)	Th (ppm)	U (ppm)
RPR	22	27	3	16	61

Table 3.3: RPR XRF results - Traces

RPR is known to contain fluoride, this is of some concern environmentally. It is likely that RPR contains a mixture of hydroxyapatite and fluorapatite, the ratios will depend on origin. As F was not measured by ICP-MS or XRF the fluoride levels of our RPR sample are unknown.

3.1.5 Particle Sizer

To test the effectiveness of manually crushing RPR with a mortar and pestle a Malvern Instruments Mastersizer 3000 was used to measure particle size for unprocessed RPR and mortar and pestle crushed RPR. The Mastersizer 3000 measures the distribution of particles over a size range from 0.05μm to 3500μm. Selected readings are summarised in Table3.4 and the volume/size distributions are shown in .

Specific Surface Area (SSA) is a measurement of the total surface area of a unit mass of a solid.[82] Calculating SSA from a particle size distribution requires assumptions about particle shape and density, this method does not account for particle porosity. SSA measurements are not necessarily comparable across different substances, instruments and measurement techniques. In this case the substance measured is the same, only the particle size distribution changes, so we have a valid comparison.

The Dv 50 of a substance is the maximum diameter below which 50% of particles (by mass) exist. Similarly Dv 10 is the maximum diameter below which 10% of particles exist and Dv 90 is the maximum diameter below which 90% of particles exist.

Manual crushing was done by placing about 10 g of RPR in a mortar and grinding with the pestle using a circular motion. Grinding continued until the

motion of the pestle felt noticeably smoother and continued grinding appeared to have little further effect. Crushed RPR appeared to be a paler grey colour and felt more powdery to touch. However on close inspection large grains were still visible. Due to the hardness of RPR manually crushing took considerable effort even for small amounts.

	RPR unprocessed	RPR Mortar and Pestle Crushed
Specific Surface Area	48.29 m^2kg^{-1}	173.5 m^2kg^{-1}
Dv 10	86.4 μm	44.7 μm
Dv 50	148 μm	134 μm
Dv 90	246 μm	240 μm

Table 3.4: RPR Particle Size - Malvern Mastersizer 3000 results

Unprocessed RPR shows fairly uniform grain size with a Dv 10 of 86.4 μm, Dv 50 of 148 μm and Dv 90 of 246 μm Fig 3.4. This is consistent with results from SEM imaging. The SSA of this sample was 48.29 m^2kg^{-1}.

Mortar and Pestle Crushed RPR had a slightly broader size distribution with a Dv 10 of 44.7 μm, Dv 50 of 134 μm and Dv 90 of 2406 μm. Compared to unprocessed RPR the Dv 50 and Dv 90 are only slightly smaller but the Dv 10 is almost half the diameter Fig. 3.5. This suggests that smaller particles of RPR are readily crushed by mortar and pestle but average to large particles are barely affected. Although the SSA of the mortar and pestle crushed RPR is significantly higher at 173.5 m^2kg^{-1} the overlapped size distributions shows this is due to a relativity small increase in the number of fines rather than a significant reduction in average particle size.

From this result it appears that manually crushing with a mortar and pestle is not an effective method of reducing the particle size of RPR. Further efforts to crush RPR used mechanical milling.

3.1.6 RPR pH stability: UV-Vis Spectroscopy of phosphate ions

Spectra of molybdenum blue complex showed a consistent absorbance peak at 830 nm, this peak was used for all calculations. There was a strong correlation. With 11 data points a linear regression using the least squares method, with intercept set to zero (all spectra were recorded against a blank sample) gave R^2=0.9943, indicating good agreement with the linear absorbance to phosphate concentration model.

RPR appears to have a buffering effect on solutions. For HNO_3 and $NaHCO_3$ solutions with initial pH ranging from 2.92 to 8.51 gave final pH in a narrow range from 7.35 to 7.87.

For solutions with initial pH below approximately 4 phosphate dissolution rates were low, resulting in phosphate concentrations below 4 ppm. Below pH 3 phosphate concentrations climbed sharply.

3.1.7 FTIR

On the recorded FTIR spectra of as supplied RPR a strong peak was observed at 1044 cm^{-1} indicative of P-O stretching and a doublet peak around 605 cm^{-1} and 570 cm^{-1} were indicative of O-P-O bending. A doublet peak was observed at 1429 cm^{-1} and 1460 cm^{-1}, and a small peak at 880 cm^{-1}. This is characteristic with carbonate C-O vibrational modes. Peaks at 3430 cm^{-1} and 1640 cm^{-1} were also observed, as with blank KBr. These peaks are consistent with water O-H vibrational modes, presumably from absorbed moisture in the KBr disks. Overall the structure is consistent with that of a combination of calcium phosphate (hydroxyapatite) and calcium carbonate.[83] This fits our expectation that RPR is mainly consisting of hydroxyapatite with some carbonate substitution. The FTIR spectrum of RPR is shown in 3.6.

3.1.8 ICP-MS

Two samples of unprocessed RPR were submitted for ICP-MS analysis. Concentrations of up to 25 elements were measured.

For several elements there were multiple readings from different isotopes. If there was a discrepancy between the two generally the major isotope would be favoured, unless that atomic mass if particularly affected by interference. In the case of Ca the dominant isotope ^{40}Ca is unusable as its signal is swamped by ^{40}Ar from the plasma torch. In this case the Ca concentrations calculated from ^{43}Ca and ^{44}Ca differed significantly. ^{44}Ca giving lower results than ^{43}Ca. By comparing the results from the two isotopes with concentrations measured by EDX, XRF and published RPR analysis results it was determined that ^{44}Ca gave more accurate readings in these tests. As the natural abundance ^{44}Ca (2.086%) is far higher than that of ^{43}Ca (0.135%) this discrepancy in the results from the two isotopes does not seem unusual. All reported Ca concentrations from ICP-MS are from the ^{44}Ca results.

For some elements multiple species were used by the internal ICP-MS calculations. In these cases where the element has a very high affinity for oxygen the mass spectrometry data for the atomic ion and the single oxide ion were both used to calculate the overall concentration. In the case of P both ^{31}P and [P-O]$^{+}$ M^{+}=47 were used, this is represented as "31-47 P" on the ICP-MS results reports. Arsenic and Silicon used similar internal calculations for their results.

Silicon results from the first set of ICP-MS results were anomalous. Results indicated implausibly high levels of silicon, over 50% of the total sample weight. Silicon is known to suffer from interference in ICP-MS measurements, with Si A=28 it has the same mass as N_2 and CO, both species which form in the plasma torch. Silicon, in the form of silica is a minor component of RPR and is relatively inert chemically. For these reasons Si measurements were not requested for later ICP-MS analyses.

From the first batch of ICP-MS samples the technician noted difficulties due to matrix interference. In order to eliminate the effects of matrix interference it was necessary to dilute the solution samples. Later the method for preparing digestion samples was modified to reduce concentration to 10% of the original method. At this concentration the ICP-MS results were of sufficiently high precision for the elements of interest while avoiding the matrix interference observed with earlier samples.

ICP-MS results for the two unprocessed RPR samples are shown in Table 3.6. Raw results from the ICP-MS solution samples and calculated concentrations in the solid RPR are shown. The first RPR sample was measured at the original high concentration and the second RPR was measured at the lower concentration. The Cd:P ratio of the first sample was 349.8 ppm and for the second sample 371.5 ppm. These values are higher than the permitted maximum Cd:P ratio for fertiliser in New Zealand (280 ppm) but are well within the normal range of values for RPR. Assuming that these results are representative of a larger batch this RPR would need to be blended with less contaminated RPR before it could be sold or manufactured as fertiliser.

The major elements found in RPR were Ca at 28.1%/23.6% sample 1/sample 2 and P at 10.6%/9.3%. This is consistent with results from EDX and XRF. Other significant elements were Na 0.98%/0.79%, Mg 0.36%/0.25%, Al 0.39%/0.20%, S 1.35%/1.58% and Fe 0.35%/0.35%. Cadmium levels in the two samples were 37.1 ppm and 34 ppm. Other trace elements detected included V, Cr, Mn, Zn, As, Ba and Pb. Uranium was also detected, there was a significant variation between the two samples at 781 ppm and 69.4 ppm.

The remaining sample mass is made up from elements not detected by ICP-MS, such as oxygen and carbon, as well as silicon which could not be measured accurately for these samples.

Although both samples are from the same batch there are significant differences in both the major and trace element concentrations. This variability was observed through all RPR samples submitted. Due to the very small samples used for ICP-MS digestions (0.2g) it is difficult to sufficiently blend a substance such as RPR. EDX analysis results indicate that individual grains of RPR differ significantly in composition, and from particle sizer results it is clear that RPR is difficult to reduce particle size without using motorised crushing equipment. We therefore

have to accept a degree of variability and uncertainty of the results for ICP-MS analysis of RPR, in that the results for a small sample cannot be considered as a precise representation of the bulk composition. There would be two approaches to increase sample homogeneity, the first would be to finely crush a large amount of RPR then blend the powdered rock together. This would take considerable time using the equipment available, as the ring mill can only handle a few tens of grams in each batch. The other approach would be to use significantly larger digestion samples. This would require a proportional increase in reagent (conc. HNO_3 and HCl) usage.

Figure 3.1: Reactive Phosphate Rock 40x magnification

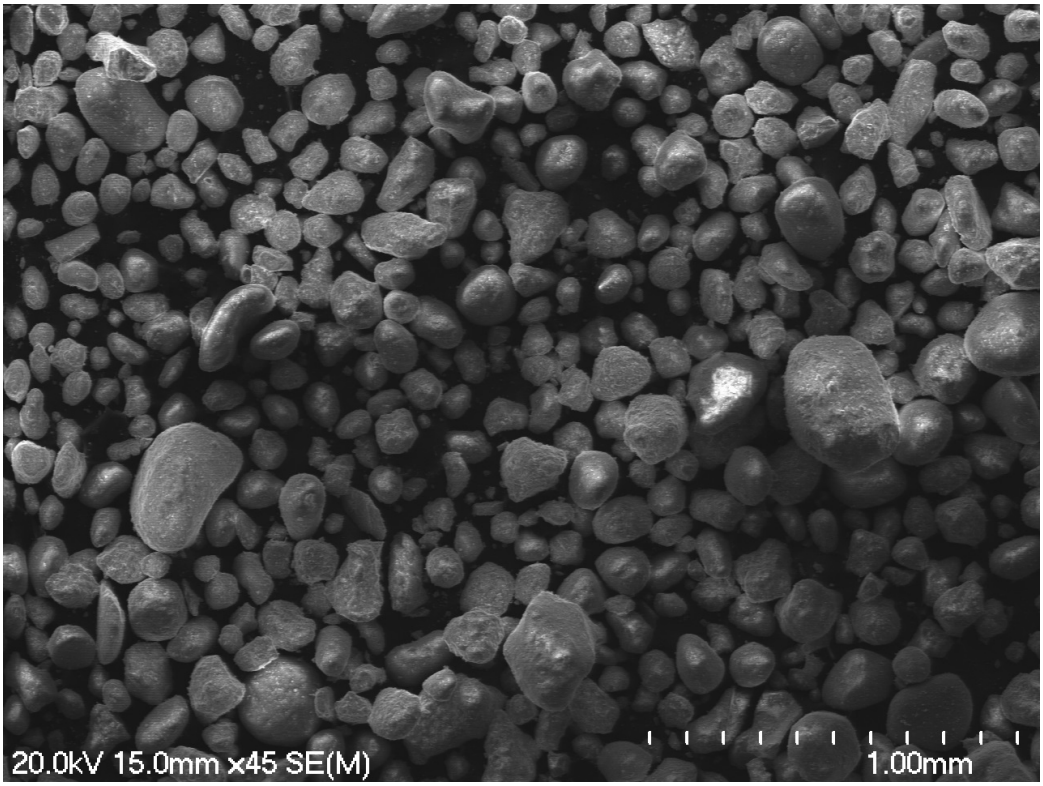

Figure 3.2: SEM micrograph of Reactive Phosphate Rock

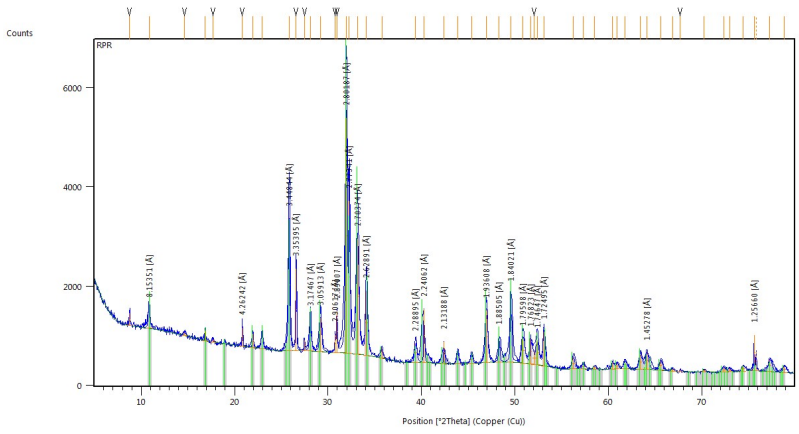

Figure 3.3: RPR XRD.

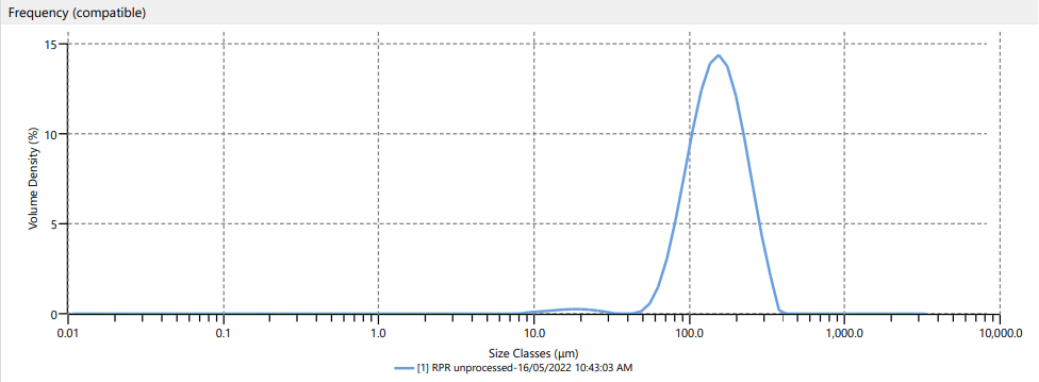

Figure 3.4: Unprocessed RPR particle sizer results.

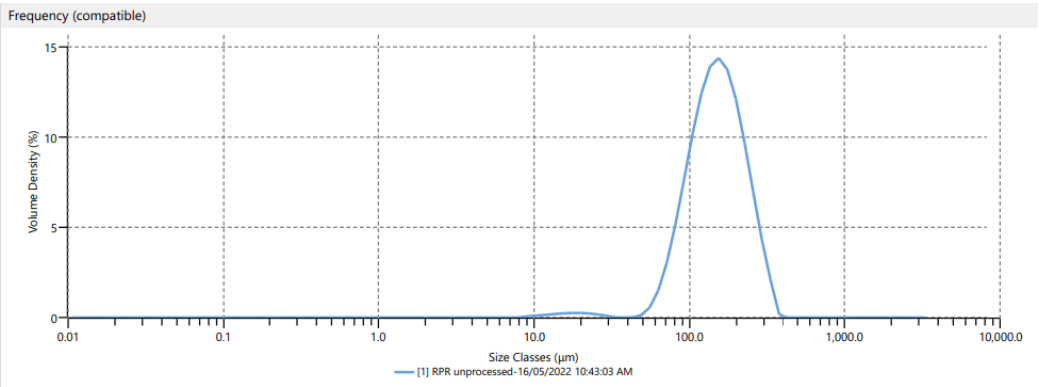

Figure 3.5: Mortar and Pestle crushed RPR sizer results.

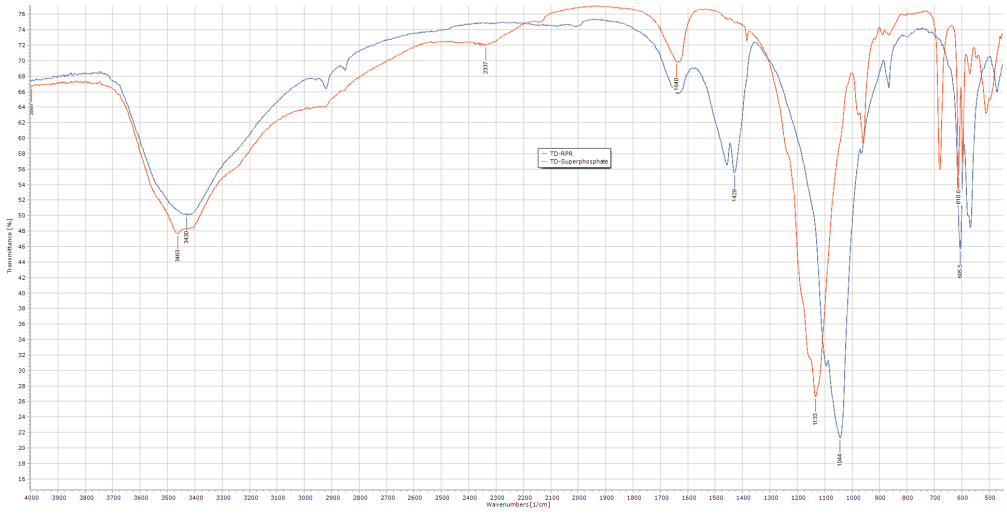

Figure 3.6: FTIR spectra of RPR and Super Phosphate.

Solution	RPR (g)	pH (initial)	pH (final)	$[PO_4^{3-}]$ (ppm)
H_2O (A)	1.0394	5.69	7.72	<0.1
H_2O (B)	1.0399	5.59	7.77	<0.1
HNO_3 0.0001% (A)	1.0016	4.72	7.75	2.6
HNO_3 0.0001% (B)	1.0256	4.76	7.65	2.3
HNO_3 0.001% (A)	1.0040	3.94	7.73	2.8
HNO_3 0.001% (B)	1.0274	3.90	7.66	2.6
HNO_3 0.01% (A)	1.0142	2.95	7.43	13.9
HNO_3 0.01% (B)	1.0041	2.92	7.35	14.3
HNO_3 0.01% (A)	1.0174	1.99	4.33	50.0
HNO_3 0.1% (B)	1.0201	1.97	4.26	45.0
HNO_3 1% (A)	1.0329	1.13	2.34	582
HNO_3 1% (B)	1.0139	1.09	2.34	577
CH_3COOH 0.0004% (A)	1.0274	4.36	7.69	2.7
CH_3COOH 0.0004% (B)	1.0309	4.43	8.42	3.5
CH_3COOH 0.004% (A)	1.0094	3.77	6.98	16.9
CH_3COOH 0.004% (B)	1.0223	3.95	8.16	4.7
CH_3COOH 0.04% (A)	1.0093	3.49	5.76	26.0
CH_3COOH 0.04% (B)	1.0086	3.48	5.42	21.9
CH_3COOH 0.04% (A)	1.0202	3.00	4.30	41.6
CH_3COOH 0.4% (B)	1.0064	2.99	4.27	41.2
CH_3COOH 4% (A)	1.0156	2.50	3.51	282
CH_3COOH 4% (B)	1.0257	2.48	3.51	255
$NaHCO_3$ 0.001% (A)	1.0134	6.37	7.77	0.2
$NaHCO_3$ 0.001% (B)	1.0062	6.49	7.86	<0.1
$NaHCO_3$ 0.01% (A)	1.0081	7.52	7.87	<0.1
$NaHCO_3$ 0.01% (B)	1.0143	7.53	7.80	<0.1
$NaHCO_3$ 0.01% (A)	1.0161	8.46	7.83	0.1
$NaHCO_3$ 0.1% (B)	1.0023	8.51	7.75	<0.1
$NaHCO_3$ 1% (A)	1.0110	8.28	7.77	2.8
$NaHCO_3$ 1% (B)	1.0094	8.29	7.85	3.3

Table 3.5: TDX013 initial/final pH and dissolved phosphate concentration.

Element	Solution 1 (ppb)	RPR 1 (ppm)	Solution 2 (ppb)	RPR 2 (ppm)
Na	39505.15	9827	3170.1	7933
Mg	14340.01	3567	988.2	2473
Al	15758.61	3920	813.5	2035
K	3719.23	925	467.9	1170
Ca	1128455.75	280710	94259.6	235884
P	425938.13	105954	37147.9	92962
S	54175.24	13476	6319.3	15813
V	262.04	65.2	23.5	58.8
Cr	603.07	150	53.5	134
Mn	262.45	65.3	41.1	103
Fe	14206.61	3533	1402.7	3510
Co	<0.000	0	0.2	0.6
Ni	<0.000	0	5.0	12.5
Cu	<0.000	0	6.0	15.1
Zn	328.27	81.7	28.3	70.7
Sr	8096.24	2013	651.9	1631
As	40.86	10.2	3.9	9.8
Se	6.33	1.57	1.8	4.5
Ag	<0.000	0	N/A	N/A
Cd	149	37.1	13.8	34
Ba	322.77	80.3	67.6	169
Hg	1.07	0.27	N/A	N/A
Tl	<0.000	0	0.3	0.7
Pb	21.44	5.33	3.9	9.7
U	3140.5	781	27.7	69.4

Table 3.6: RPR ICP-MS results

3.2 Mussel Shells

3.2.1 Mussel Shell FTIR

FTIR spectra were obtained of crushed mussel shell (unheated) as well as samples that had been heated at 300°C , 600°C , and 900°C .

The 900°C shell spectrum differed significantly from the other shell spectra. A strong, narrow peak at 3650cm^{-1} was present. This peak is due to O-H stretching in calcium hydroxide and indicates that calcination of $CaCO_3$ to CaO, followed by partial hydration to $Ca(OH)_2$ had occurred. This is consistent with the altered physical appearance of the 900°C heated shell. Calcium oxide will in turn undergo carbonation by interaction with CO_2 in air. As the samples had sat in air for several months prior to recording the spectra it is not possible to determine if the carbonate present in the 900°C shell spectrum is from un-reacted solid or from entirely from carbonation of $Ca(OH)_2$.

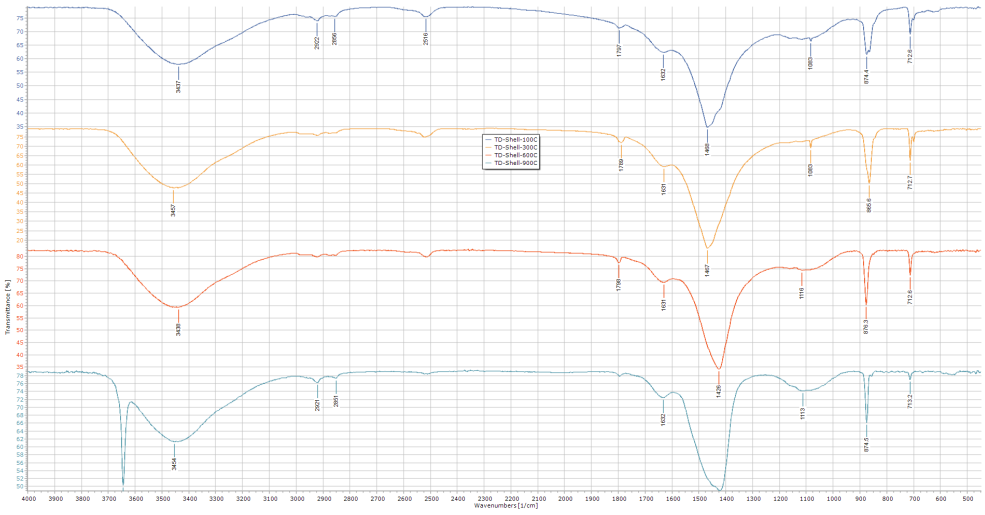

Figure 3.7: FTIR spectra heated mussel shells

3.2.2 Mussel Shell X-ray Fluoresce

Major element analysis showed that the calcium and carbon oxides made up the great majority (96-98%) of the fusion disc samples. This is consistent with expectations that mussel shells are made up of calcium carbonate with a small amount of organic matrix and trace levels of other minerals.

Sample	SiO_2 (%)	Al_2O_3 (%)	TiO_2 (%)	MnO (%)	Fe_2O_3 (%)
Shell 100°C	1.15	0.27	0.019	0.004	0.0881
Shell 300°C	0.01	0.04	0.013	0.006	0.03836
Shell 600°C	0.00	0.02	0.009	0.001	0.03594
Shell 900°C	0.23	0.08	0.011	0.004	0.08903
Sample	MgO (%)	CaO (%)	Na_2O (%)	K2O (%)	P2O5 (%)
Shell 100°C	0.156	51.56	0.864	0.05	0.020
Shell 300°C	0.131	53.969	0.833	0.09	0.020
Shell 600°C	0.166	54.708	0.836	0.02	0.020
Shell 900°C	0.215	66.343	0.766	0.04	0.021
Sample	SO3 (%)	SrO (Sr - ppm)	BaO (Ba - ppm)	CO2 (%)	Sum (%)
Shell 100°C	0.35	857	3	45.27	99.901
Shell 300°C	0.36	901	3	44.48	100.098
Shell 600°C	0.46	892	3	43.71	100.086
Shell 900°C	0.56	1058	3	31.49	99.979

Table 3.7: Mussel Shell XRF results - Majors

3.2.3 RPR X-ray Diffraction

For mussel shells dried at 100°C the best Highscore match to the recorded scatter pattern was for two compounds: calcium carbonate (aragonite) with a score of 64, Displacement [°2Th.] of 0.000 and Scale Factor of 0.618; and calcium carbonate (calcite) with a score of 60, Displacement [°2Th.] of 0.000 and Scale Factor of 0.895. The relative composition was 65% aragonite and 35% calcite.

For mussel shells heated to 300°C the best Highscore match to the recorded scatter pattern was for two compounds: calcium carbonate (calcite) with a score of 75, Displacement [°2Th.] of 0.000 and Scale Factor of 0.311; and calcium carbonate (aragonite) with a score of 70, Displacement [°2Th.] of 0.000 and Scale Factor of 0.981. The relative composition was 52% calcite and 48% aragonite.

For mussel shells heated to 600°C the best Highscore match to the recorded scatter pattern was for one compound: calcium carbonate (calcite) with a score of 82, Displacement [°2Th.] of 0.000 and Scale Factor of 0.879.

For mussel shells heated to 900°C the best Highscore match to the recorded scatter pattern was for two compounds: calcium hydroxide with a score of 70, Displacement [°2Th.] of 0.000 and Scale Factor of 0.942; and calcium carbonate (calcite) with a score of 66, Displacement [°2Th.] of 0.000 and Scale Factor of 0.798. The relative composition was 52% calcium hydroxide and 48% calcite.

As expected from the physical appearance of the samples calcination had occurred to shells heated to 900°C but not at 600°C or lower. A significant amount

Sample	Sc (ppm)	V (ppm)	Cr (ppm)	Co (ppm)	Ni (ppm)
Shell 100°C	74	1	0	3	3
Shell 300°C	77	2	0	3	3
Shell 600°C	75	1	0	3	3
Sample	Cu (ppm)	Zn (ppm)	Ga (ppm)	As (ppm)	Rb (ppm)
Shell 100°C	5	4	1	9	6
Shell 300°C	5	4	1	9	34
Shell 600°C	5	5	1	9	6
Sample	Sr (ppm)	Y (ppm)	Zr (ppm)	Nb (ppm)	Mo (ppm)
Shell 100°C	833	0	11	0	4
Shell 300°C	796	0	12	0	4
Shell 600°C	722	0	12	0	4
Sample	Sn (ppm)	Sb (ppm)	Cs (ppm)	Ba (ppm)	La (ppm)
Shell 100°C	0	0	33	3	0
Shell 300°C	0	0	30	4	0
Shell 600°C	0	0	33	4	0
Sample	Ce (ppm)	Nd (ppm)	Pb (ppm)	Th (ppm)	U (ppm)
Shell 100°C	0	9	3	8	3
Shell 300°C	0	5	3	9	3
Shell 600°C	0	5	3	6	3

Table 3.8: Mussel Shell XRF results - Traces

of calcium carbonate was observed in the 900°C sample, indicating incomplete calcination. It is also possible that some calcium hydroxide converted back to calcium carbonate by absorbing CO_2 from the air over the several months that passed between heating the shell samples and measuring their diffraction patterns. It is interesting to note that the crystal structure of $CaCO_3$ changes with heating. For shells heated to 100°C the major crystal structure was aragonite, by 600°C all $CaCO_3$ was converted to Calcite. Unheated shells were not tested here as all samples were dried at 100°C in preparation for XRF/XRD analysis. The thermodynamic equlibrium between calcite and aragonite has been studied extensively[84,85,86]. As calcite and aragonite have slightly different physical properties this may have applications to the use of mussel shells as a source of calcium ions in solution.

3.2.4 ICP-MS

Greenshell mussel shell contained low levels of Cadmium. Mussels, as with other shellfish species, absorb cadmium from the environment. It has been reported for

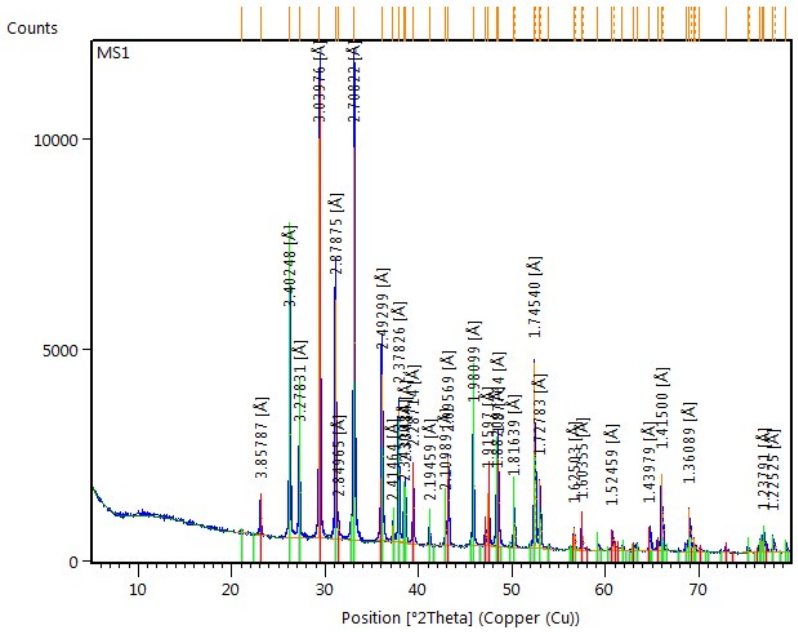

Figure 3.8: Mussel Shell 100°C XRD.

other shellfish species that the majority of accumulate cadmium is found in their meat and relativity little is deposited in their shells.[87]

Only one shell sample was analysed. Further testing would be required to establish the average cadmium levels in mussel shell and to determine if there are any variations due to mussel farm location, size of shell (age of the mussel) or other factors.

The cadmium concentration found in this mussel shell sample was 2.45 ppm. This is low compared to RPR and so should not prove to be an issue for use as a calcium ion source for decontamination. There may however be something of an image problem. Using a decontamination product that is known to be already contaminated itself invites criticism. Other sources of calcium ions such as limestone are also known to contain cadmium.[88]

3.2.5 UV-Vis Mussel Shell Solutions

Although prepared under the same conditions solutions of mussel shell heated to 300°C and unheated mussel shell had different colour. 300°C shell solution was bright yellow in colour while unheated shell solution was very pale yellow, almost colourless. This corresponds to the recorded UV-Vis spectra of these (undiluted) solutions Fig. 3.12. The 300°C shell solution showed a strong peak at 240 nm,

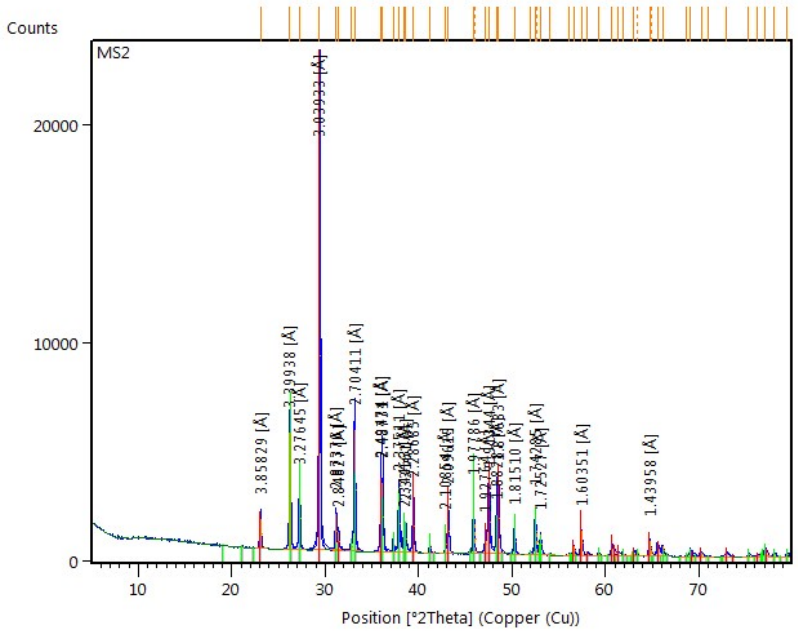

Figure 3.9: Mussel Shell 300°C XRD.

extending into the visible region (>400 nm). This peak was also observed for the unheated shell solution but the absorbance was much lower and extension into the visible region was minimal. It is not clear why heating mussel shells enhances the solution colour. It is possible that the high temperature caused organic compounds within the mussel shell to undergo a Maillard reaction or some form of pyrolysis to produce coloured species. Mussel shells are known to contain proteins, polysaccharides and glycoproteins,[89] any of which could contribute to this observed colour change.

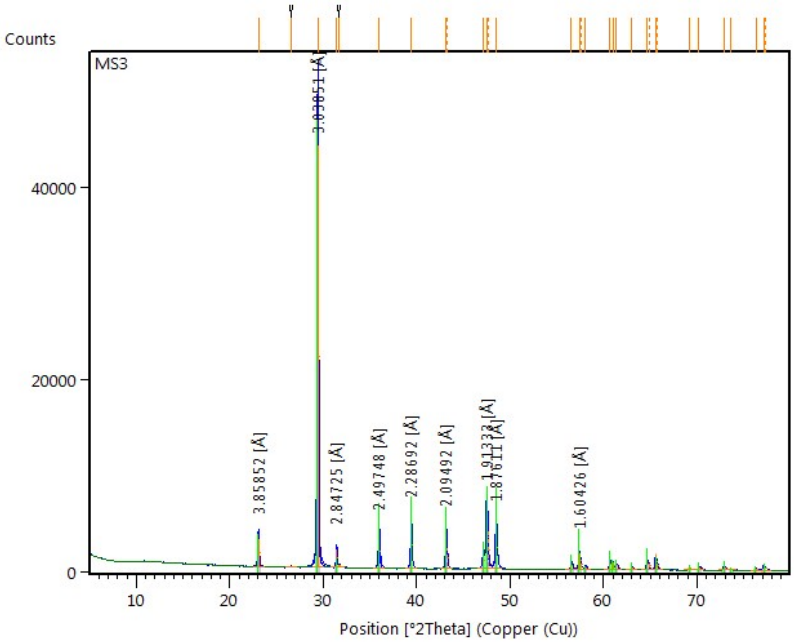

Figure 3.10: Mussel Shell 600°C XRD.

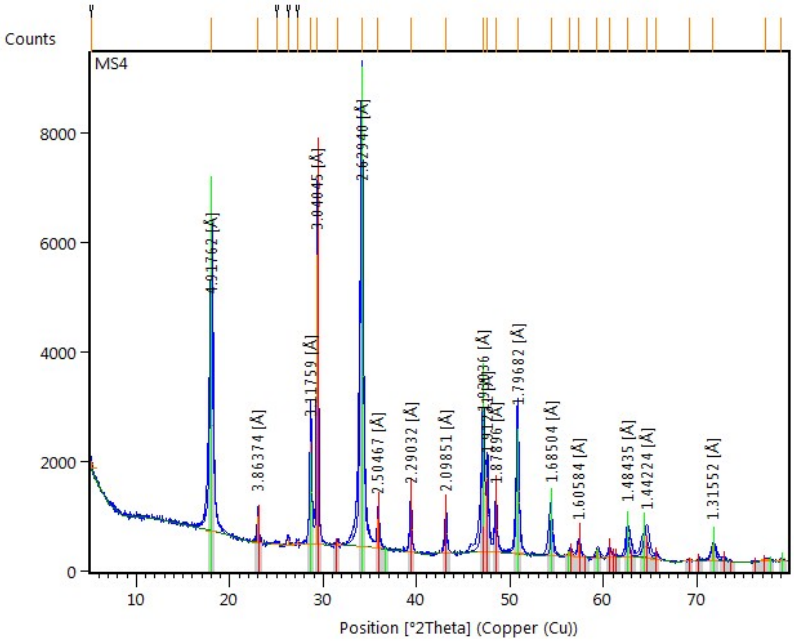

Figure 3.11: Mussel Shell 900°C XRD.

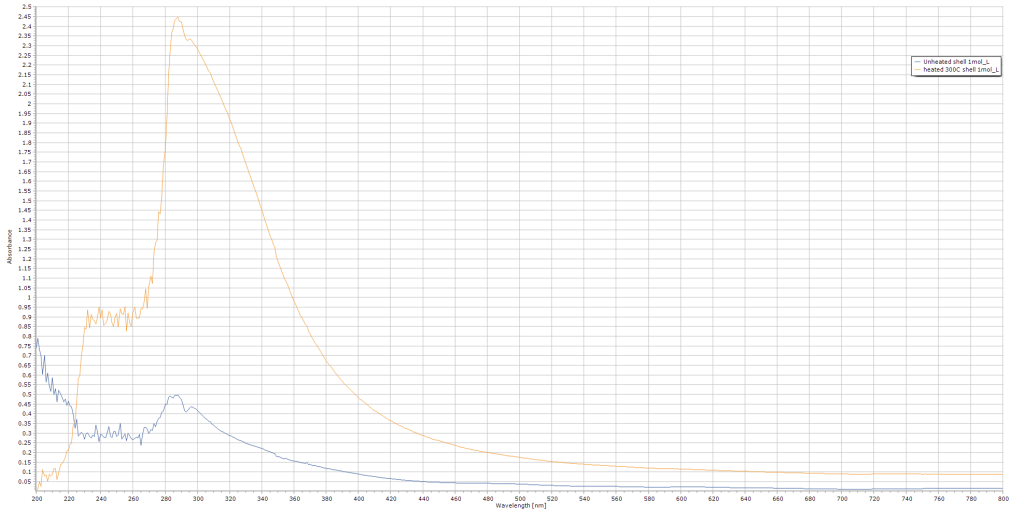

Figure 3.12: UV-Vis spectra of HCl dissolved mussel shell solutions.

3.3 SSP and other Fertilisers

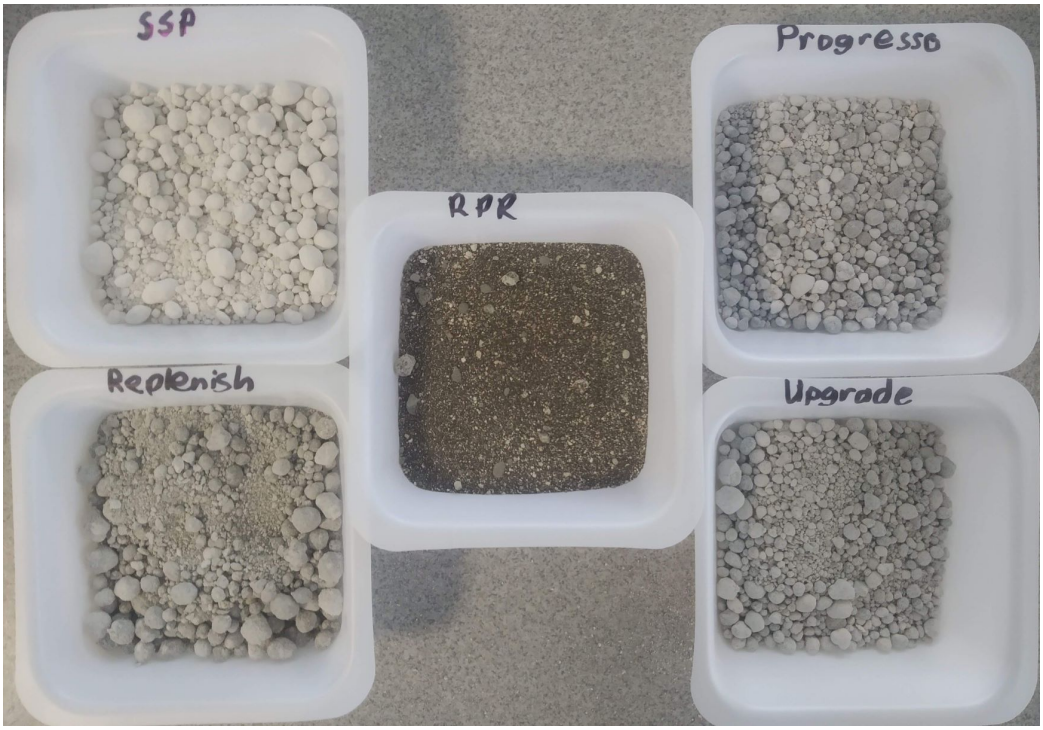

Figure 3.13: RPR, SSP, Progresso, Replenish and Upgrade fertilisers.

3.3.1 FTIR

SSP

Compared to RPR the characteristic P-O vibrational modes were observed at slightly higher wavenumbers. The strong P-O stretch peak was observed at 1133 cm^{-1} and the O-P-O bend doublet at 780 cm^{-1} and 610 cm^{-1}. No carbonate peaks were observed. The spectrum recorded was consistent with published single super phosphate FTIR spectra.[90]

The observations are consistent our expectations based on the SSP manufacturing process. Carbonates in RPR will react with sulphuric acid, releasing CO_2 gas. The difference in location of the P-O stretch reflects the different chemical structure of RPR and SSP. In RPR the phosphate ions are contained in a calcium phosphate (apatite) crystalline lattice, whereas SSP contains mono calcium phosphate. The FTIR spectrum of SSP is shown in Fig.3.6.

Other Fertilisers

FTIR spectra for "Progresso" and "Replenish" were very similar to that of SSP. The location of the P-O stretch peak at 1136 cm^{-1} (Progresso) and 1134 cm^{-1} (Replenish) are the same energy as for SSP. There were no prominent peaks on these spectra that were not observed for SSP.

For "Upgrade" a strong peak at 1428 cm^{-1} and a sharp peak at 875 cm^{-1} were observed. This is characteristic with carbonate C-O vibrational modes. The location of the P-O stretch peak was at 1138 cm^{-1}. Overall the FTIR spectrum of Upgrade is markedly different from both RPR and SSP.

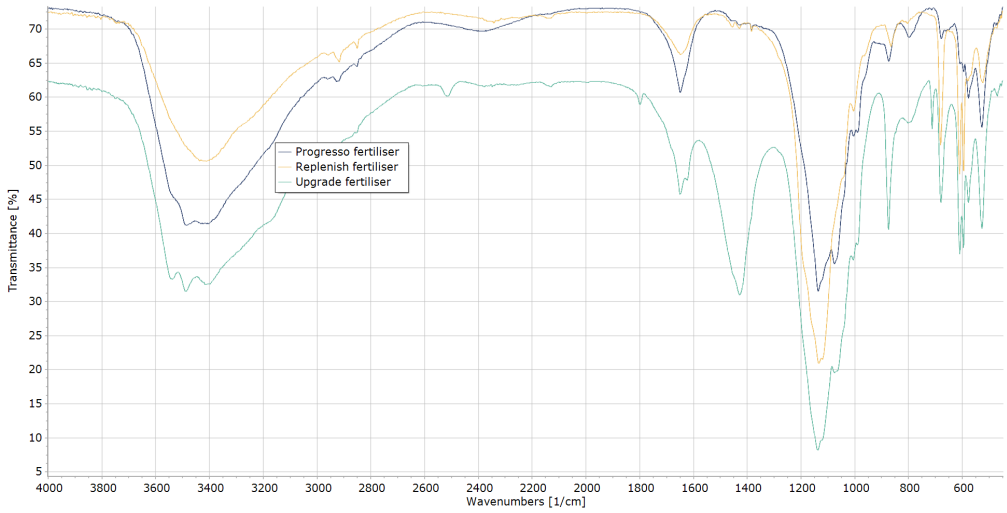

Figure 3.14: FTIR spectra of "Progresso", "Replenish" and "Upgrade" fertilisers.

3.3.2 SSP X-ray Fluoresce

XRF results for SSP were anomalous. The calculated sum composition amounts to 115% of the weighed sample mass. We observed unexpected results for CO_2 content. Since SSP is manufactured by treating RPR with concentrated sulphuric acid we would expect that carbonates present would react and the carbon lost as CO_2 gas. A possible explanation for these results is from evaporation of H_2O contained in gypsum as water of crystallisation during heating. The mass of lost H_2O would then have been attributed to CO_2 by the loss on ignition calculation.

3.3.3 SSP X-ray Diffraction

The best Highscore match to the recorded scatter pattern was for two compounds: Calcium Sulphate with a score of 70, Displacement [°2Th.] of 0.000 and Scale

Sample	SiO_2 (%)	Al_2O_3 (%)	TiO_2 (%)	MnO (%)	Fe_2O_3 (%)
SSP	3.25	0.68	0.039	0.027	0.4463
Sample	MgO (%)	CaO (%)	Na_2O (%)	K2O (%)	P2O5 (%)
SSP	0.364	30.536	0.196	0.14	20.801
Sample	SO3 (%)	SrO (Sr - ppm)	BaO (Ba - ppm)	CO2 (%)	Sum (%)
SSP	28.15	487	229	30.37	115.074

Table 3.9: SSP XRF results - Majors

Sample	Sc (ppm)	V (ppm)	Cr (ppm)	Co (ppm)	Ni (ppm)
SSP	31	39	64	6	24
Sample	Cu (ppm)	Zn (ppm)	Ga (ppm)	As (ppm)	Rb (ppm)
SSP	13	125	1	17	8
Sample	Sr (ppm)	Y (ppm)	Zr (ppm)	Nb (ppm)	Mo (ppm)
SSP	343	50	30	0	4
Sample	Sn (ppm)	Sb (ppm)	Cs (ppm)	Ba (ppm)	La (ppm)
SSP	0	0	10	184	66
Sample	Ce (ppm)	Nd (ppm)	Pb (ppm)	Th (ppm)	U (ppm)
SSP	126	73	3	4	14

Table 3.10: SSP XRF results - Traces

Factor of 0.908; and Hydrogen Calcium Phosphate Hydrate with a score of 55, Displacement [°2Th.] of 0.000 and Scale Factor of 0.180. The calculated composition was 76% Calcium Sulphate and 24% Hydrogen Calcium Phosphate Hydrate.

3.3.4 ICP-MS

The sample of Super phosphate tested showed lower cadmium levels than the RPR samples. This is likely due to being manufactured from a less contaminated batch of RPR. The process of making super phosphate is a reaction between RPR and sulphuric acid, nothing is removed in the process so there is no apparent mechanism for reducing cadmium levels. The Cd:P ratio of this sample was below the industry maximum level of 280 ppm.

The sample of "Progresso" fertiliser did not contain detectable levels of cadmium, its phosphorous content was 24% higher than super phosphate. A sample of "Replenish" fertiliser contained about 24% less phosphorus than RPR and had a Cd:P ratio of 244 ppm. A sample of "Upgrade" fertiliser contained about

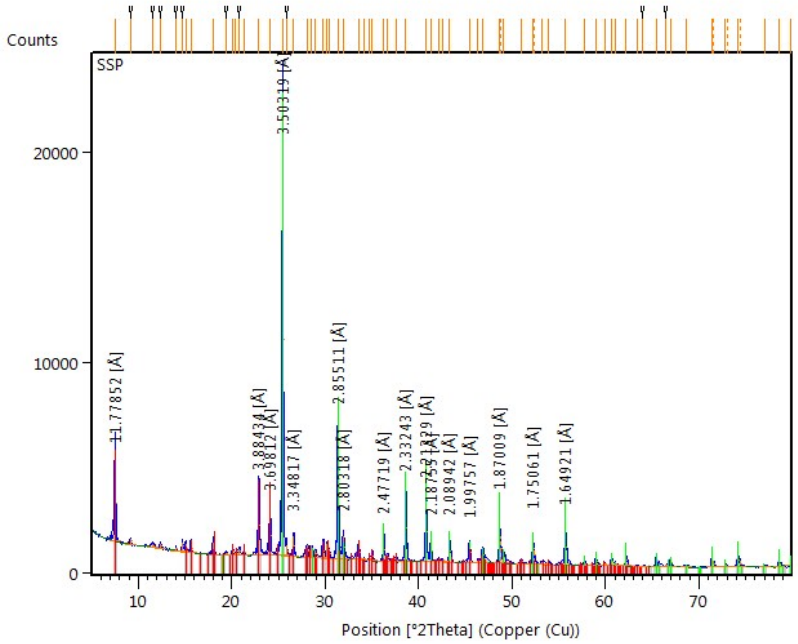

Figure 3.15: SSP XRD.

38% less phosphorus than RPR and had a Cd:P ratio of 237 ppm.

A summary of the major plant nutrient content, as well as cadmium, for RPR, Super phosphate, Progresso, Replenish and Upgrade is provided in Table**??**. Nitrogen was not measured by ICP-MS so nitrogen content of the fertilisers is not available.

Fertiliser	Ca	P	K	S	Mg	Cd	Cd:P
RPR	31.60%	9.29%	0.12%	1.56%	0.25%	34.3 ppm	370 ppm
Super phosphate	19.33%	9.85%	0.12%	9.96%	0.21%	12.9 ppm	131 ppm
Progresso	15.09%	12.23%	0.23%	1.34%	0.61%	0	-
Replenish	25.60%	7.08%	0.11%	6.96%	0.20%	17.3 ppm	244 ppm
Upgrade	28.01%	5.73%	0.15%	3.54%	0.25%	13.6 ppm	237 ppm

Table 3.11: Fertiliser ICP-MS results

From the relative concentrations of P, Cd, S and Ca it appears probable that Replenish and Upgrade are blends containing super phosphate or RPR while Progresso is blended from another more highly refined phosphate fertiliser.

3.4 Heated RPR Cd extraction

There was no evidence of correlation between elevated temperature (50-90°C) and RPR Cd levels with $Ca(NO_3)_2$ extraction. There was a statistically significant difference between RPR Cd levels for $Ca(NO_3)_2$ extractions at neutral pH (6.75) and mildly acidic pH (3.22). P and Cd results from ICP-MS digestion samples are summarised in Table3.12.

Sample	Solution	pH	Temperature	P (ppb)	Cd (ppb)	Cd:P (ppm)
1	$1molL^{-1}$ $Ca(NO_3)_2$	6.75	50°C	444542.33	124.62	280.3
2	$1molL^{-1}$ $Ca(NO_3)_2$	6.75	60°C	320345.9	90.81	283.5
3	$1molL^{-1}$ $Ca(NO_3)_2$	6.75	70°C	482369.44	141.24	292.8
4	$1molL^{-1}$ $Ca(NO_3)_2$	6.75	80°C	439256.24	111.87	254.7
5	$1molL^{-1}$ $Ca(NO_3)_2$	6.75	90°C	395978.17	142.24	359.2
6	$1molL^{-1}$ $Ca(NO_3)_2$	3.22	50°C	515916.45	122.11	236.7
7	$1molL^{-1}$ $Ca(NO_3)_2$	3.22	60°C	531945.05	118.68	223.1
8	$1molL^{-1}$ $Ca(NO_3)_2$	3.22	70°C	496241.46	111.46	224.6
9	$1molL^{-1}$ $Ca(NO_3)_2$	3.22	80°C	490037.47	115.29	235.3
10	$1molL^{-1}$ $Ca(NO_3)_2$	3.22	90°C	475139.89	110.02	231.6

Table 3.12: Heated $Ca(NO_3)_2$ extractions: Cd and P in RPR residues

A graph of Cd:P ratio of RPR residues against extraction solution temperature is shown in Fig.3.16. Linear regression can be used to determine if there is evidence of a directly proportional relationship between two variables, in this case temperature and Cd:P ratio, or if there is no evidence of a relationship (the null hypothesis). Using linear sum of squares regression on pH 6.75 extractions gives an equation of $y = 1.2896x + 203.83$, where y is the Cd:P level in residual RPR and x is temperature, the R^2 value is 0.2728. The contribution from the temperature term is small and the R^2 value is very poor so there is no evidence to reject the null hypothesis. For pH 3.22 extractions the sum of squares linear regression model gives and equation of $y = 0.019x + 228.92$ and an R^2 value of 0.0024. This is a very weak contribution from the temperature term and an exceptionally poor R^2 value. Again there is no evidence to reject the null hypothesis.

If we assume that there is in fact no correlation between temperature and Cd:P in RPR residues then the effects of pH can be compared using a t-test. The null hypothesis is that there is zero difference in mean Cd:P values between extraction at the two pH levels. The results obtained from a two sample t-test, assuming unequal variances and a 95% confidence interval($\alpha = 0.05$), are summarised in Table 3.13. The resulting two-tailed P value is 0.022503, thus the null hypothesis is rejected, this is moderate evidence of a true difference between Cd:P ratios of

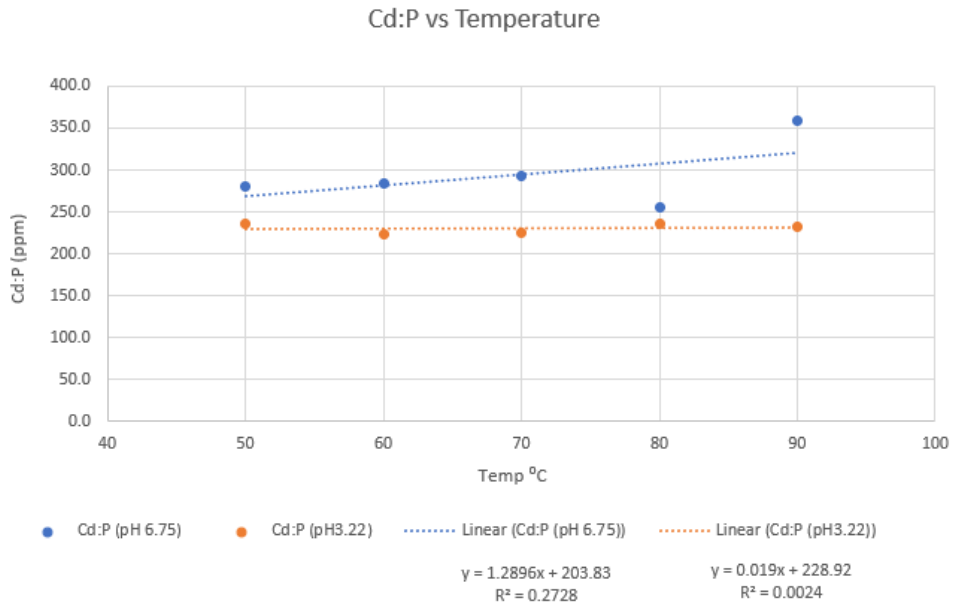

Figure 3.16: Cd:P vs temperature for $Ca(NO_3)_2$ extractions

RPR subjected to extraction solutions at pH 6.75 and pH 3.22. This is a promising result that suggests that adding a small amount of acetic acid to calcium nitrate extraction solutions can have a significant effect of Cd extraction. More trials would be required to establish confidence in these results.

	Cd:P (pH 6.75)	Cd:P (pH 3.22)
Mean	294.101	230.244
Variance	1524.382	37.790
Observations	5	5
Hypothesised Mean Difference	0	
df	4	
t stat	3.61267	
P(T$\leq$ t) two tail	0.022503	
t Critical two-tail	2.77645	

Table 3.13: Solution pH Heated $Ca(NO_3)_2$ extractions: t-test results

For $CaCl_2$ extraction solutions there appeared to be a slight difference in Cd levels between high temperature (90°C) and room temperature (20°C) Table3.14. Cd levels in the extraction solution were higher at 90°C than 20°C while residual Cd levels in the RPR were slightly lower. Using a two sample t-test, assuming unequal variances and a 95% confidence interval($\alpha = 0.05$) there is moderate

evidence of a true difference between Cd levels in the extraction solution (P value 0.022109), while there is insufficient evidence to reject the null hypothesis for a difference in Cd levels in the RPR residues (P value 0.155471). More trials are necessary to establish if there is a benefit to heating $CaCl_2$ extraction solutions.

Sample	Solution	Temperature	Solution Cd (ppb)	RPR Cd (ppb)
1	Shell $CaCl_2$ (1 $molL^{-1}$)	20	74.4	12.8
2	Shell $CaCl_2$ (1 $molL^{-1}$)	20	73.7	12.7
3	Shell $CaCl_2$ (1 $molL^{-1}$)	90	107.5	11.9
4	Shell $CaCl_2$ (1 $molL^{-1}$)	90	109.8	12.2

Table 3.14: Heated $CaCl_2$ Cd extraction results

3.5 Microwave heated RPR extraction

3.5.1 Effects of Microwave heating time

ICP-MS results for microwave heated calcium chloride extractions showed progressively lower Cd:P with increased microwave irradiation time. Extraction solutions showed a corresponding increase in Cd levels with increasing microwave irradiation. All microwave irradiated samples showed reduced Cd:P compared to the control sample. Microwave heating without calcium ions (RPR in water) was not effective in extracting Cd. To test for a linear correlation between microwave irradiation time and Cd concentration in extraction solution a linear sum of squares regression was used, resulting in an equation of $y = 81.1x + 171$ where y is dissolved Cd (ppm) and x is microwave irradiation time (min). The relatively large positive controlled variable term is promising, consistent with increased Cd extraction with microwave irradiation. The R^2 value was 0.8798, this indicates a weak correlation, there is insufficient evidence to reject the null hypothesis. Similarly for Cd levels remaining in the RPR residues a linear sum of squares regression gave an equation of $y = -0.774x + 28.1$ where y is Cd concentration in RPR(ppm) and x is microwave irradiation time (min). In this case the negative controlled variable term is consistent with increased Cd extraction with microwave irradiation. Again the R^2 value, 0.8989, was too low to reject the null hypothesis. The seemingly promising results but low statistical significance indicate that larger sample sizes should be used.

Sample	Solution	Microwave time	solution P (ppb)	solution Cd (ppb)
1	1molL^{-1} $CaCl_2$	0 min	57354.6	292.1
2	1molL^{-1} $CaCl_2$	2 min	87001.9	326.0
3	1molL^{-1} $CaCl_2$	4 min	60990.8	452.3
4	1molL^{-1} $CaCl_2$	7 min	71140.7	529.5
5	1molL^{-1} $CaCl_2$	12 min	165205.1	1281.0
6	H_2O	12 min	472356.9	115.4

Table 3.15: Microwave heated extractions: Cd and P dissolved into extraction solution

3.5.2 Effects of Cd stabilising ligands

From the results of TDX020 solutions containing 1M $CaCl_2$ and 0.1% ligand (Mercaptosuccinic acid (MSA), potassium bitartrate or EDTA) did not show improved Cd extraction compared to $CaCl_2$ solutions without ligands Fig 3.19. Calcium

Sample	Solution	Microwave time	RPR P (ppm)	RPR Cd (ppm)	Cd:P (ppm)
1	1molL^{-1} $CaCl_2$	0 min	105612.8	29.6	280.1
2	1molL^{-1} $CaCl_2$	2 min	99509.1	24.8	249.2
3	1molL^{-1} $CaCl_2$	4 min	98918.3	25.5	257.9
4	1molL^{-1} $CaCl_2$	7 min	100508.0	22.3	221.6
5	1molL^{-1} $CaCl_2$	12 min	98323.5	19.3	196.3
6	H_2O	12 min	98402.4	34.7	352.7
RPR	-	-	92916.2	34.4	370.2

Table 3.16: Microwave heated extractions: Cd and P in RPR residues

chloride extractions solutions containing these ligands showed lower concentrations of cadmium after microwave extraction than solutions with no ligand present. This test only considered a small number of ligands at a single concentration and pH. There are many other possible ligands and limitless combinations of salt concentration, ligand concentration and pH, some of which may have significantly different effects. Far more investigation is required before drawing any conclusions on the effects on Cd complexing ligands on extraction potential.

Code	Solution	Ca (ppb)	P (ppb)	Cd (ppb)
TDX020-1	1M $CaCl_2$	97039	53046	8.1
TDX020-2	2M $CaCl_2$	127408	64368	10.6
TDX020-3	3M $CaCl_2$	95885	50865	7.0
TDX020-4	1M $CaCl_2$ + MSA	119747	59630	16.7
TDX020-5	1M $CaCl_2$ + Potassium tartrate	121698	60123	11.3
TDX020-6	1M $CaCl_2$ + EDTA	117498	61338	11.5

Table 3.17: TDX020 microwave extraction RPR residues ICP-MS digestion results

Code	Solution	Ca (ppb)	P (ppb)	Cd (ppb)
TDX020-1	1M $CaCl_2$	357774	306.5	28.9
TDX020-2	2M $CaCl_2$	596167	79.7	27.1
TDX020-3	3M $CaCl_2$	906747	184.7	27.5
TDX020-4	1M $CaCl_2$ + MSA	467662	56.6	16.9
TDX020-5	1M $CaCl_2$ + Potassium tartrate	320848	63.6	23.4
TDX020-6	1M $CaCl_2$ + EDTA	354100	102.5	24.4

Table 3.18: TDX020 microwave extraction solutions ICP-MS results

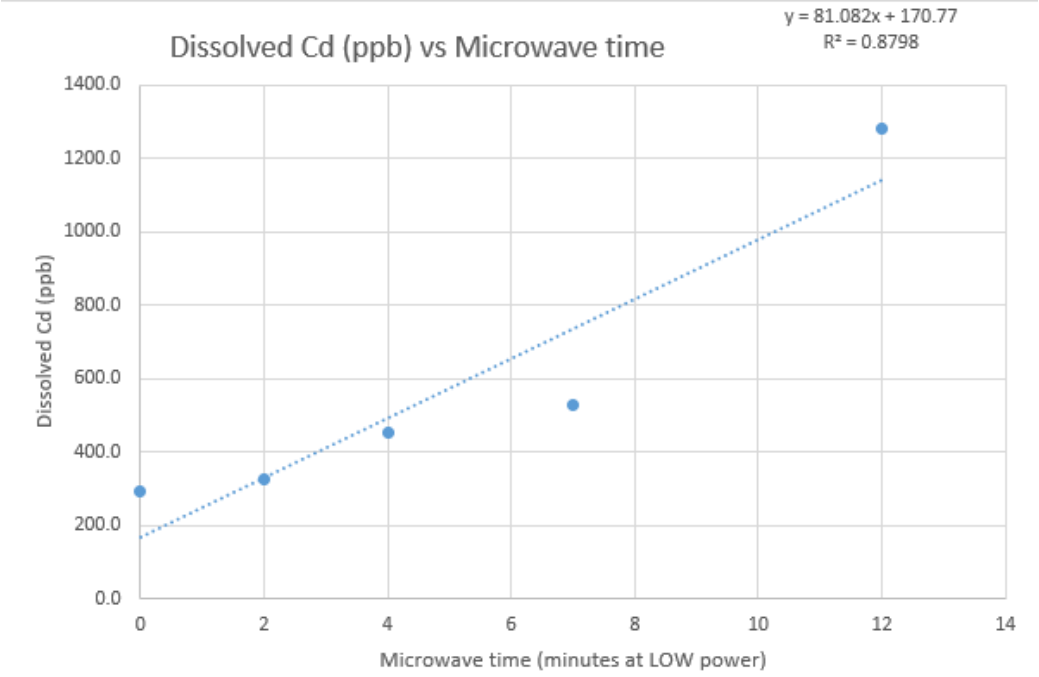

Figure 3.17: Cd concentration in microwave extraction solutions.

3.5.3 Effects of $CaCl_2$ concentration

$CaCl_2$ solutions of 1 mol L^{-1}, 2 mol L^{-1} and 3 mol L^{-1} were tested with microwave extraction. From this test there is no evidence that higher $CaCl_2$ concentrations significantly enhanced Cd extraction over a 1 molL^{-1} extraction. With the three samples tested there was very little variation in extracted Cd, as shown in Table 3.20. Applying linear sum of squares regression results in an equation of $y = -68.2x + 2920.9$ where x is calcium chloride concentration (mol L^{-1}) and y is extracted Cd (ppb), see Figure 3.20. The contribution of the controlled variable (x) is very small. The R^2 value of 0.5052 is very poor, therefore these results provide no evidence of a correlation between $CaCl_2$ concentrations and Cd extraction, though with only three data point it is unlikely that we would observe a statistically significant result.

Similarly the residual cadmium levels in RPR samples after microwave extraction showed no correlation to $CaCl_2$ concentrations of 1 mol L^{-1}, 2 mol L^{-1} and 3 mol L^{-1}. Applying linear sum of squares regression results in an equation of $y = -7.75x + 167$ where x is calcium chloride concentration (mol L^{-1}) and y is residual Cd:P (ppm), see Figure 3.21. The contribution of the controlled variable (x) is small. The R^2 value of 0.311 is very poor, therefore these results provide no evidence of a correlation between $CaCl_2$ concentrations and Cd extraction, though

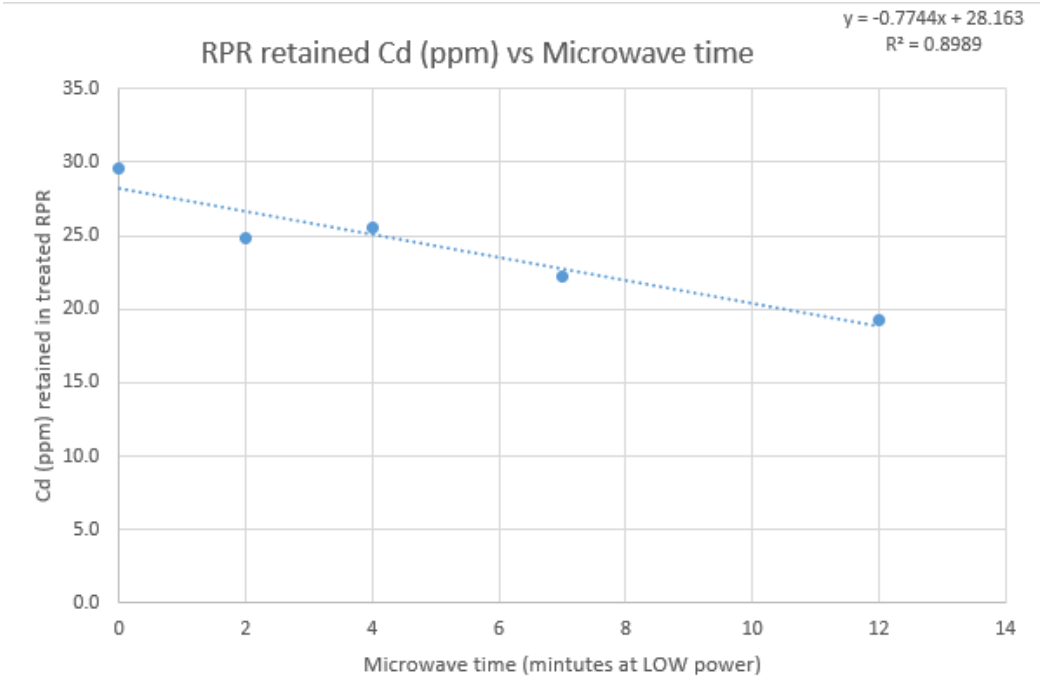

Figure 3.18: Cd concentration in RPR after microwave extraction.

once again it is unlikely that we would observe a statistically significant result from only three data points.

$[CaCl_2]$ (mol L^{-1})	[Cd] ppb
1	2891.7
2	2706.6
3	2755.3

Table 3.19: Extracted cadmium vs calcium chloride concentration, with microwave heating.

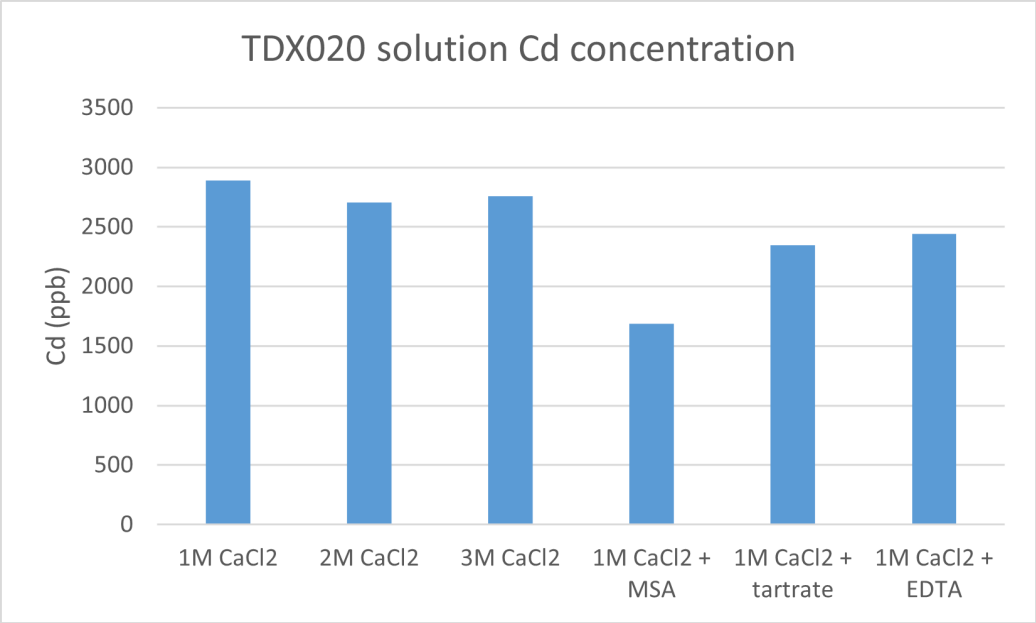

Figure 3.19: Cd concentrations in microwave $CaCl_2$ extraction solutions with ligands.

[$CaCl_2$] (mol L^{-1})	Cd:P (ppm)
1	153
2	165
3	137

Table 3.20: Residual Cd:P in RPR vs calcium chloride concentration, after microwave extraction.

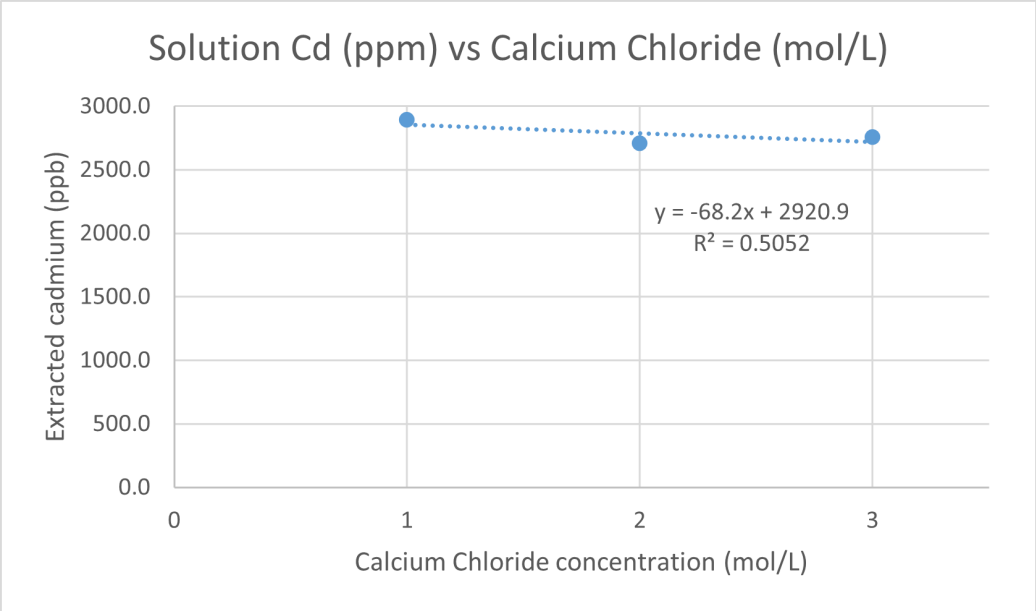

Figure 3.20: Results of increased $CaCl_2$ concentration on Cd extraction by microwave method.

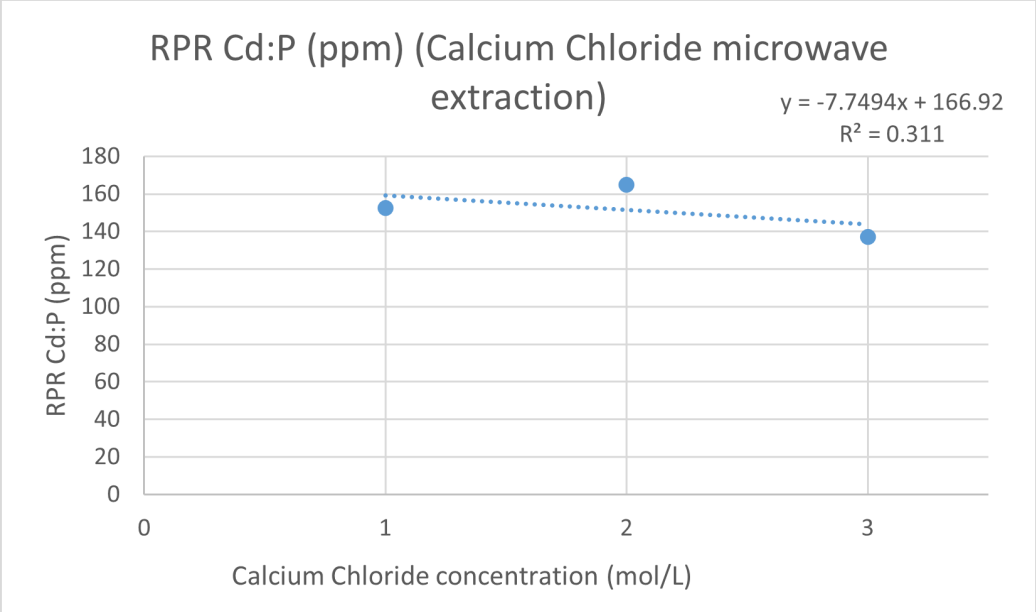

Figure 3.21: Results of increased $CaCl_2$ concentration on residual Cd in RPR.

3.6 Column RPR Cd extraction

3.6.1 TDX012, TDX014 and TDX015

The following solutions were tested in extraction columns:
$CaCl_2$ (1 mol L^{-1});
Mussel shell dissolved in HCl (unknown concentration):
KCl (2 mol L^{-1});
Mussel shell dissolved in HNO_3 (unknown concentration):
$Ca(CH_3COO)_2$ (1 mol L^{-1});
$Ca(NO_3)_2$ (1 mol L^{-1});
$MgCl_2$ (1 mol L^{-1});
Distilled water.

Distilled water was the least effective extracting agent, removing far less Cd than any of the salt solutions. $CaCl_2$ extractions showed consistently the best results of the tested solutions. $Ca(CH_3COO)_2$ was less effective than $CaCl_2$ but better than $Ca(NO_3)_2$. $MgCl_2$ (1 mol L^{-1}) and KCl (2 mol L^{-1}) were more effective than $Ca(NO_3)_2$.

These results suggest that both cation and anion have an effect on Cd extraction. Since water alone was ineffective at extracting cadmium it appears that ions in solution are driving the reaction by either displacing cadmium ions from the crystal lattice or by stabilising cadmium ions in solution.

Of the anions tested Cl^- had the greatest Cd extraction effect. This could be due to Cd^{2+} ions forming a chloride complex in solution, thereby stabilising dissolved Cd^{2+}. Cadmium is known to form a number of chloride complexes in aqueous solution; the most favoured complex depends on solution conditions including concentration, temperature and pH.[91] This also suggests that it may be possible to achieve more effective Cd extraction by using ligands that selectively bind to Cd^{2+}.

The concentration of Cd in extraction solutions are shown in Fig. 3.22. For all the solutions prepared from lab salts the first extraction solution contained the highest levels of Cd, followed by the second and then the third. This was not the case when water or as prepared dissolved shell solutions were used, in these cases very low levels of Cd were recorded in each extraction solution. ICP-MS results also showed that the shell solutions used contained much lower calcium concentrations, approximately 0.1 mol L^{-1}, compared to 1 mol L^{-1} for the other calcium salt solutions.

The cadmium levels in treated RPR samples are shown in Fig.3.23. These results broadly correspond to the extraction solution results. The $CaCl_2$ column RPR had the lowest Cd levels while the distilled water and mussel shell dissolved in HCl were very similar to untreated RPR. The RPR sample treated with mussel

shell dissolved in HNO_3 had Cd levels significantly higher than untreated RPR. RPR treated with other salt extraction solutions showed decreased levels of Cd which roughly corresponded to the levels of Cd recorded in the solutions.

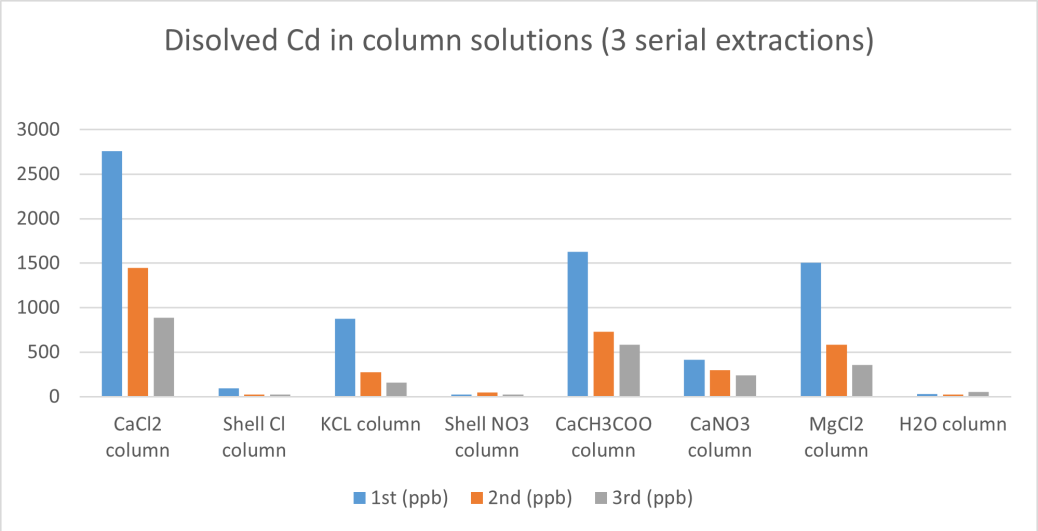

Figure 3.22: Cd levels in column extraction solutions.

For the cations Ca^{2+} was more effective than Mg^{2+} or K^{+}. These results suggest that Ca^{2+} is better able to substitute for Cd^{2+} in the hydroxyapitite lattice than Mg^{2+} or K^{+}. Sodium salts were not tested as Na^{+} ions are known to be a common source of matrix interference in ICP-MS. Following the results from calcium, magnesium and potassium chlorides it appears that NaCl should be tested for cadmium extraction potential. Na^{+} has a similar ionic radius to Cd^{2+} and sodium salts are readily available. It would also be possible to use sodium salts of other anions, such as SO_4^{2-}, which are not soluble as a calcium salt.

3.6.2 TDX018

The following salt solutions were tested in extraction columns:
Mussel shell dissolved in HCl (equivalent to $CaCl_2$ (1 mol L^{-1}));
Mussel shell - heated to 300°C dissolved in HCl (equivalent to $CaCl_2$ (1 mol L^{-1}));
$CaCl_2$ (1 mol L^{-1});
$CaCl_2$ (1 mol L^{-1}) with 0.1% EDTA;

Results for Cd concentrations in these extraction solutions are shown in Fig.3.24

Following the results of TDX012, TDX014 and TDX015 more concentrated shell solutions were prepared for testing. The extraction results with these solutions were considerably improved (compare Fig.3.22).

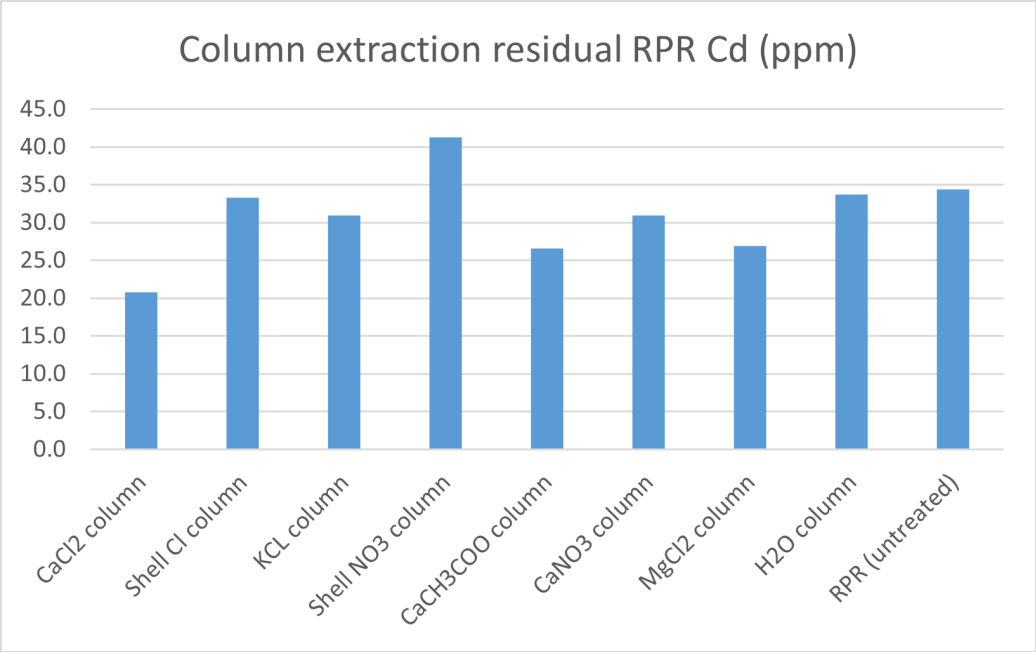

Figure 3.23: Residual Cd levels in RPR after column extraction.

EDTA, which forms stable complexes with many metal ions, was tested in combination with $CaCl_2$. A $CaCl_2$ (1 mol L^{-1}) with 0.1% EDTA solution did not appear to enhance Cd extraction over a $CaCl_2$ solution (1 mol L^{-1}) without EDTA. In this case the amount of cadmium in the first extraction solution was significantly lower when EDTA was present. For the second and third extractions EDTA solution showed similar levels of cadmium to the $CaCl_2$ solutions without EDTA. Cd levels across the three EDTA extraction solutions were similar whereas with the other $CaCl_2$ extractions there was a clear trend for reduced Cd concentrations in subsequent extractions. This test was only conducted once, with a single combination of $CaCl_2$ concentration, EDTA concentration and pH. More testing is required before we can make any conclusions on the effects of EDTA on cadmium extraction.

Solutions derived from mussel shells and mussel shells which had been heated to 300°C appeared to contain similar levels of cadmium after column extraction. Compared to a control solution from lab $CaCl_2$ both appear to show significantly lower levels of cadmium on the first extraction and compatible levels on the second and third extraction. As only one test was conducted more repeats would be required before making any conclusions regarding the effectiveness of cadmium extraction solutions of dissolved mussel shells compared to those made from refined calcium salts.

The levels of cadmium remaining in RPR after column extraction, as measured

by ICP-MS from digestion samples, were compared Fig. 3.25. These results did not correspond to the trends recorded for cadmium in the extraction solutions. In this case the extraction solution which extracted the largest amount of cadmium (lab $CaCl_2$ 1 mol L^{-1}) had significantly higher residual Cd levels than any of the other samples. This could be due to random variation among digestion samples due to the small sample size used. It is possible that the RPR in the different columns started with significantly different levels of Cd. This appears to be unlikely as all four columns were filled from the same RPR source, however it cannot be ruled out without taking multiple digestion samples from each column and using statistical tests to determine the variance among RPR digestion samples. Without further tests we are unable to draw meaningful conclusions from this comparison.

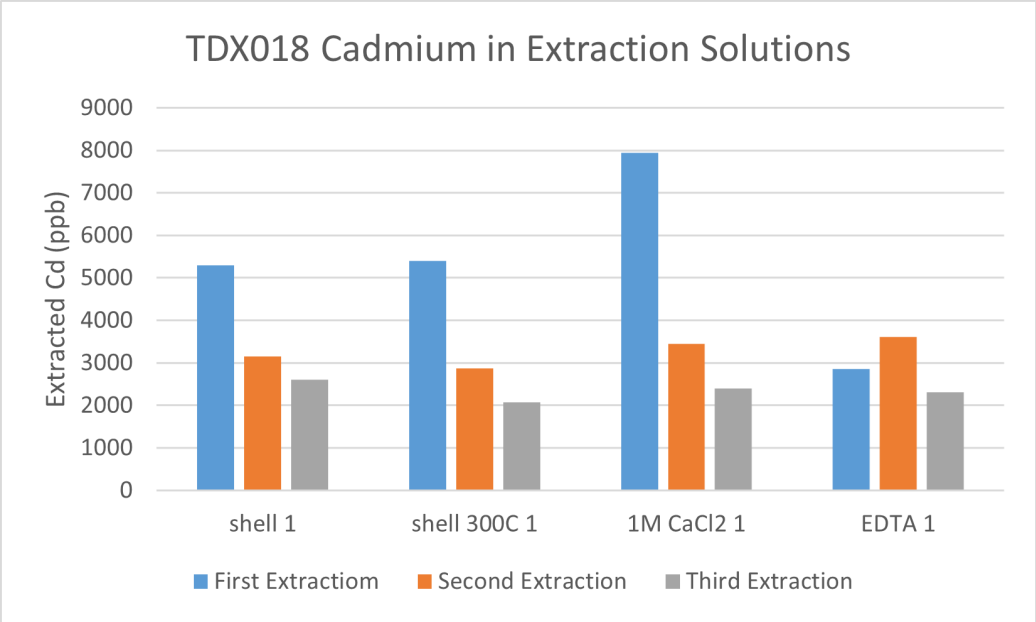

Figure 3.24: TDX018 cadmium extracted into solutions.

3.6.3 RPR FTIR after Cd extraction

FTIR spectra of 30 samples of RPR which had been subject to various Cd extraction attempts were obtained.

Nearly all the spectra appear similar, there were no significant shifts in the P-O peaks and no notable new peaks were observed. The C-O peaks were still present. This is unlike FTIR spectra for SSP (formed by treating RPR with concentrated H_2SO_4), where C-O peaks are absent and the P-O peaks are shifted. This suggests

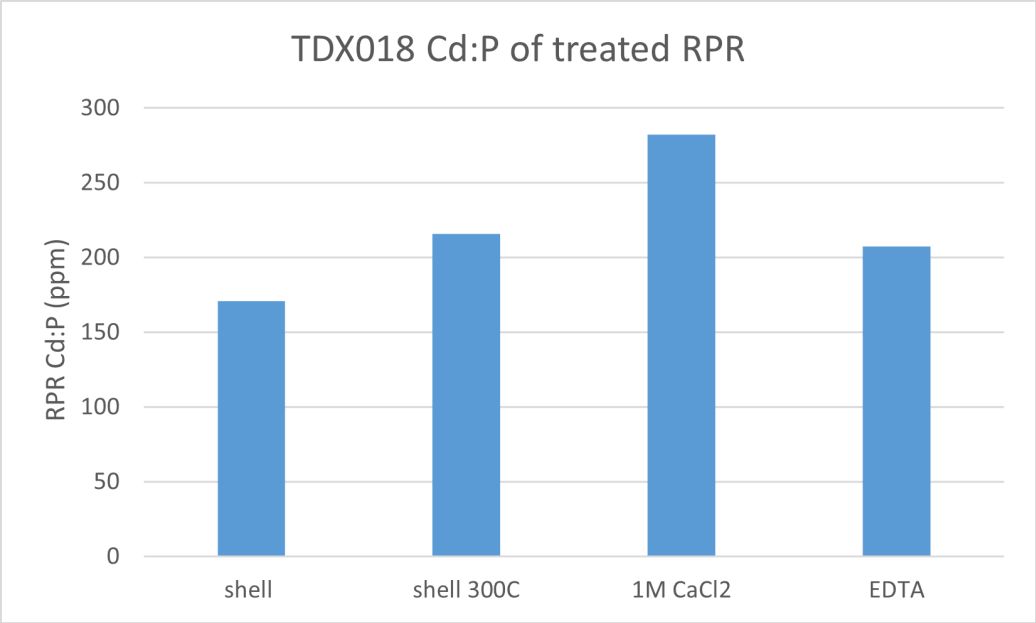

Figure 3.25: TDX018 Cd:P of treated RPR samples from columns.

that exposure to the tested extraction solutions does not significantly alter the phosphate chemistry of RPR.

For TDX015-1 (extraction with calcium acetate) a sharp peak is observed at 1620 cm^{-1}. This is consistent with the C=O stretch mode of acetate ions. For TDX015-2 (extraction with calcium nitrate) a sharp peak at 1380 cm^{-1} is observed. This is consistent with an N-O stretch vibrational mode. It would appear that these two samples still contained residues of their extraction solutions.

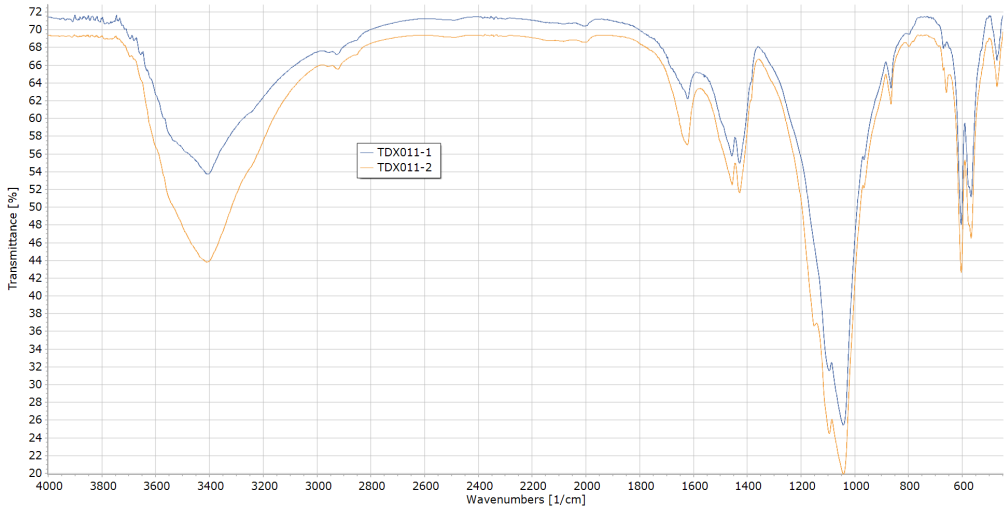

Figure 3.26: FTIR spectra TDX011 after treatment

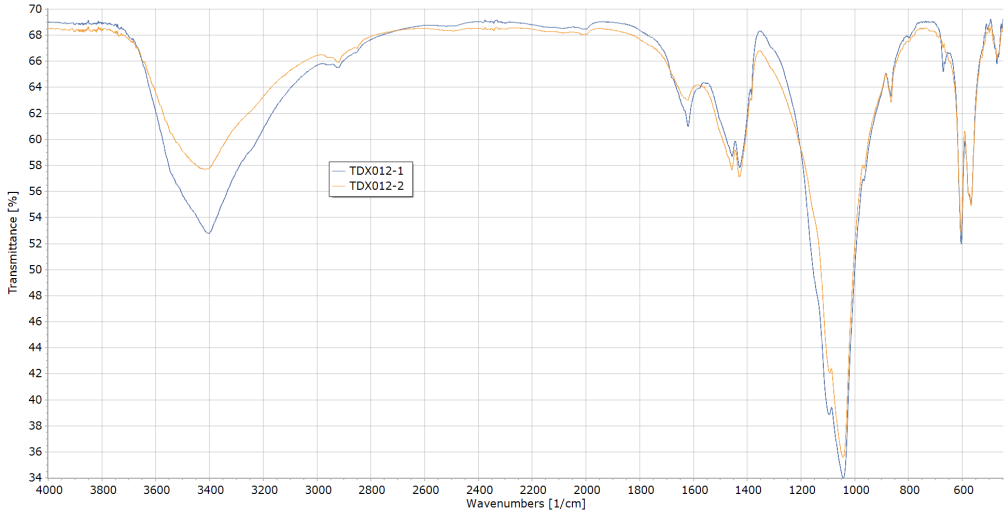

Figure 3.27: FTIR spectra TDX012 after treatment

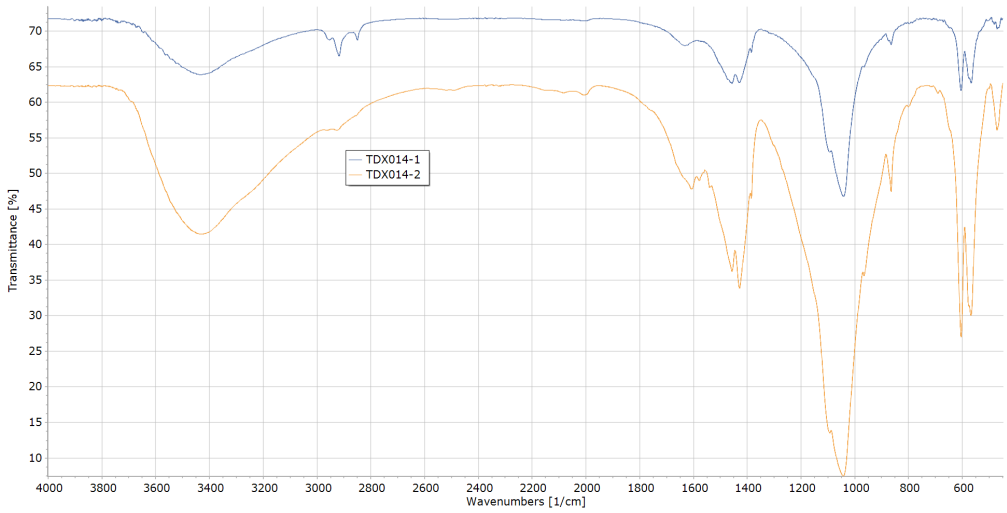

Figure 3.28: FTIR spectra TDX014 after treatment

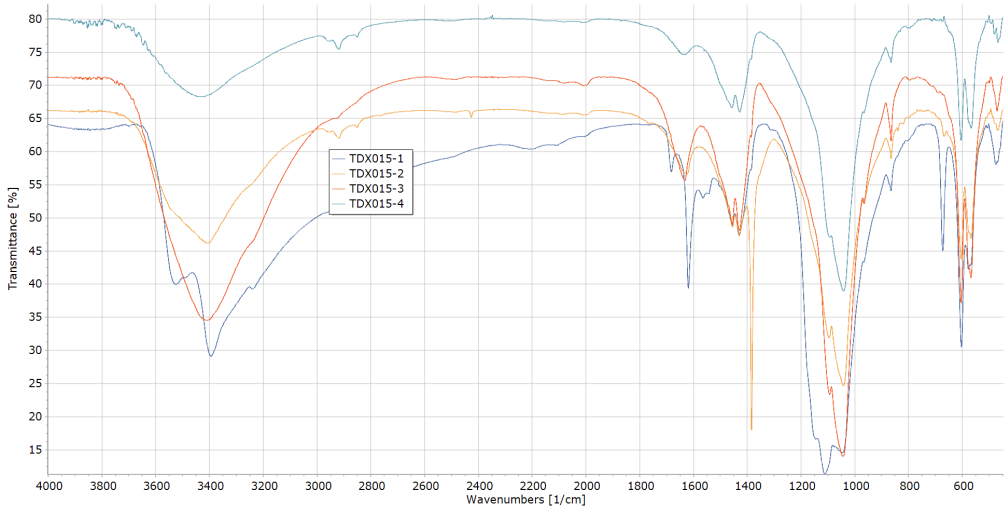

Figure 3.29: FTIR spectra TDX015 after treatment

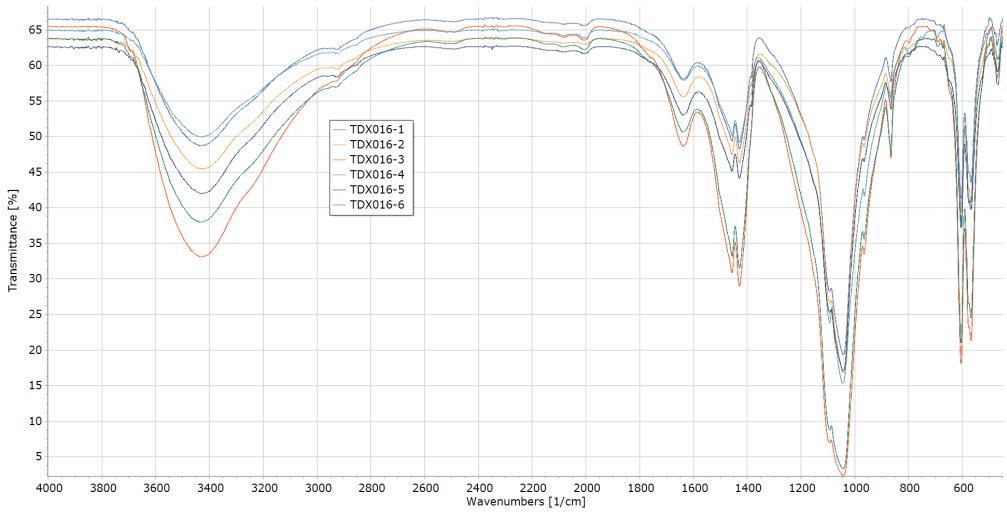

Figure 3.30: FTIR spectra TDX016 after treatment

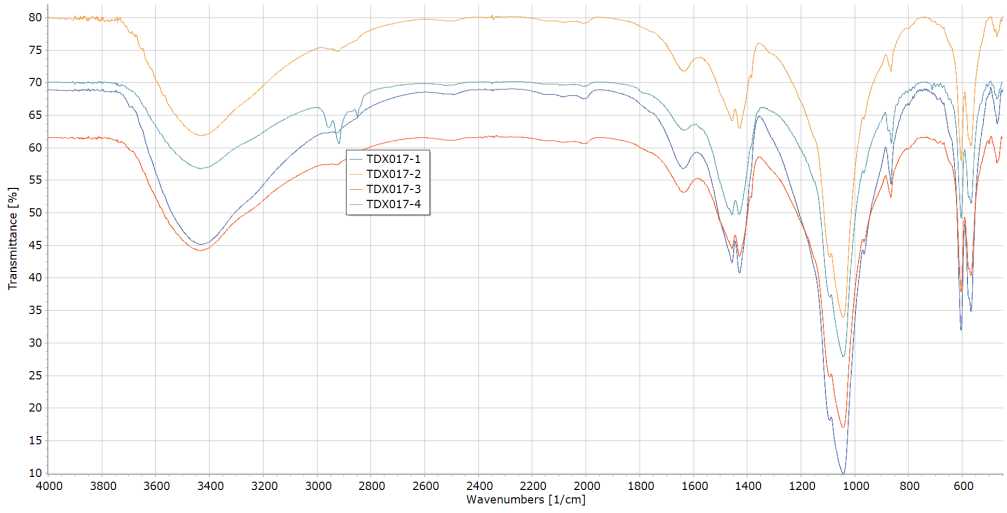

Figure 3.31: FTIR spectra TDX017 after treatment

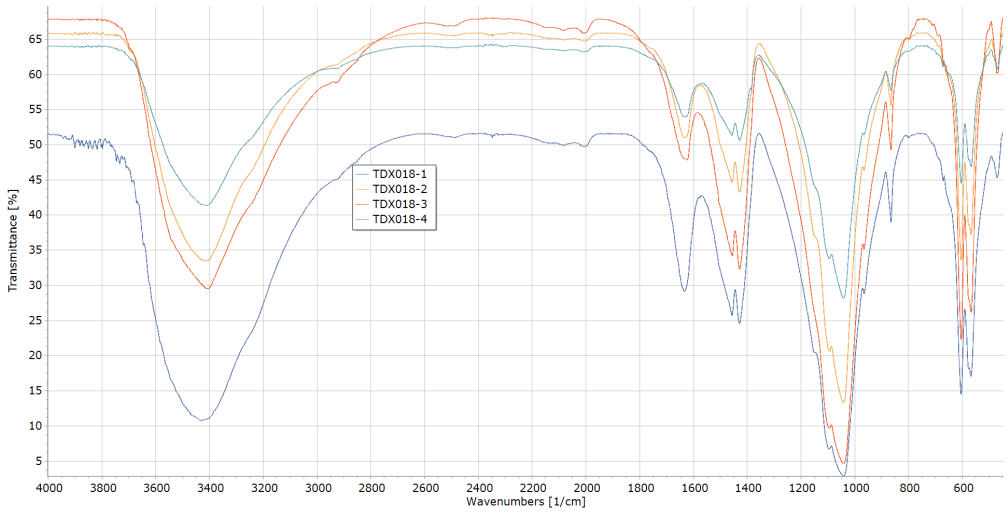

Figure 3.32: FTIR spectra TDX018 after treatment

Figure 3.33: FTIR spectra TDX020 after treatment

3.7 Phosphate dissolution in Cadmium Extraction Solutions

The aim of this project is to reduce cadmium contamination if phosphate fertiliser. The intention is to selectively remove cadmium into solution while leaving phosphate in the solid phase as RPR. Although the phosphate in RPR has been shown to have limited solubility above pH 4 it is inevitable that some will be lost into solution. Using an extraction solution with high Ca^{2+} concentration also disfavours phosphate loss as the concentration gradient will limit the further dissolution of calcium ions from the RPR Calcium Phosphate lattice. Dissolving phosphate into solution is counter productive for RPR based fertiliser as it has must be recovered as before it can be used for manufacturing fertiliser. The effectiveness of cadmium extraction can be compared using Cd:P ratio. If the Cd:P ratio of an extraction solution is significantly higher than the Cd:P ratio of RPR then the extraction method can be considered to be effective.

3.7.1 Column Extractions TDX008, TDX009 and TDX011

Early column extractions showed extremely promising results, in some cases cadmium levels in the extraction solutions were higher than phosphate levels. $CaCl_2$ extraction solutions showed considerably higher Cd:P ratios than $Ca(NO_3)_2$ extraction solutions. Large columns appeared to be more efficient in extracting cadmium than small columns. This may be due to poor flow rates, small columns were easily blocked by gas bubbles.

Code	Solution	Column type	Solution Cd:P (ppm)
TDX008-1	H_2O	Small	0
TDX008-4	0.5M $Ca(NO_3)_2$	Small	5784
TDX009-1	0.5M $Ca(NO_3)_2$	Large	39695
TDX009-2	1M $Ca(NO_3)_2$	Large	631011
TDX011-1	0.5M $CaCl_2$	Large	2528083
TDX011-2	1M $CaCl_2$	Large	2376542

Table 3.21: TDX011 Cd:P ratios of extraction solutions and RPR residues.

3.7.2 Column Extractions TDX012, TDX014 and TDX015

Results of these column extractions are summarised in Table 3.22. RPR Cd:P are reported only for the third extraction as in all cases the sample was taken after

all three extraction solutions had been applied. All extraction solutions showed elevated relative levels of cadmium compared to the final RPR residue.

Code	Solution	Extraction	Solution Cd:P (ppm)	RPR Cd:P (ppm)
TDX012-1-1	$CaCl_2$	1st	375277	-
TDX012-1-2	$CaCl_2$	2nd	494323	-
TDX012-1-3	$CaCl_2$	3rd	447571	224
TDX012-2-1	Shell $CaCl_2$	1st	46844	-
TDX012-2-2	Shell $CaCl_2$	2nd	23391	-
TDX012-2-3	Shell $CaCl_2$	3rd	16778	342
TDX014-1-1	KCl	1st	588750	-
TDX014-1-2	KCl	2nd	155802	-
TDX014-1-3	KCl	3rd	95662	331
TDX014-2-1	Shell $Ca(NO_3)_2$	1st	41958	-
TDX014-2-2	Shell $Ca(NO_3)_2$	2nd	61086	-
TDX014-2-3	Shell $Ca(NO_3)_2$	3rd	17623	430
TDX015-1-1	$Ca(CH_3COO)_2$	1st	481400	-
TDX015-1-2	$Ca(CH_3COO)_2$	2nd	271304	-
TDX015-1-3	$Ca(CH_3COO)_2$	3rd	260604	279
TDX015-2-1	$Ca(NO_3)_2$	1st	179741	-
TDX015-2-2	$Ca(NO_3)_2$	2nd	229354	-
TDX015-2-3	$Ca(NO_3)_2$	3rd	292235	472
TDX015-3-1	$MgCl_2$	1st	816697	-
TDX015-3-2	$MgCl_2$	2nd	750064	-
TDX015-3-3	$MgCl_2$	3rd	387891	289
TDX015-4-1	H_2O	1st	29649	-
TDX015-4-2	H_2O	2nd	26960	-
TDX015-4-3	H_2O	3rd	2463	343

Table 3.22: TDX012, TDX014 and TDX015 Cd:P ratios of column extraction solutions and RPR residues.

3.7.3 Column Extractions TDX018

Results of these column extractions are summarised in Table 3.23. RPR Cd:P are reported only for the third extraction as in all cases the sample was taken after all three extraction solutions had been applied. All extraction solutions showed highly elevated relative levels of cadmium compared to the final RPR residue. In some cases levels of cadmium in the extraction solution were higher than phosphorus

(giving a Cd:P over 1 million ppm). This is good evidence that For the two $CaCl_2$ solutions derived from mussel shell there was a trend for increasingly high Cd:P ratio for subsequent extractions. For the $CaCl_2$ + EDTA the situation was reversed, each subsequent extraction the Cd:P ratio decreased. There was no clear trend for the lab $CaCl_2$ solution. Overall we cannot draw any conclusions for trends from sequential extraction and Cd:P ratio.

Code	Solution	Extraction	Solution Cd:P (ppm)	RPR Cd:P (ppm)
TDX018-1-1	Shell $CaCl_2$	1st	125076	-
TDX018-1-2	Shell $CaCl_2$	2nd	594802	-
TDX018-1-3	Shell $CaCl_2$	3rd	1769262	171
TDX018-2-1	Shell 300°C $CaCl_2$	1st	211652	-
TDX018-2-2	Shell 300°C $CaCl_2$	2nd	454244	-
TDX018-2-3	Shell 300°C $CaCl_2$	3rd	591896	216
TDX018-3-1	$CaCl_2$	1st	417681	-
TDX018-3-2	$CaCl_2$	2nd	1108632	-
TDX018-3-3	$CaCl_2$	3rd	717211	282
TDX018-4-1	$CaCl_2$ + EDTA	1st	630231	-
TDX018-4-2	$CaCl_2$ + EDTA	2nd	572500	-
TDX018-4-3	$CaCl_2$ + EDTA	3rd	287520	207

Table 3.23: TDX018 Cd:P ratios of column extraction solutions and RPR residues.

3.7.4 Heated Extraction TDX017

The Cd:P ratio of Shell $CaCl_2$ extraction solutions were highly variable, all were significantly higher than the Cd:P ratios of RPR residues. There is no obvious correlation between temperature and solution Cd:P ratio.

Code	Solution	Temp. (°C)	Solution Cd:P (ppm)	RPR Cd:P (ppm)
TDX017-1	Shell $CaCl_2$	20	2546	338
TDX017-2	Shell $CaCl_2$	20	3102	447
TDX017-3	Shell $CaCl_2$	90	1804	306
TDX017-4	Shell $CaCl_2$	90	5439	317

Table 3.24: TDX017 Cd:P ratios of extraction solutions and RPR residues.

3.7.5 Microwave Extractions TDX016

The Cd:P ratio of $CaCl_2$ extraction solutions were variable, all were significantly higher than the Cd:P ratios of RPR residues. This is evidence that cadmium is being selectively extracted over phosphate. There is no obvious correlation between microwave time and solution Cd:P ratio. Increased microwave time was correlated to higher concentrations of both Cd and P in the extraction solution. When water was used as an extraction solution the Cd:P ratio was far lower than for $CaCl_2$ extraction solutions. With water extraction solution the dissolved P concentration was higher than for $CaCl_2$ while the concentration of Cd was lower. Overall the Cd:P ratio in water extraction solution was similar to that of RPR. There is no evidence that water selectively extracts cadmium over phosphate as observed for calcium chloride solutions. However only a single test was carried out so we cannot draw conclusions based on this data alone.

Code	Solution	Microwave time (°C)	Solution Cd:P (ppm)	RPR Cd:P (ppm)
TDX016-1	1M $CaCl_2$	0	5092	280
TDX016-2	1M $CaCl_2$	2	3747	249
TDX016-3	1M $CaCl_2$	4	7416	258
TDX016-4	1M $CaCl_2$	7	7443	222
TDX016-5	1M $CaCl_2$	12	7754	196
TDX016-6	H_2O	12	244	353

Table 3.25: TDX016 Cd:P ratios of microwave extraction solutions and RPR residues.

3.7.6 Microwave Extractions TDX020

The Cd:P ratio of $CaCl_2$ extraction solutions were variable, all were significantly higher than the Cd:P ratios of RPR residues. This is evidence that cadmium is being selectively extracted over phosphate. Cadmium levels in TDX020 extraction solutions were relatively consistent, most of the variation in Cd:P ratio was due to phosphorus levels 3.18. There is no obvious correlation between $CaCl_2$ and solution Cd:P ratio, the three samples showed similar cadmium levels but significant variation in phosphorous levels. Solutions containing ligands also showed variable results, all showed higher solution Cd:P ratios than $1\text{molL}-1$ $CaCl_2$ but also showed higher Cd:P in the RPR. Overall the effects of these ligands are inconclusive, more trials are required before we can draw any conclusions.

Code	Solution	Microwave time (°C)	Solution Cd:P (ppm)	RPR Cd:P (ppm)
TDX020-1	1M $CaCl_2$	12	94333	153
TDX020-2	2M $CaCl_2$	12	339471	165
TDX020-3	3M $CaCl_2$	12	149143	137
TDX020-4	1M $CaCl_2$ + MSA	12	298214	281
TDX020-5	1M $CaCl_2$ + Potassium tartrate	12	368512	188
TDX020-6	1M $CaCl_2$ + EDTA	12	238120	187

Table 3.26: TDX020 Cd:P ratios of microwave extraction solutions and RPR residues.

4. Conclusions

The aim of this project was to test the possibility for waste mussel shells to be used for reducing cadmium in phosphate fertilisers. A multi stage approach was used so each step can be assessed individually.

- The results obtained provide some evidence that contact with aqueous calcium chloride caused cadmium to diffuse out to RPR and into solution.
- ICP-MS results of $CaCl_2$ extraction solutions show consistently elevated levels of cadmium. This in of itself is not enough to conclude that cadmium is being removed. We also need to consider the levels of phosphorous in solution. The ratio of Cd:P in extraction solutions was consistently higher than in RPR digestion samples. This indicates that cadmium is being selectively extracted over phosphorous.
- There are also indications that cadmium levels in RPR are reduced by calcium chloride solution extraction. ICP-MS results from RPR digestion samples showed high variance for cadmium, phosphorous, calcium and other elements. RPR appears to be a very heterogeneous substance at a granular level, as evidence from the optical microscopy and SEM-EDX results. A more consistent method for preparing ICP-MS digestion samples is required to obtain substantive results. The ICP-MS digestion method used only 0.2g of RPR for each sample, possibly using significantly larger amount of RPR would improve the consistency of results. It is also possible that finely crushing the RPR and thoroughly mixing would increase the RPR homogeneity and allow small samples to give representative results.
- It appears that fairly high calcium ion concentrations are required for effective cadmium extraction. Extraction solutions with a 1 mol:$^{-1}$ calcium concentration were considerably more effective than 0.1 mol:$^{-1}$ solutions. There did not appear to be a significant change in cadmium extraction by increasing calcium ion concentration to 2 or 3 mol:$^{-1}$. Further studies would be required to establish the optimal concentration for extraction solutions.

- A handful of common calcium salts were tested for effectiveness in cadmium extraction. With the requirement for high solubility in water the nitrate, chloride and acetate salts were identified as the most suitable. Of these salts calcium chloride appeared to be the most effective at extracting cadmium from RPR. Chloride salts of potassium and magnesium were also tested. Overall from the results obtained it appears that $CaCl_2$ is the most effective extraction agent among the compounds tested.

- Microwave heating appears to enhance cadmium extraction over a short time period. Further testing would be required to determine if this is the result of very high temperatures (short term boiling), selective heating of polar molecules or other effects. The effects of conventional heating were less clear, further tests would be required to determine what effect if any solution temperature has on cadmium extraction rate and total extraction potential.

- Crushed greenshell mussel shells dissolved readily in mineral acids although a considerable amount of foaming occurred. Using rapid stirring can minimise this problem. A small amount of insoluble residue is easily removed by filtration. Using a known amount of acid and a slight excess of crushed shell ensures a solution known calcium concentration and approximately neutral pH. There does not appear to be any benefit to heating mussel shells before dissolving in acid. Shells that had been heated to 300°C were slightly easier to crush than unheated shells but they produced strong pungent smell when dissolved in acid. Heating mussel shells to 900°C converted the $CaCO_2$ to CaO. This also burned off any residual organic compounds. As the CO_2 has already been driven off there is considerably less foaming, however a considerable amount of energy is required by the calcination process. Further research is required to determine if the optimal method for producing calcium ion solutions from mussel shells. Mussel shells were found to contain low levels of cadmium. This could be a potential issue for use as a cadmium extracting agent.

Overall there are several promising results which indicate that cadmium extraction by ion exchange with calcium ions in aqueous solution has the potential to be developed into a viable method for reducing cadmium contamination in fertilisers.

4.1 Further Research

As with most research the results of this project raise more questions and suggest possible future research.

A variety of salt solutions were tested, there are of course many others available. Suitable salts must be soluable in reasonably high concentrations and have low environmental impact when their residue is present in fertiliser. Possible cations include Li^+, Na^+, K^+, Mg^{2+}, Ca^{2+}, Fe^{2+}, Fe^{3+}, Zn^{2+} and NH_4^+. Possible anions include NO_3^-, Cl^-, acetate (CH_3COO^-), HCO_3^-/CO_3^{2-}, SO_4^{2-}, oxalate ($C_2O_4^{2-}$), tartrate ($C_4H_4O_6^{2-}$, PO_4^{3-} as well as numerous other organic and inorganic ions. This creates a large number of possible salts that could be tested. Some combinations will not work as they are are insoluble or sparingly soluble while others may react with RPR.

Some rationalisation can be used in order to target potentially suitable salts. The function of the cation is to displace Cd^{2+} from the apatite lattice. Ca^{2+} appears to be highly suitable; it has the same charge and similar ionic radius to Cd^{2+}. Displacement of Ca^{2+} is not an issue with calcium salts and there are no additional environmental impacts to consider. Na^+ is a possible cation of interest due to its similar ionic radius to Cd^{2+} while also being readily available and forming soluble salts with nearly all anions. Sodium salts were not tested in this project as high sodium levels in ICP-MS solution are a common source of interference. Among cations Cl^- was the most effective. It is hypothesised that the main function of the cations in cadmium extraction is to stabilise the Cd^{2+} in solution. Chloride is known to form complexes with cadmium ions in solution[93] but there may be other anions with a greater stabilising effect.

Stabilising cadmium ions in solution could be further enhanced using complex forming ligands.[94] This approach was briefly explored without apparent success. However there are many untested ligands available which are able to complex with Cd^{2+}, some of which may have a greater effect on cadmium extraction potential. Given the very low concentrations of cadmium present in solution it only small amounts of a suitable ligand would be required. In order to be effective a ligand must have high selectivity for Cd^{2+} over Ca^{2+} and other ions in solution as the relative concentration of cadmium ions is very low. Dimercaptosuccinate was suggested as a potential ligand for Cd^{2+} but it could not be obtained in time for testing.

Once cadmium has been removed from RPR into solution it will be necessary at some stage to capture the cadmium ions and so allow the extraction solution to be recycled. Due to the low levels of cadmium in the extraction solution bulk methods such as recrystallisation or precipitation appear unfavourable. More advanced methods such as ion exchange resins,[95] electrodialysis[96] or biosorption[97] could be used to "clean up" the extraction solution in situ by removing dissolved cadmium ions. This would allow the extraction solution to be recycled and would greatly decrease the amount of cadmium contaminated waste produced by the extraction process.

Throughout this project it has been proposed that ion exchange between

aqueous calcium ions and cadmium ions in the RPR latices is able to occur and that this forms the mechanism for enhanced cadmium extraction. However no direct evidence of this kind of ion exchange has been presented. Methods that could prove that calcium ions from solution are being incorporated into the apatite crystal structure, such as radioisotope labelling,[98] are beyond the scope of this project but could form the basis for further research.

The ultimate aim of this research is to reduce toxic contamination in fertiliser. In order for any process to achieve this it must be function as a part of the fertiliser industry. While this is well outside the scope of this project any future research should make considerations for feasibility and practicality in an industrial setting. While any new process must first be tested and verified in a controlled setting before being adapted industrially it is beneficial to have an awareness of the industry when planning research. For this reason consulting with the fertiliser industry; from mining, to manufacturing to the end users should be considered when planning future research.

Bibliography

[1] Rujitanapanich, S.; Kumpapan, P.; Wanjanoi, P. *Energy Procedia* **2014**, *56*, 112–117.

[2] Schlesinger, W. H.; Bernhardt, E. S. In *Chapter 12 - The Global Cycles of Nitrogen and Phosphorus*; Schlesinger, W. H., Bernhardt, E. S. B. T. B. T. E., Eds.; Academic Press: Boston, 2013; pp 445–467.

[3] Paytan, A.; McLaughlin, K. *Chem. Rev.* **2007**, *107*, 563–576.

[4] Buend\'\ia, C.; Kleidon, A.; Porporato, A. *Biogeosciences* **2010**, *7*, 2025–2038.

[5] Bennet, E.; Elser, J. *Nature* **2011**, *478*, 29–31.

[6] Smith, J. P.; Lehr, J. R. *J. Agric. Food Chem.* **1966**, *14*, 342–349.

[7] Kaleeswari, R. K.; Subramanian, S. *Agric. Rev.* **2001**, *22*, 121–126.

[8] Schipper, L. A.; Sparling, G. P.; Fisk, L. M.; Dodd, M. B.; Power, I. L.; Littler, R. A. *Agric. Ecosyst. Environ.* **2011**, *144*, 95–101.

[9] Rahimzadeh, M. R. M. R.; Rahimzadeh, M. R. M. R.; Kazemi, S.; Moghadamnia, A. A. *Casp. J. Intern. Med.* **2017**, *8*, 135–145.

[10] Salmanzadeh, M.; Schipper, L. A.; Balks, M. R.; Hartland, A.; Mudge, P. L.; Littler, R. *Agric. Ecosyst. Environ.* **2017**, *247*, 84–90.

[11] Podgaiskyte, V., &. V. *J. Environ. Eng. Landsc. Manag.* **2009**, *17*, 219–225.

[12] Yaacoubi, H.; Zidani, O.; Mouflih, M.; Gourai, M.; Sebti, S. *Procedia Eng.* **2014**, *83*, 386–393.

[13] Monteiro, R. J. R.; Lopes, C. B.; Rocha, L. S.; Coelho, J. P.; Duarte, A. C.; Pereira, E. *J. Environ. Chem. Eng.* **2016**, *4*, 1199–1208.

[14] Boparai, H. K.; Joseph, M.; O'Carroll, D. M. *J. Hazard. Mater.* **2011**, *186*, 458–465.

[15] Nogawa, K.; Kobayashi, E.; Okubo, Y.; Suwazono, Y. *BioMetals* **2004**, *17*, 581–587.

[16] Pearson, A.; Gibbs, M.; Lau, K.; Edmonds, J.; Alexander, D.; Nicolas, J. *2016 New Zealand Total Diet Study Consultation paper*; Ministry for Primary Industries, 2018.

[17] Schnug, E.; Jacobs, F.; Stöven, K. In *Guano: The White Gold of the Seabirds*; Mikkola, H., Ed.; IntechOpen: Rijeka, 2018; p Ch. 6.

[18] Giurgiu, A. M.; Onac, B. P.; Tudor, T.; Fornós, J. J. *ICS Proc.* **2013**, 483–485.

[19] Doughty, R. *AAG Rev. Books* **2014**, *2*, 83–85.

[20] Barnum, D. W. *J. Chem. Educ.* **2003**, *80*, 1393.

[21] Rouwenhorst, K. H. R.; Travis, A. S.; Lefferts, L. 1921–2021: A Century of Renewable Ammonia Synthesis. 2022.

[22] Roberts, T. *Better Crop. with Plant Food* **2019**, *103*, 6–8.

[23] Njira, K. *African J. Food, Agric. Nutr. Dev.* **2015**, *15*, 9777–9783.

[24] Ciceri, D.; Manning, D. A. C.; Allanore, A. *Sci. Total Environ.* **2015**, *502*, 590–601.

[25] Zenda, T.; Liu, S.; Dong, A.; Duan, H. Revisiting Sulphur—The Once Neglected Nutrient: It's Roles in Plant Growth, Metabolism, Stress Tolerance and Crop Production. 2021.

[26] Gerendás, J.; Führs, H. *Plant Soil* **2013**, *368*, 101–128.

[27] Craighead, M.; Rd, D.; Rangiora, R. D.; Zealand, N. *Magnesium* **2001**, 53–62.

[28] Brock, J.; Caradus, J.; Hay, M. *Proc. New Zeal. Grassl. Assoc.* **1989**, *39*, 25–39.

[29] Edmeades, D.; Mcbride, R. *Proc. New Zeal. Grassl. Assoc.* **2012**, 217–224.

[30] Mohanta, R. *Norman Borlaug and Green Revolution*; 2009.

[31] Cassman, K. G.; Dobermann, A. *Ambio* **2022**, *51*, 17–24.

[32] Good, A. G.; Beatty, P. H. *PLoS Biol.* **2011**, *9*, e1001124.

[33] Bhagowati, B.; Ahamad, K. U. *Ecohydrol. Hydrobiol.* **2019**, *19*, 155–166.

[34] Andersen, J. H.; Carstensen, J.; Holmer, M.; Krause-Jensen, D.; Richardson, K. Editorial: Research and Management of Eutrophication in Coastal Ecosystems . 2019; https://www.frontiersin.org/articles/10.3389/fmars.2019.00768.

[35] Hallegraeff, G. *Phycologia* **1993**, *32*.

[36] Young, N.; Sharpe, R. A.; Barciela, R.; Nichols, G.; Davidson, K.; Berdalet, E.; Fleming, L. E. *Harmful Algae* **2020**, *98*, 101901.

[37] CHEBET, A. *Int. J. Contemp. Res. Rev.* **2021**, *12*, 20355?20360.

[38] Kurkute, S. *Int. J. Res. Appl. Sci. Eng. Technol.* **2018**, *6*, 341–346.

[39] Khan, J.; Mohammadi, N. **2019**,

[40] Abraham, E. *New Zeal. J. Agric. Res.* **2020**, *63*, 202–219.

[41] Chernysh, Y.; Yakhnenko, O.; Chubur, V.; Roubík, H. Phosphogypsum Recycling: A Review of Environmental Issues, Current Trends, and Prospects. 2021.

[42] Benredjem, Z.; Delimi, R. *Phys. Procedia* **2009**, *2*, 1455–1460.

[43] Benredjem, Z.; Delimi, R.; Khelalfa, A. *Arab. J. Chem.* **2016**, *9*, S446–S450.

[44] Benredjem, Z.; Delimi, R.; Khelalfa, A.; Saaidia, S.; Mehellou, A. *Sep. Sci. Technol.* **2016**, *51*, 718–726.

[45] Wang, W. Z.; Brusseau, M. L.; Artiola, J. F. *J. Contam. Hydrol.* **1997**, *25*, 325–336.

[46] Jalali, M.; Moradi, F. *Environ. Monit. Assess.* **2013**, *185*, 8831–8846.

[47] Reeder-Myers, L. et al. *Nat. Commun.* **2022**, *13*.

[48] Nagai, K. *Zoolog. Sci.* **2013**, *30*, 783–793.

[49] FAO. 2020, *The State of World Fisheries and Aquaculture 2020. Sustainability in action*; Rome.

[50] Aquaculture New Zealand, AQUACULTURE FOR NEW ZEALAND A sector overview with key facts and statistics for 2020 Primary industry of the future. 2020; https://drive.google.com/file/d/12G2OxGx-Wv-icEnv1{_}4VnEJ02PFoKeUQ/view.

[51] Montery Bay Aquarium Seafood Watch, Marine Mussels. 2020; https://www.seafoodwatch.org/recommendation/mussels/green-mussels-mussels-worldwide-off-bottom-culture?species=3454.

[52] DAVIDSON, J. M. *Rec. Auckl. Inst. Museum* **1967**, *6*, 203–228.

[53] Miller, P.; Sunde, M. *Poult. Sci.* **1975**, *54*, 1422–1433.

[54] Eziefula, U. G.; Ezeh, J. C.; Eziefula, B. I. *Constr. Build. Mater.* **2018**, *192*, 287–300.

[55] Bailey, W. *William Mary Q.* **1938**, *18*, 1–12.

[56] Strömberg, A.-M.; Karlsson, H. T. *Chem. Eng. Sci.* **1988**, *43*, 2095–2102.

[57] Carran, D.; Hughes, J. J.; Leslie, A.; Kennedy, C. *Int. J. Archit. Herit.* **2012**, *6*, 117–146.

[58] Gray, C. W.; McDowell, R. W. *New Zeal. J. Agric. Res.* **2016**, *59*, 185–193.

[59] Ghorbani, Y.; Franzidis, J. P.; Petersen, J. *Miner. Process. Extr. Metall. Rev.* **2016**, *37*, 73–119.

[60] Pasero, M.; Kampf, A. R.; Ferraris, C.; Pekov, I. V.; Rakovan, J.; White, T. J. *Eur. J. Mineral.* **2010**, *22*, 163–179.

[61] Yan, W. Q.; Nakamura, T.; Kawanabe, K.; Nishigochi, S.; Oka, M.; Kokubo, T. *Biomaterials* **1997**, *18*, 1185–1190.

[62] Cummings, L. J.; Snyder, M. A.; Brisack, K. *Methods Enzymol.* **2009**, *463*, 387–404.

[63] Chen, X.; Wright, J. V.; Conca, J. L.; Peurrung, L. M. *Water. Air. Soil Pollut.* **1997**, *98*, 57–78.

[64] Peckham, S.; Awofeso, N. *ScientificWorldJournal.* **2014**, *2014*, 293019.

[65] Lee, C.-K.; Kim, H.-S.; Kwon, J.-H. *Environ. Eng. Res.* **2005**, *10*, 205–212.

[66] Wilschefski, S. C.; Baxter, M. R. *Clin. Biochem. Rev.* **2019**, *40*, 115–133.

[67] Berzas Nevado, J. J.; Rodríguez Martín-Doimeadios, R. C.; Krupp, E. M.; Guzmán Bernardo, F. J.; Rodríguez Fariñas, N.; Jiménez Moreno, M.; Wallace, D.; Patiño Ropero, M. J. *J. Chromatogr. A* **2011**, *1218*, 4545–4551.

[68] Jarošová, M.; Milde, D.; Kuba, M. *Czech J. Food Sci.* **2014**, *32*, 354–359.

[69] Lum, T.-S.; Sze-Yin Leung, K. *J. Anal. At. Spectrom.* **2016**, *31*, 1078–1088.

[70] Swinehart, D. F. *J. Chem. Educ.* **1962**, *39*, 333.

[71] Ma, Z.; Merkus, H. G.; de Smet, J. G. A. E.; Heffels, C.; Scarlett, B. *Powder Technol.* **2000**, *111*, 66–78.

[72] Armenise, I.; Kustova, E. *J. Phys. Chem. A* **2018**, *122*, 8709–8721.

[73] Jenkins, R.; Manne, R.; Robin, R.; Senemaud, C. *X-Ray Spectrom.* **1991**, *20*, 149–155.

[74] Melquiades, F. L.; Appoloni, C. R. *J. Radioanal. Nucl. Chem.* **2004**, *262*, 533–541.

[75] Alfeld, M.; de Viguerie, L. *Spectrochim. Acta Part B At. Spectrosc.* **2017**, *136*, 81–105.

[76] Vernon-Parry, K. D. *III-Vs Rev.* **2000**, *13*, 40–44.

[77] Lynch, V.; Miotti, L. *J. Archaeol. Sci. Reports* **2017**, *16*, 299–308.

[78] Reiter, M. *Conversion Factors Needed for Common Fertilizer Calculations*; 2020; pp 1–4.

[79] Crouch, S. R.; Malmstadt, H. V. *Anal. Chem.* **1967**, *39*, 1084–1089.

[80] College of Science, U. o. C. *Coll. Sci. Determ. Phosphate Conc. Soil. (n.d.).*

[81] Dudley, G. B.; Richert, R.; Stiegman, A. E. *Chem. Sci.* **2015**, *6*, 2144–2152.

[82] Everett, D. H. *Pure Appl. Chem.* **2019**, *31*, 577–638.

[83] Jastrzbski, W.; Sitarz, M.; Rokita, M.; Bułat, K. *Spectrochim. Acta - Part A Mol. Biomol. Spectrosc.* **2011**, *79*, 722–727.

[84] Salje, E.; Viswanathan, K. *Contrib. to Mineral. Petrol.* **1976**, *55*, 55–67.

[85] Ukita, M.; Toyoura, K.; Nakamura, A.; Matsunaga, K. *J. Appl. Phys.* **2016**, *120*, 142118.

[86] Tone, T.; Koga, N. *ACS Omega* **2021**, *6*, 13904–13914.

[87] AbdAllah, A. T.; Moustafa, M. A. *Environ. Pollut.* **2002**, *116*, 185–191.

[88] Rambeau, C. M.; Baize, D.; Saby, N.; Matera, V.; Adatte, T.; Föllmi, K. B. *Environ. Earth Sci.* **2010**, *61*, 1573–1585.

[89] Martínez-García, C.; González-Fonteboa, B.; Martínez-Abella, F.; López, D. C. *Constr. Build. Mater.* **2017**, *139*, 570–583.

[90] Plotegher, F.; Ribeiro, C. *Mater. Res.* **2016**, *19*, 98–105.

[91] Bazarkina, E. F.; Pokrovski, G. S.; Zotov, A. V.; Hazemann, J. L. *Chem. Geol.* **2010**, *276*, 1–17.

[92] Shannon, R. D. *Acta Crystallogr. Sect. A* **1976**, *32*, 751–767.

[93] Bazarkina, E. F.; Pokrovski, G. S.; Zotov, A. V.; Hazemann, J.-L. *Chem. Geol.* **2010**, *276*, 1–17.

[94] Elliott, H. A.; Denneny, C. M. *J. Environ. Qual.* **1982**, *11*, 658–663.

[95] Wong, C.-W.; Barford, J. P.; Chen, G.; McKay, G. *J. Environ. Chem. Eng.* **2014**, *2*, 698–707.

[96] Marder, L.; Bernardes, A. M.; Zoppas Ferreira, J. *Sep. Purif. Technol.* **2004**, *37*, 247–255.

[97] Butter, T. J.; Evison, L. M.; Hancock, I. C.; Holland, F. S.; Matis, K. A.; Philipson, A.; Sheikh, A. I.; Zouboulis, A. I. *Water Res.* **1998**, *32*, 400–406.

[98] Lokhande, R. S.; Singare, P. U.; Kolte, A. R. **2007**, *95*, 595–600.